UNIVERSITY OF TROMSØ UIT

FACULTY OF SCIENCE AND TECHNOLOGY
DEPARTMENT OF GEOLOGY

Ice stream dynamics inferred from seismic geomorphology from the Bjørnøyrenna and Nordkappbanken area, SW Barents Sea

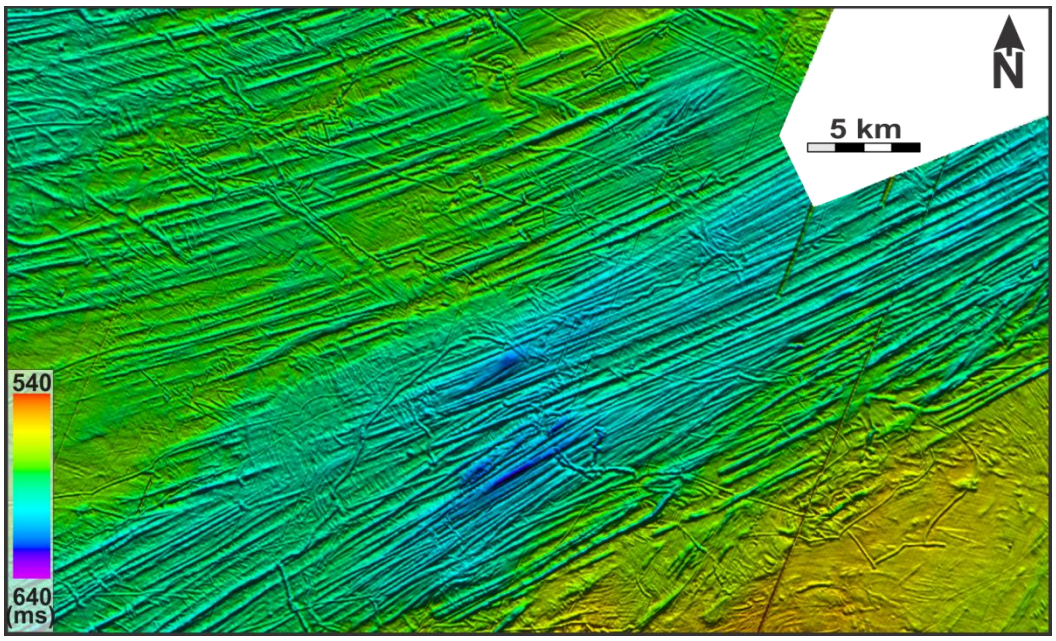

Mohammad Ibrahim Khan

GEO-3900 Master's Thesis in Geology

May 2013

GEO-3900

MASTER'S THESIS IN GEOLOGY

Ice stream dynamics inferred from seismic geomorphology from the Bjørnøyrenna and Nordkappbanken area, SW Barents Sea

Mohammad Ibrahim Khan

May, 2013

ABSTRACT

The aim of this master thesis is to investigate ice streams dynamics in Bjørnøyrenna and Nordkappbanken areas in south-west Barents Sea shelf Ice streams are responsible for the drainage of majority of ice from ice sheet and play a key role in the dynamic nature and stability of ice sheets, based mainly on six 3D seismic data sets,. Regional 2D lines are also used to establish the regional stratigraphy and for correlation purposes. A total of 15 horizons were interpreted in the various cubes. On all the sub-surface horizons, depressions and megascale glacial lineations (MSGLs) were observed, the latter being indicative of fast flowing paleo-ice streams. Most of these surfaces exhibit multiple generations of MSGLs indicating changes in ice stream source areas or flow of different ice streams. The paleo-ice streams on the seafloor are attributed to deglaciation of the Barents Sea while some of the subsurface paleo-ice streams may have formed during the Last Glacial Maximum (LGM). Glaciotectonic origin is inferred for most of the depressions with some being additionally attributed to fluid flow expulsion. Channels are inferred to be formed from glacial melt-water.

فَبِأَيِّ آلاءِ رَبِّكُمَا تُكَذِّبَانِ

The Holy Quran 55:13

So which of the favors of your Lord would you deny?

The Holy Quran 55: 13

ACKNOWLEDGEMENTS

First of all I would like to offer my sincere thanks my supervisors Professor Karin Andreassen and Bjarne Rafaelsen for their continue help and support throughout this Master Thesis. I am grateful for all the suggestions, comments and constructive feedback throughout the study period. I would also like to extend my gratitude for their contribution in my personal development and my potential future career.

I am thankful to Statoil, ASA and TGS, Norway for providing seismic data for this study. I also appreciate all the help I received from Denis Ruther in understanding ArcGIS software.

I would like to show appreciation to my fellow MSc students especially Morten and Audun for all the discussions and sharing ideas throughout this study period. Special thanks to my all friends especially Atif, Tanveer and Adnan for making my stay in Tromsø a memorable one.

Finally, I am extremely thankful to my family especially my parents and grandmother without whose prayers and support, I would have not made it this far. I would like to express gratitude to my wife for the patience, love, support and looking after my two kids through these years which made it possible for me to pursue my study.

Mohammad Ibrahim Khan

May, 2013

Contents

1. Introduction

1.1 Objectives

Preliminary observations suggest that sub glacial erosion had been a common geological process in the southwest Barents Sea shelf during the deglaciation of Barents Sea Ice sheet as indicated by the presence of megascale glacial lineations (MSGL) and irregular depressions within the glacigenic sediments above URU. The MSGLs are produced by fast flowing ice streams which are corridors of fast flowing ice within an ice sheet. These are helpful in depicting the dynamics of an ice sheet (Clark et al. 2003; Andreassen et al. 2008). Large erosional depressions are also common occurring elements in the study area. At various places these depressions seem to have a relationship with the underlying fluid flow and shallow gas accumulations.

The primary objective of this master thesis was to study the ice streams dynamics using 3D seismic data in the subsurface horizons in the glacigenic sediments as well as to establish if there is any relationship between the depressions and shallow gas accumulations.

1.2 The study area

The study area is located in the southwestern Barents Sea (Fig. 1.1). The Barents Sea is an epicontinental sea with its present continental shelf covering an area of ~1.4x106 km^2 with an average depth of around 250 meters. The deepest part on the shelf area reaches more than 500 meters (Laberg et al. 2012, Solheim and Elverhøi, 1993).

The Barents Sea is bounded by the Arctic Ocean in the north, the Norwegian-Greenland Sea in the west, northern Norway in the south and Novaya Zemlya in the east separating the Barents Sea from the Kara Sea. The bathymetry of Barents Sea shelf is characterized by shallow banks and over-deepened troughs. The banks areas have water depth from 50 m to more than 300 m, separated by large transverse and over-deepened troughs with water depth of ~300 m to more than 500 m. Water depth in the study area is from about 230 to 480 meter. Large scale bathymetric features like grounding-zone wedges, megascale glacial lineations and ice berg plough marks dominate the seafloor which are interpreted to have resulted from a dynamic decay of the Barents Sea-Fennoscandian ice sheet following the Last Glacial Maximum (Andreassen et al. 2008; Winsborrow et al. 2010; Knies et al. 2009; Andreassen et al. 2007a). The ice sheets through its ice streams, zones of fast flowing ice compared to the surrounding ice sheet, imprinted the seafloor creating large elongated troughs into the underlying bedrock and sediments which is inferred as the Bear Island Trough or Bjørnøyrenna (Andreassen et al. 2007, b; Andreassen et al.2008; Vorren and Laberg, 1997) (Fig. 1.1 B). The water depth at Bjørnøyrenna varies between 300 and 500 m. It is 750 km long, 150-200 km wide. It is bounded by shallow banks like Tromsøflaket in the southwest and Nordkappbanken in the southeast which have water depths around 200-300 m while the Bjørnøya Island lies to the northwest of Bjørnøyrenna (Fig. 1.1 B). The Bjørnøyrenna Trough extends into large fan-shaped mouth fan termed as Bjørnøya Trough Mouth Fan (BTMF) (Vorren et al. 1988; Vorren and Laberg 1997; Andreassen et al. 2008).

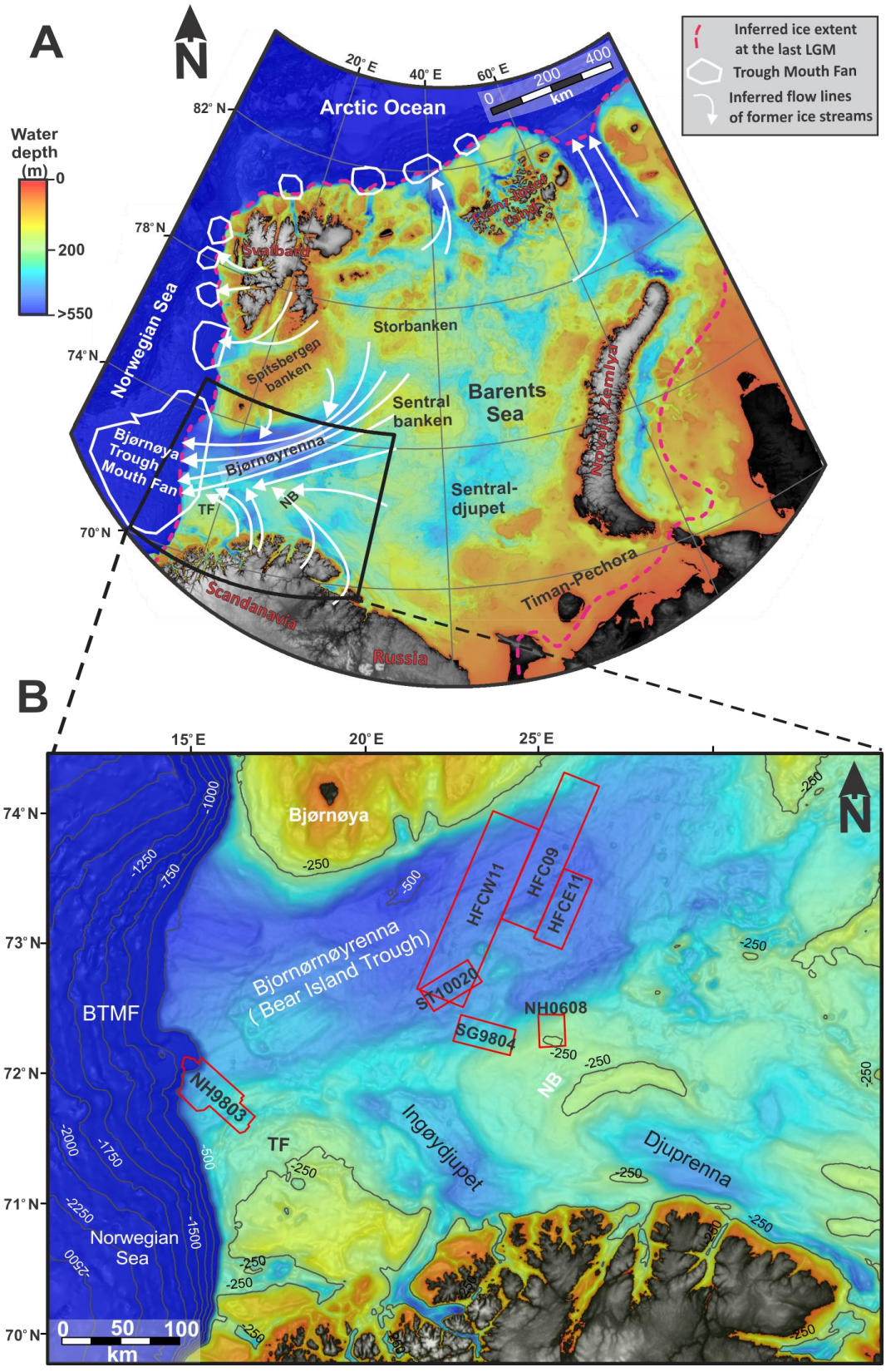

Figure 1.1 A) Map showing large scale IBCAO bathymetry map (raw data from Jackobssen et al. 2012) of the Barents Sea and extent of the Last Glacial Maximum of Barents Sea and Fennoscandian Ice Sheets (shape file from Svensden et al. 2004). Flow lines of major ice streams are indicated by white arrows,

modified from Andreassen et al. (2008). ***B)*** *IBCAO bathymetry map of SW Barents Sea, red polygons show location of the 3D surveys used. The survey NH9803 is used only for profile in Fig. 1.7. BTMF: Bear Island Trough Mouth Fan.*

1.2 Geological Settings of the Barents Sea

The Barents Sea covers the continental shelf of north-western Eurasia and has some the deepest sedimentary basins in the world; it is bounded by young passive margins to the west and north which are related to Cenozoic opening of the Norwegian-Greenland Sea and Eurasian Basin (Gudlaugsson et al. 1998, Faleide et al. 1993a, Faleide et al. 1984). To the north lies the Svalbard archipelago and Franz Joseph Land. Towards the east, the shelf is delimited by the extension of the Ural mountain chain through Novaja Zemlya and in the south by the Baltic Shield (Larssen et al. 2002). The region has an intracratonic setting with several tectonic phases since the Caledonian orogenic movements terminated in Early Devonian times. Many highs and lows can be seen from regional profiles in the Barents Sea. The region is divided into different smaller basins.

The Barents Sea has a complex geological history with various episodes of tectonics, subsidence and erosion. Faleide et al (1993a and 2010) has described the geological history of western Barents Sea in 3 rift phases; Late Devonian-Carboniferous, Middle Jurassic-Early Cretaceous and Early Tertiary with several tectonic pulses within each phase. Late Paleozoic crustal extension affected most of the Barents Sea causing westward migration of rifting, formation of well-defined rifts and pull apart basins in the SW part while strike slip faults development in the north (Faleide et al. 1993a). Breivik et al. 1995 has documented that a major rifting event took place in Early Carboniferous and culminated in Middle Carboniferous followed by a second phase in Permian-Early Triassic. The former rifting gave rise to several extensional basins with synrift deposits, separated by fault bounded highs. Late Mesozoic-Early Cenozoic tectonic events gave rise to the present deep sedimentary basins in SW Barents Sea (Breivik et al. 1998). Dore, A.G 1991, describes the formation of the region by continental collision forming Caledonian orogeny and later followed by continental separation forming the rifts. The region is underlain by thick sequence of more than 15km, in some areas ranging from upper Paleozoic to Cenozoic rocks (Faleide et al. 2010; Glørstad et al. 2010; Gudlaugsson et al. 1998, Faleide et al. 1993a). Basement is rarely seen on seismic data (Faleide et al. 1993a). Regionally the sequence

in Barents Sea is thick and undeformed except the south-west Barents Sea where it is deformed by Late Mesozoic and Cenozoic tectonic movements making structural correlation locally difficult (Faleide et al. 1993a). “Many structural elements in the region reflect Jurassic and later tectonism: not least a Tertiary phase of differential uplift had a profound effect on the final sculpting of the province” (Nyland *et al.* 1992).

The western Barents Sea having thick sequence of upper Paleozoic to Cenozoic sediments is divided in 3 distinct regions (Dimakis et al. 1998).

1. Svalbard Platform containing flat successions of upper Paleozoic and Mesozoic.
2. Basin Province between Svalbard Platform and Norwegian Coast having sub basins and highs that contain Jurassic-Cretaceous Sediments and Paleocene-Eocene towards the west.
3. The continental Margin which can be further divided into three regions
    a) Southern sheared Margin along the Senja Fracture zone.
    b) Volcanism Associated central rift complex SW of Bjørnøya.
    c) Northern, initially sheared followed by rifting margin along the Hornsund Fault Zone.

1.3 Structural Elements in the study area

Structural Elements in the region are described in detail by Gabrielsen at al. 1990 and Larssen et al. 2002. "The entire western Barents Sea rift system is believed to reflect the grain of the Caledonide orogeny ('Barents Sea Caledonides') (Dore`, 1991)" which is characterized by a predominant NE-SW strike direction (Gudlaugsson et al. 1998). Structurally, the Barents Sea continental shelf is dominated by ENE-WSW to NE-SW and NNE-SSW to NNW-SSE trends with local influence of WNW-ESE striking elements (Gabrielsen et al. 1990). The southern part has fault complexes with ENE-WSW trends which border the Hammerfest and Nordkapp Basins, in the North, a sub parallel zone to the southern part is defined by the Veslemøy High and the fault complexes separating the Loppa High from the Bjørnøya Basin (Fig. 1.2). The oldest Paleozoic structures like Nordkapp Basin and Finnmark Platform characterize the SW region while Mesozoic basins; Tromsø and Bjørnøya in the west and the youngest basins like Sørvestsnaget Basin are adjacent to Norwegian-Greenland Sea (Reemst et al. 1994).

1) Loppa High

Most of the 3D surveys are located on Loppa High (Fig. 1.2). The Loppa High is a triangular shaped sedimentary high between Hammerfest and Bjørnøya Basin which is faulted towards the Bjørnøya Basin and flexure or faulted towards the Hammerfest Basin (Faleide et al. 1984). The southern side is bounded by the Asterias Fault Complex, eastern and south-east by a monocline towards the Hammerfest Basin and to the west by the Ringvassøy-Loppa and Bjørnøyrenna Fault complexes (Gabrielsen et al. 1990).

2) Bjarmeland Platform

The Bjarmeland Platform represents the areas bounded between Sentralbanken and Gardarbanken High in the north, Nordkapp and Hammerfest basin in the south and, Loppa high and Fingerdjupet subbasin in the west (Fig. 1.2). As a result of Tertiary uplift, the platform sediments gently dip towards the south and progressively older sediments subcrop to the north under URU (upper regional unconformity).

Bjarmeland Platform represents a stable structural element since the Late Paleozoic (Gabrielsen et al. 1990). The Bjarmeland Platform started to develop as a stable platform in Late Carboniferous time. Late Mesozoic and Tertiary tectonism gave rise to the present Loppa High

and Fingerdjupet subbasin which marks the western termination of Bjarmeland Platform (Gabrielsen et al. 1990).

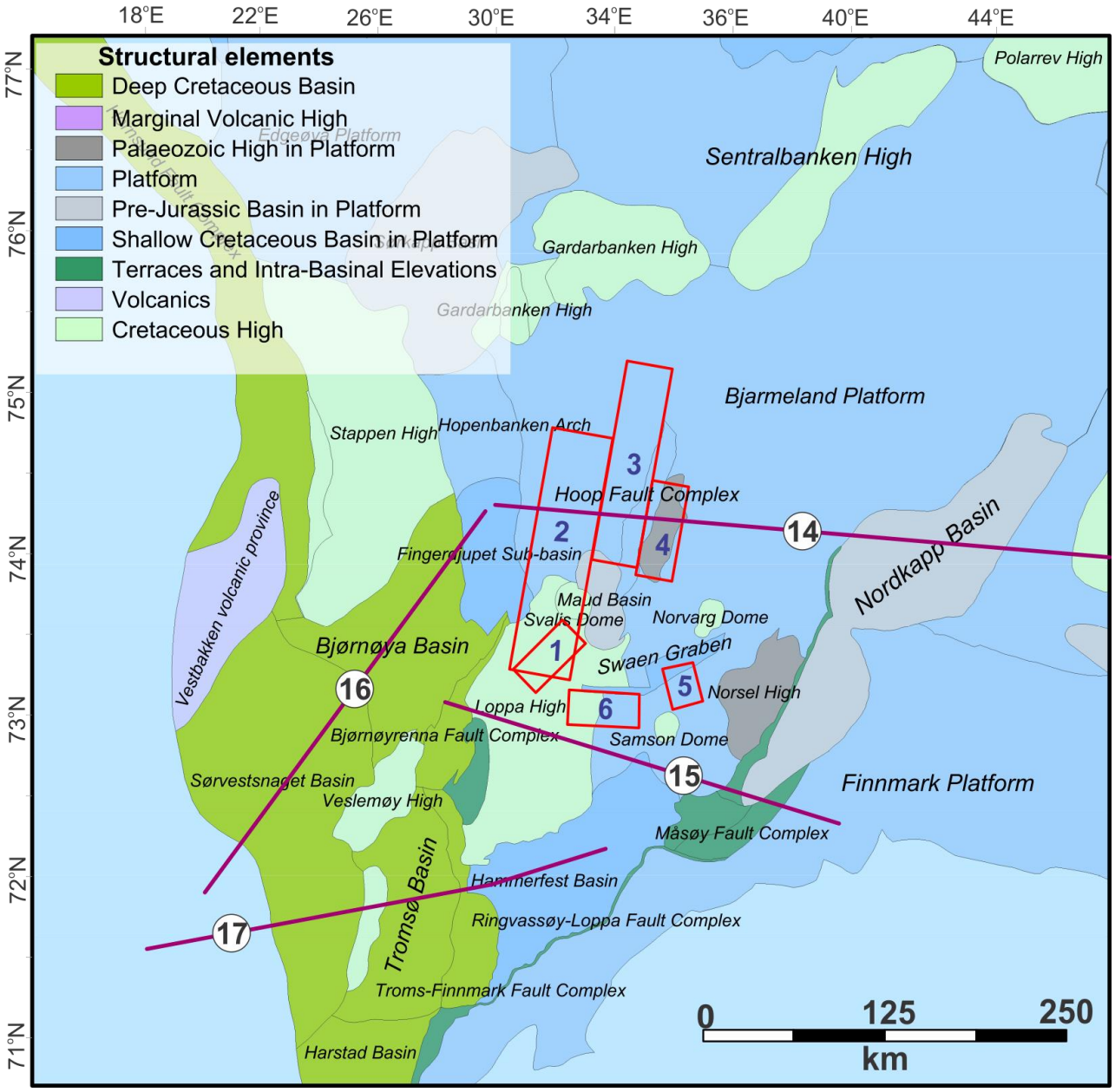

Figure 1.2: Main Structural Elements in the study area with respect to geo-referenced 3D surveys in SW Barents Sea modified from www.npd.no. . 1: ST10020; 2:HFCW11; 3: HFC09; 4: HFCE11; 5: NH 0608; 6: SG9804. 2D seismic profiles 14-17 can be seen in figure 1.3.

1.4 Geological Evolution of Barents Sea

The Western Barents Sea has can be divided into 3 major rift phases; post Caledonian which are Late Devonian-Carboniferous, Middle Jurassic-Early Cretaceous and Early Tertiary with several tectonic pulses in each rift phase (Faleide et al. 2010). These events gave rise to different structures in the region (Fig. 1.3). Devonian tectonics were dominated both by extensional and compressional events as known from Svalbard (Faleide et al. 2010).

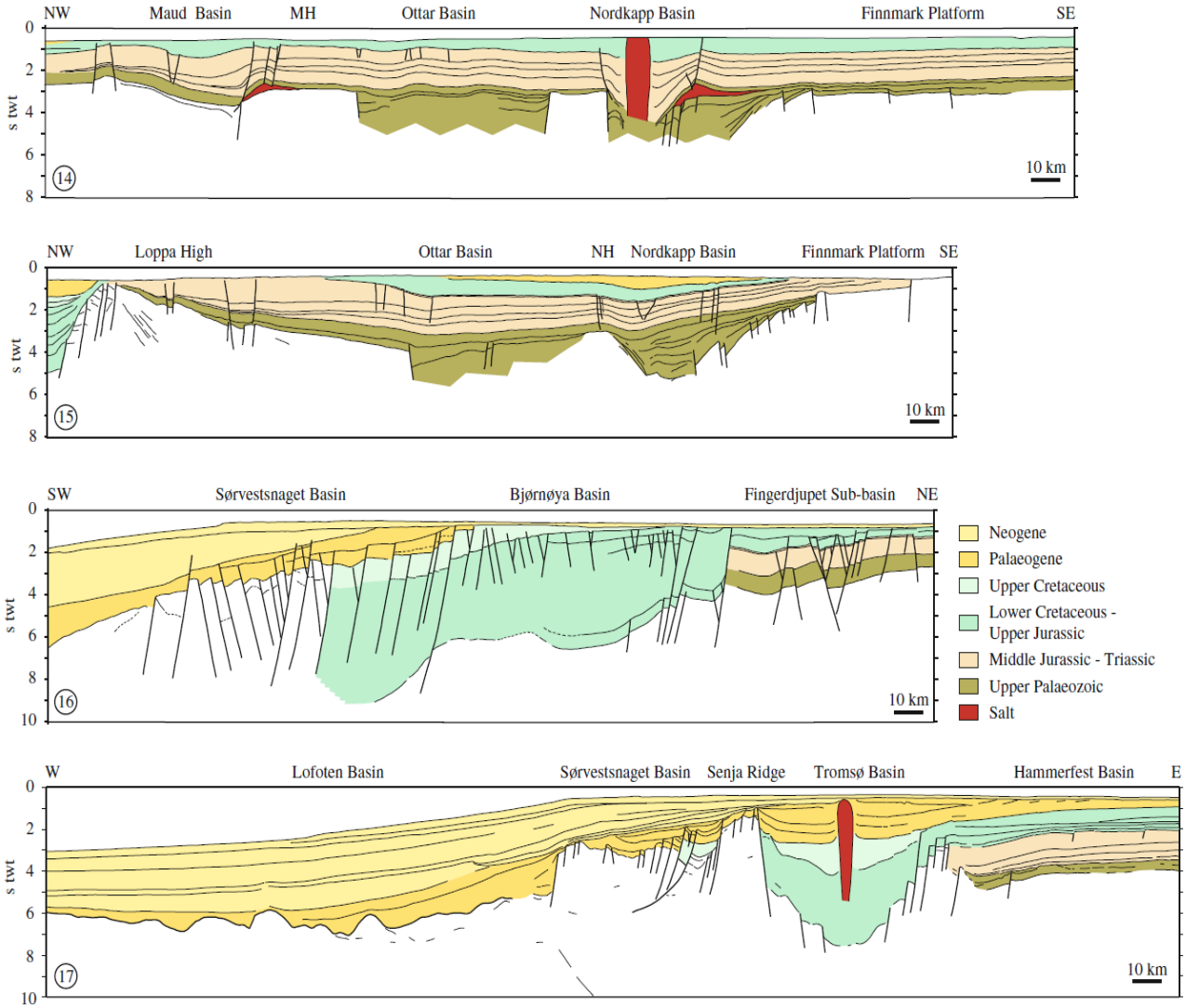

Figure 1.3: Regional geo-seismic profiles in SW Barents Sea from Faleide et al. 2010.The location of the respective lines can be seen in figure 1.2.

During Lower to Lower Upper Carboniferous clastics were mainly deposited in extensional basins. Mid Carboniferous extension formed a 300km wide and 600km long fan shaped rift zone which can be attributed to direct continuation of NE Atlantic rift between

Greenland and Norway as well as subordinate link to the Arctic rift. The rifting during this period caused formation of several extensional basins like Tromsø, Bjørnøya, Nordkapp, Fingerdjupet, Maud and Ottar Basins with syn-rift deposits separated by fault bounded highs (Faleide et al. 2010). Towards the end of Carboniferous faults movement ceased in eastern area. Late Carboniferous-Permian age platform successions were deposited with dolomites in the lower part passing to evaporites (mapped regionally in SW Barents Sea) to massive limestone during Early Permian followed by clastic deposition late Permian(Faleide et al. 2010). The western area was affected by faulting, erosion and uplift during Permian and Early Triassic which can be depicted from western Margin of Loppa High. The erosional surface can be mapped from Loppa High to Stappen High (Faleide et al. 2010).

Clastic deposition took place during the Triassic with Uralian Highlands acting as a main source of sediments along with Baltic shield. Salt movement in the Nordkapp Basin as well as some other salt basins in the region was probably triggered during this period due to differential loading. The Triassic sequence mainly consists of sandstones and shale. Continental deposition dominated a large part of the region during the middle Triassic except for central and Northern basins where marine conditions dominated. In the end of Triassic regression and erosion took place. During Lower-Middle Jurassic Sandstone deposition took place in the entire region forming the present day reservoirs in SW Barents Sea (Faleide et al. 2010). In late Triassic regional subsidence took place and large volumes of sediments were deposited (Faleide et al. 2008).

During Lower-Middle Jurassic sandstone deposition took place in the entire region forming the present day reservoirs in SW Barents Sea. The late Middle Jurassic boundary is marked by the rifting phase in SW Barents Sea while unconformities in upper Jurassic reflect faulting and sea level changes. The lithologies in this sequence reflect relatively deep and quiet marine conditions (Faleide et al. 2010). Regional extension with strike slip movements along old structures during Late Jurassic- Early Cretaceous gave rise to Bjørnøya, Tromsø and Harstad rift basins (Faleide et al. 2010). The Middle-Late Jurassic rifting phase gave rise to block faulting in Hammerfest and Bjørnøya Basins and deposition of Upper Jurassic shales in restricted basins. Tromsø and Bjørnøya basins are also interpreted to have initiated subsidence during this period (Faleide et al. 1993a and 1993b).

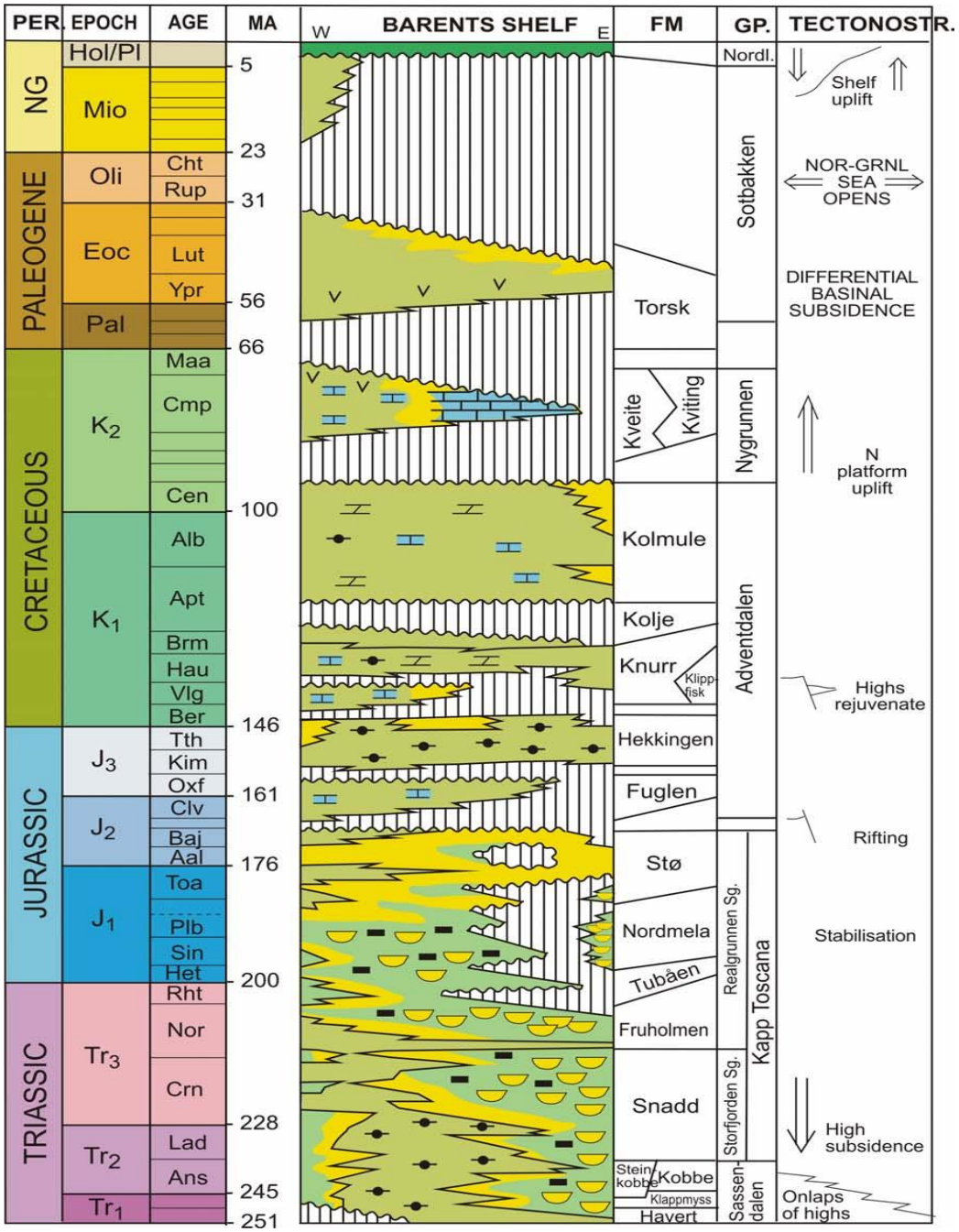

Figure1.4: Mesozoic and Cenozoic development of SW Barents Sea. Worsely (2006).

The rifting continued in the Early Cretaceous which gave rise to numerous faults in SW Barents Sea (Faleide et al. 2010). Faleide et al. 1993a has suggested three tectonic phases during Early Cretaceous which strongly affected the Tromsø and Bjørnøya Basins. Three sedimentary units can be recognized in the Lower Cretaceous with dominant lithology of shales and claystone along with thin interbeds of silt, limestone and dolomite in SW Barents Sea (Faleide et al. 2010). High amplitude reflectors observed in Northern Tromsø Basin are interpreted as deep water

clastic fans derived from uplifted Loppa High by Faleide et al. 1993a). Rapid subsidence took place at the end of Early Cretaceous rift phase with deposition of 5-6km thick sequence in Bjørnøya, Tromsø and Harstad Basins (Faleide et al. 1993a and 1993b). The environment of deposition for these units is dominated by marine conditions with restricted bottom circulation periodically. During Upper Cretaceous deposition continued in SW Barents Sea which subsided continuously in response to faulting (Faleide et al. 2010). Svalbard underwent uplift in Late Cretaceous (Faleide et al. 1984).Tromsø and Sørvestsnaget Basins continued to subside during Late Cretaceous. Extension during late Cretaceous gave rise to numerous faults in Veslemøy High and Bjørnøya Basin. A hiatus occurred at Cretaceous-Tertiary boundary followed by uniform Late Paleocene sequence in the entire Western Barents Sea (Faleide et al. 1993a).

Cenozoic structures are related to a two-stage opening of Norwegian-Greenland Sea and formation of sheared margin along western Barents Sea Continental margin. Continental break up was followed by rapid late Paleocene subsidence (Faleide et al. 2919). The Paleocene deposition took place in deep marine conditions in the Sørvestsnaget Basin and Vestbakken Volcanic Province. Deep marine conditions persisted in Sørvestsnaget basin during Eocene with deposition of sandy submarine fans in Middle Eocene (Ryseth et al. 2003). Senja Fracture zone was developed as a result of Norwegian-Greenland Sea opening during Eocene (Faleide et al. 2008).

Paleogene sequence is underlain unconformably by Cretaceous throughout the SW Barents Sea (Faleide et al. 2010). The western Barents Sea-Svalbard margin developed from megashear zone which linked Norwegian-Greenland Sea and Eurasia Basin in the Eocene opening. The pre-break structure, geometry at opening and direction of plate motion controlled the structure and tectonic development along the margin; The SW of Bjørnøya was associated with magmatism in Vestbakken Volcanic Province during Paleocene-Eocene and Oligocene break up while strike slip movements along Svalbard and Greenland formed the Spitsbergen Fold and Thrust Belt (Faleide et al. 2010). Deep marine conditions existed in Sørvestsnaget Basin and Vestbakken Volcanic Province with deposition of submarine fans in axial part of Sørvestsnaget Bain and Vestbakken area. Sørvestsnaget Basin experienced marine shallowing during Eocene-Oligocene transition (Ryseth et al. 2003). Rifting occurred in Early Oligocene which reactivated faults in Vestbakken Volcanic Province (Faleide et al. 2008) also resulted in extension faulting

along Senja Fracture Zone (Ryseth et al. 2003). Subsidence and burial of margins by thick sediments in clastic wedge form uplifted areas took place during late Cenozoic. Uplift and erosion of the region during late Cenozoic has removed most of Cenozoic sequence in the SW Barents Sea which is estimated around 1,000-1,500m (Faleide et al . 2010).

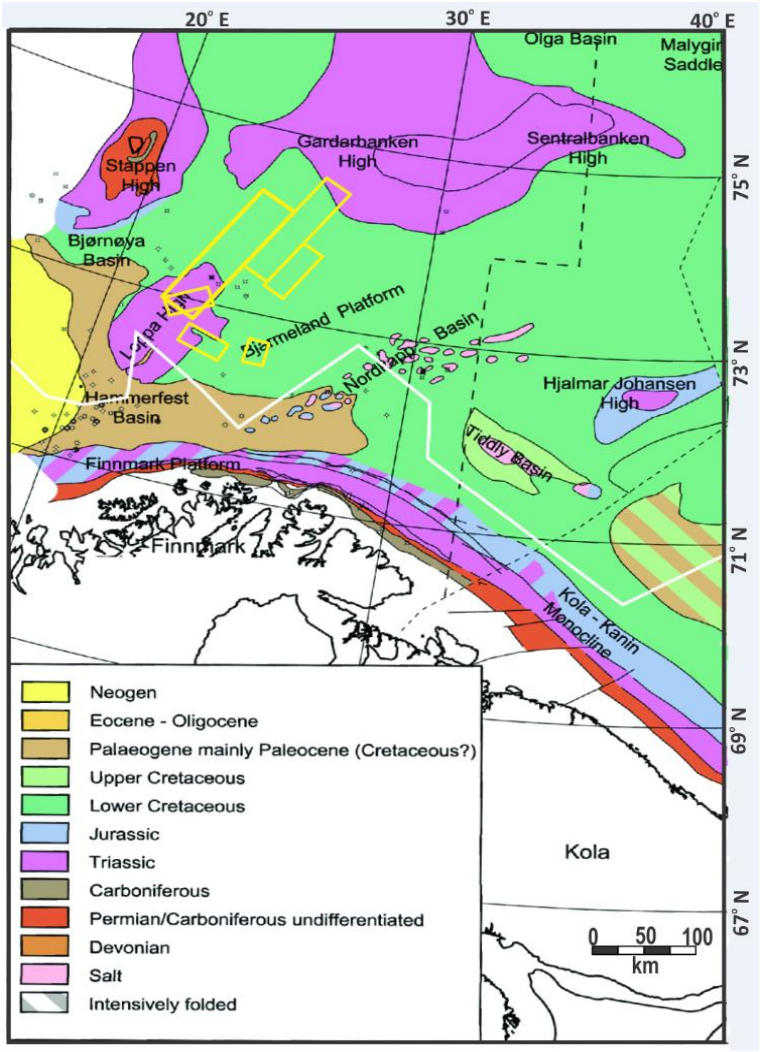

Figure 1.5: subcropping geology in the SW Barents Sea under Quaternary glacial sediments. The surveys can be seen in yellow rectangles. Modified after Henriksen et al. (2011, a).

In late Miocene uplifting of the region occurred with high magnitude eastward in Vestbakken Volcanic Province (Jabsen and Faleide, 1998). In Late Pliocene Northern Hemisphere Glaciation caused rapid progradation and high sedimentation formed depocentres in western Barents Sea (Faleide et al. 2008).Glacial deposition in submarine fans took place as a result of Plio-Pleistocene uplift and erosion caused by glaciers in the region (Dimakis et al. 1998) which underwent sediment instability due to excess pore pressure in response to enhanced deposition

forming series of submarine slides in the area (Bryan et al. 2005; Evans et al. 2005; Solheim et al. 2005; Hjelstuen et al. 2007). The erosion led to different subcropping units in the Barents Sea (Fig) below base of Quaternary glacial sediments.

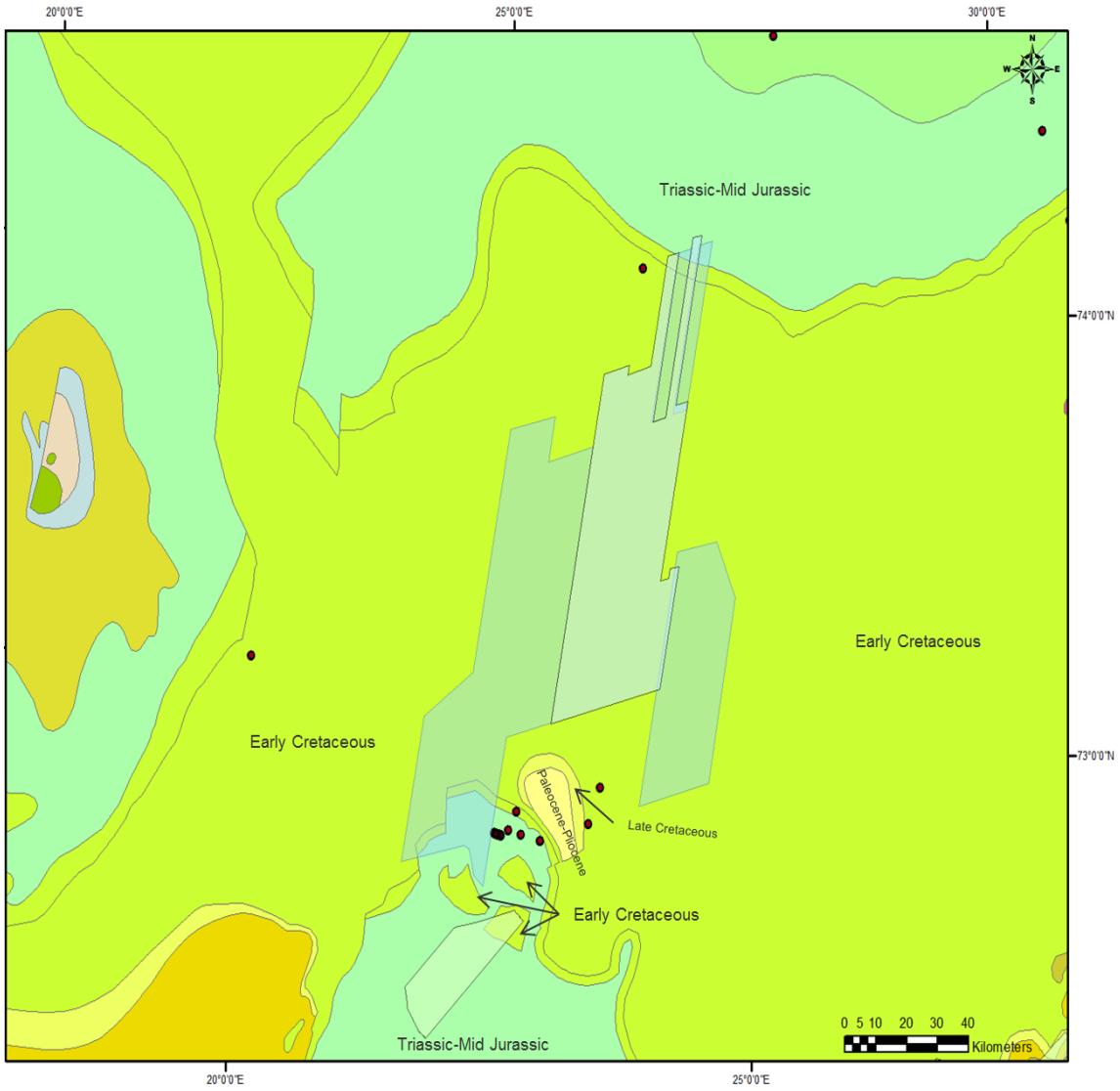

Figure 1.6: subcropping geology under Quaternary glacial sediments in the survey ST10020 and HFC surveys. Modified after Ellen Sigmond 1992.

1.5 Glacial History of Barents Sea

Barents Sea had been glaciated several times during the Late Cenozoic which is documented by many authors (Andreassen et al. 2004, 2007, Vorren et al. 2011, Knies et al. 2009, Rafaelsen et al 2007, Sættem et al. 1992a, Winsborrow et al. 2009). During the deglaciation periods sediments have been eroded and deposited throughout the Barents Sea. These glacial deposits can easily be distinguished from underlying bedrock by a pronounced seismic reflector; the upper regional unconformity (URU) (Solheim and Kristofferson, 1984, Vorren et al. 1986). The glacial package varies in thickness around 0-300m on the continental shelf areas and 900-1000m on the continental shelf break areas (Andreassen et al. 2008, Vorren et al. 2011). Several ice streams operated in the Barents Sea which influenced the sea floor geomorphology and led to development of trough mouth fans as ice streams during glacial maxima dumped eroded sediments at the continental shelf margins (Vorren and Laberg, 1997, Vorren et al. 1998, Sejrup et al. 2003, Andreassen et al 2007, 2008, Ottesen et al. 2008, Winsborrow et al 2009). The largest of these ice streams is the Bjørnøyrenna Ice stream with length and width of more than 600 km and 165 km respectively. The largest of the trough mouth fan is the 215 000 km^2 Bjørnøya Trough Mouth Fan in south west Barents Sea (Fig. 1.1) (Vorren and Laberg, 1997, Andreassen et al. 2004, Andreassen and Winsborrow 2009).

Seismostratigraphically the glacial sediments are divided into three sediment packages, GI to GIII on the Bjørnøya Trough Mouth Fan (Fig. 1.7). Seven major seismic reflectors have been identified in these packages from R1-R7 with R7 being the base of glacial deposit (Faleide et al. 1996, Andreassen et al. 2007a). Bases on paleo-magnetic, bio-stratigraphic and strontium isotope analyses, R7 has been assigned Late Pliocene age of 2.3-2.5 Ma (Knies et al. 2009). R5 is assigned an age of 1.3 to 1.5Ma (Butt et al. 2000) which implies an age of approximately 2.7Ma to 1.5Ma to the seismic unit GI. Vorren et al. (2011) have suggested an age of 0.7Ma to the seismic unit GIII. On the basis of GIII and GI ages it can be inferred that GII has an age of approx. 1.5 to 1.7Ma. Since approx. 1.5 Ma, repeated ice advances have been reported along the Western Barents Sea and Svalbard margins (Solheim et al. 1996, Laberg and Vorren 1996a, Solheim et al. 1998, Butt et al. 2000, Andreassen et al. 2004, Sejrup et al. 2005, Andreassen et al. 2007, Vorren et al. 2011).

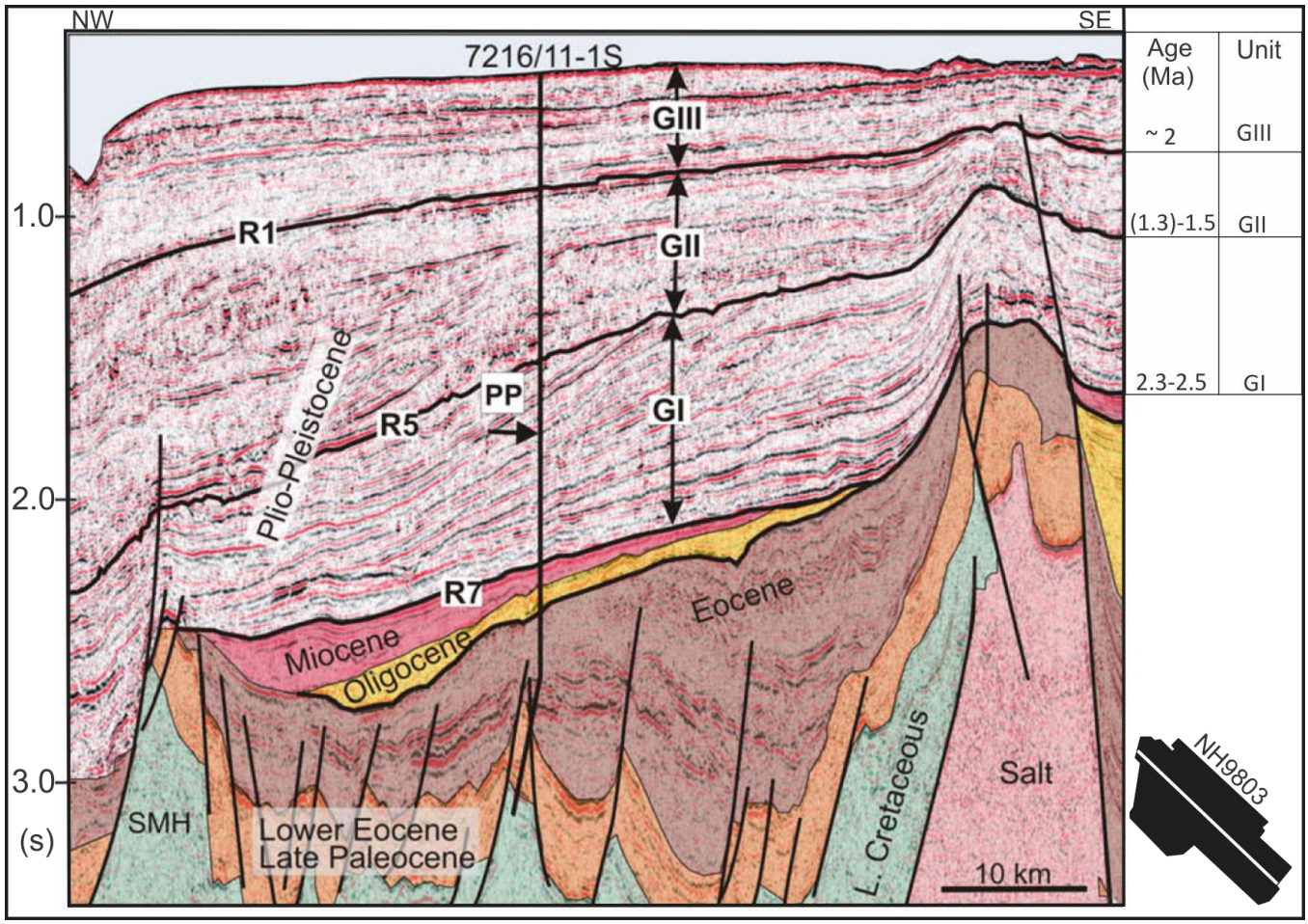

Figure 1.7: Seismic stratigraphy along an inline in the survey NH9803 (left bottom in the figure) across margin of SW Barents Sea. Glacial packages from GI-GIII and R1-R7 can be seen in the figure. The arrow PP marks the base of Plio-Pleistocene in the well 7216/11-1S. Modified after Andreassen et al. (2007a). The respective ages on the right table of R1, R5 and R7 are from Knies et al. (2009). The location of the survey NH9803 can be seen in figure 1.1 B.

According to Knies et al. (2009), the glacial history of the region can be divided into three main stages: (I) Initial growth phase (approx. 3.5-2.4 Ma), (II) transitional growth phase of ice sheet expansion (approx. 2.4-1.0 Ma) and (III) final growth phase of large scale glacial intensification (since approx. 1.0 MA) (Fig. 1.8).

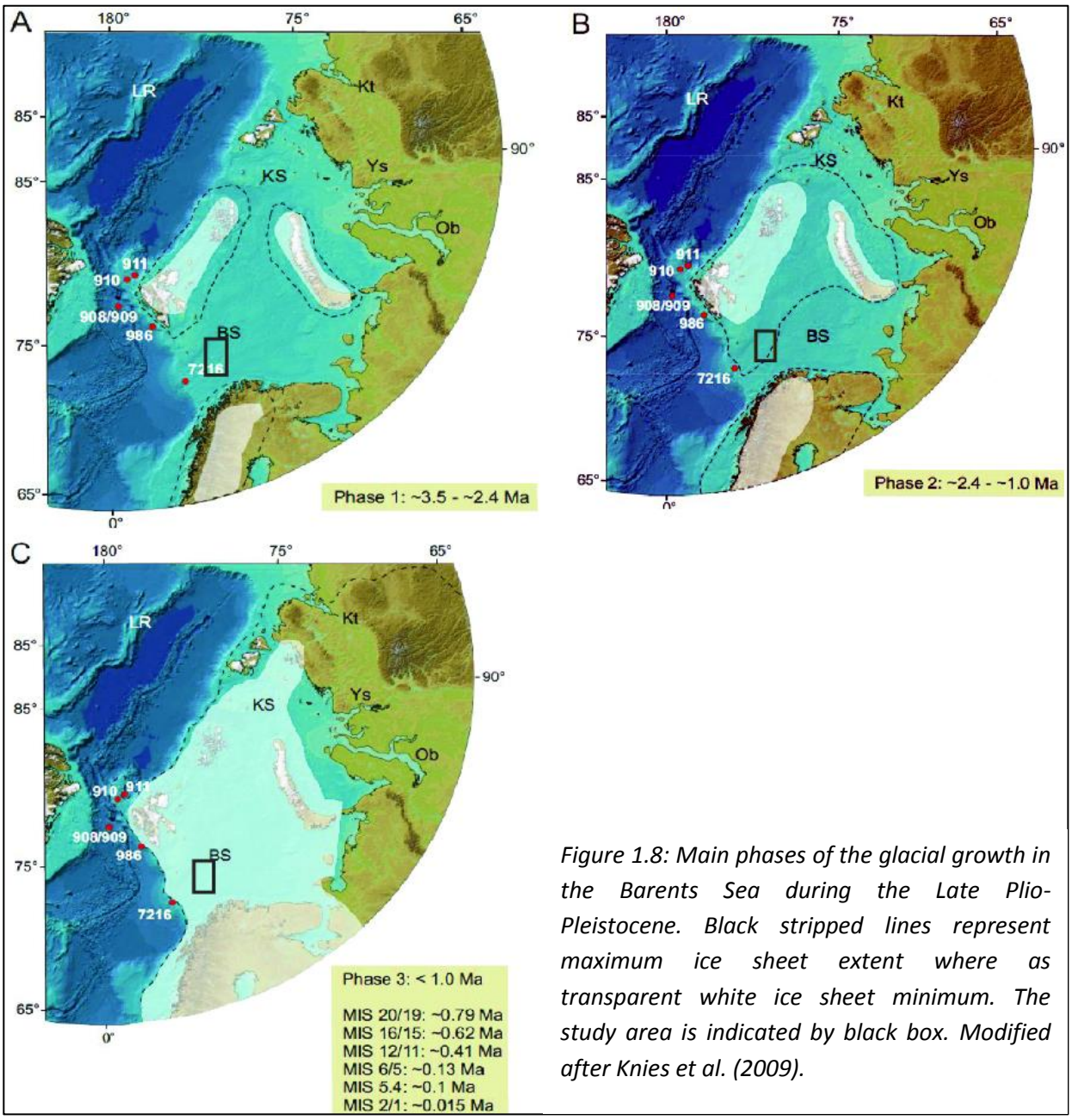

Figure 1.8: Main phases of the glacial growth in the Barents Sea during the Late Plio-Pleistocene. Black stripped lines represent maximum ice sheet extent where as transparent white ice sheet minimum. The study area is indicated by black box. Modified after Knies et al. (2009).

Large scale glaciations in the northern Barents Sea have taken place between approx. 3.5 Ma and 2.4 Ma as observed by the frequent Ice-Rafted Debris (IRD) pulses on the Yermak Plateau in this period (Knies et al. 2009). Mesozoic sediments in central and northern Barents Sea were eroded by the glaciers which were released at the coastline. This Ice sheet was of limited extent as the glacial material (IRD) on the Fram Strait diminishes suggesting that the sediments from the northern Barents Sea were not transported over long distances (Knies et al. 2009). At approx. 2.7 and 2.4 Ma, increase IRD on the Yermak Plateau as well as Western

Svalbard-Barents Sea Margin can be observed suggesting that the ice sheet extended beyond the coast line during this phase (Knies et al. 2009).

Abundant reduction in IRD onto the Yermak Plateau and Western Svalbard Margin suggests that this transitional growth phase (approx. 2.4 Ma) started with partial disintegration of the outermost ice margins with significant glacial erosion on the Yermak Plateau and Fram Strait at approx. 2.4 Ma (Knies et al. 2009). Frequent occurrence of debris flow and turbidites along Western Svalbard margin at 2.4 Ma is interpreted as response to glacial build up on land and increasing erosion rates due to fluctuating ice margin. Svalbard has been the source area for western margins (Forsberg et al. 1999).

Three mega slides along the western Barents Sea margins (Hjelstuen et al. 2007) since approx. 1 Ma (final growth phase) suggest presence of abundant glacial ice and repeated glaciations to the shelf edge (Faleide et al. 1996, Solheim et al. 1998, Andreassen et al. 2004). Andreassen et al. (2007) has reported that grounded ice reached south-western Barents Sea shelf break several times during last million years. At least 5 or 6 shelf edge glaciations have taken place since past 800, 000 years (Knies et al. 2009).

During the deglaciation of the Barents Sea, several ice streams which are corridors for fast ice flow within ice sheet left their imprints in the present day seafloor geomorphology (Andreassen et al. 2008, 2007, 2004, Rafaelsen et al. 2002, and Vorren et al. 2002). Major and oldest ice streams drained out of Bjørnøyrenna and Ingøydjupet trough from the NW Barents Sea and Scandinavian mainland. Ice streams extended to the shelf edge during this event around 18-16 ka BP during last glacial maximum (LGM) (Laberg and Vorren, 1996, Vorren et al. 1990). Shallow banks areas like Tromsøflaket may have been occupied by relatively slow-moving ice during LGM (Andreassen et al. 2008).

A 5-stage deglaciation model (Fig. 1.9) has been proposed for the Barents Sea Ice sheet (Winsborrow et al. 2009). Only those elements of deglaciation model which have affected the study area are documented here. In stage 1 (Fig 1.9 A) whole of Barents Sea shelf extending to the shelf edge was covered with ice. Ice drainage was dominated by the Bjørnøyrenna Ice Stream which was fed by large source area to the north-east and south. Along Bjørnøyrenna two branches of the ice streams, Ingøydjupet and Nordkappbanken operated in the south. Stage 1

has been assigned age of about 19 cal ka BP after Sættem et al. (1992a) and Laberg and Vorren, (1995). A significant retreat of ice margin occurred during deglaciation which was followed by a readvance in the stage 2 (Fig. 1.9 B). An age of about 17 cal ka BP is assigned to the early stage 2.

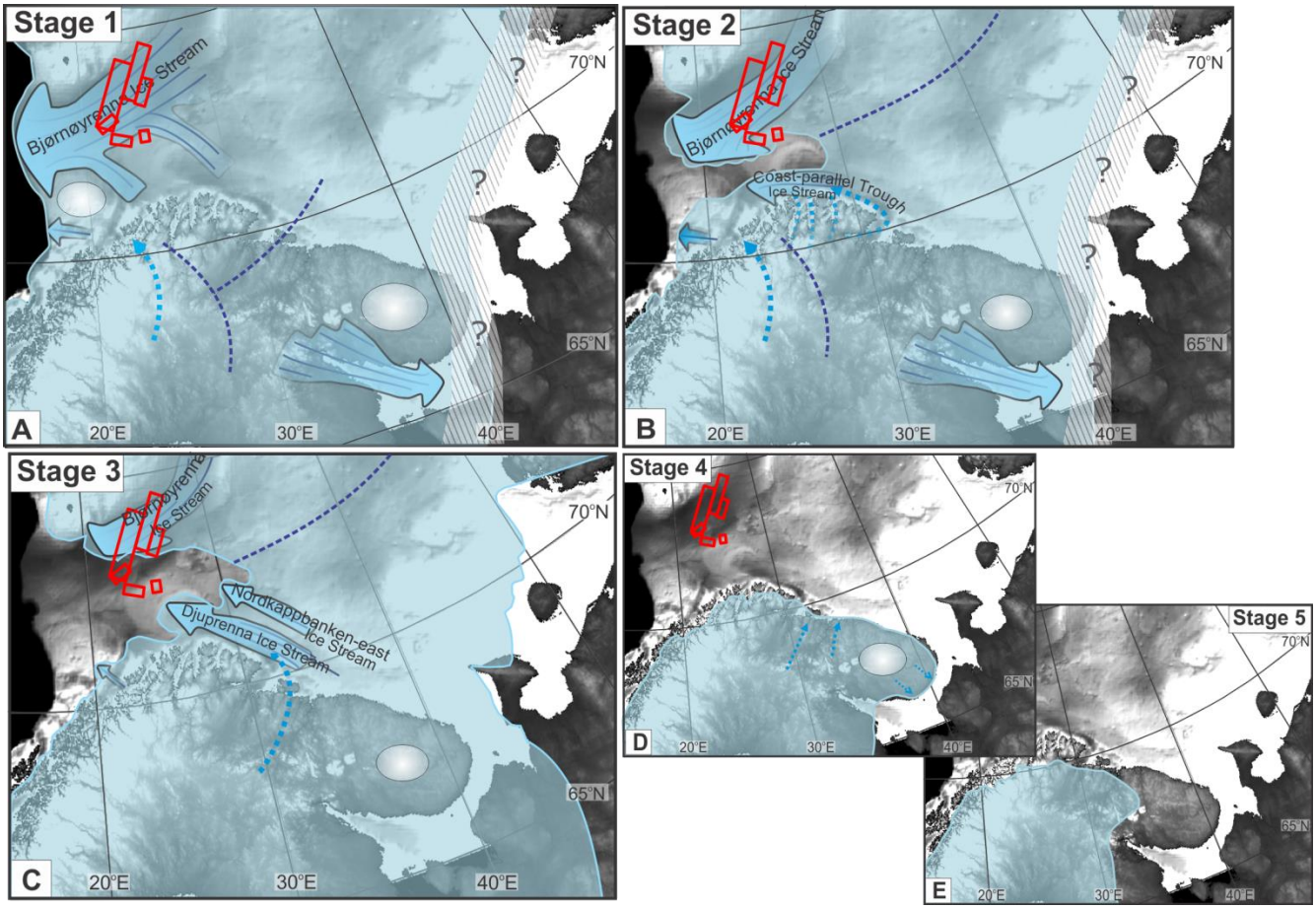

Figure 1.9: Five-stage reconstruction of the Late Weichselian maximum and subsequent deglaciation of the southern Barents Sea. Ice streams are shown as large blue arrows, warm-based ice as dashed blue arrows, cold-based ice as white discs and possible ice divides as dashed dark blue lines from Winsborrow et al. (2009).The study area is represented by red polygons.

In stage 3 (Fig. 1.9 C), the center of maximum ice volume shifted eastwards. Much of the south-western Barents Sea was ice free. Major readvance of Djuprenna and Nordkappbanken-east Ice Streams occurred during this stage. Tromsøflaket and the deepest parts of the Bjørnøyrenna were ice free while the Bjørnøyrenna Ice Stream was still active. Stage 3 is assigned an age of about 16 cal ka BP.

Stage 4 (Fig. 1.9 D) is marked by complete loss of ice cover in the southern Barents Sea with ice margin lying in outer-fjord area in northern Norway. Stage 4 has been assigned an age of about 15 cal ka BP. In the stage 5 (Fig. 1.9 E), a significant ice retreat took place on Kola Peninsula while in northern Norway, ice retreated continuously southward. Stage 5 has an approximate age of about 12-12.5 cal ka BP.

1.6 Glaciotectonic processes and landforms

Glacial erosional processes such as plucking, abrasion, and physical and chemical erosion by subglacial water (Fu and Harbor, 2011) give rise to formation of distinctive landforms (Fig. 1.10). Glaciotectonic involves both proglacial and subglacial deformation. The weight of the ice sheet and its movement is the main driving force which exerts stress on the underlying geology creating these deformations (Fig. 1.10 C & 1.11). Most of these deformations are relatively shallow not deeper than 200 m (Aber and Ber, 2011).

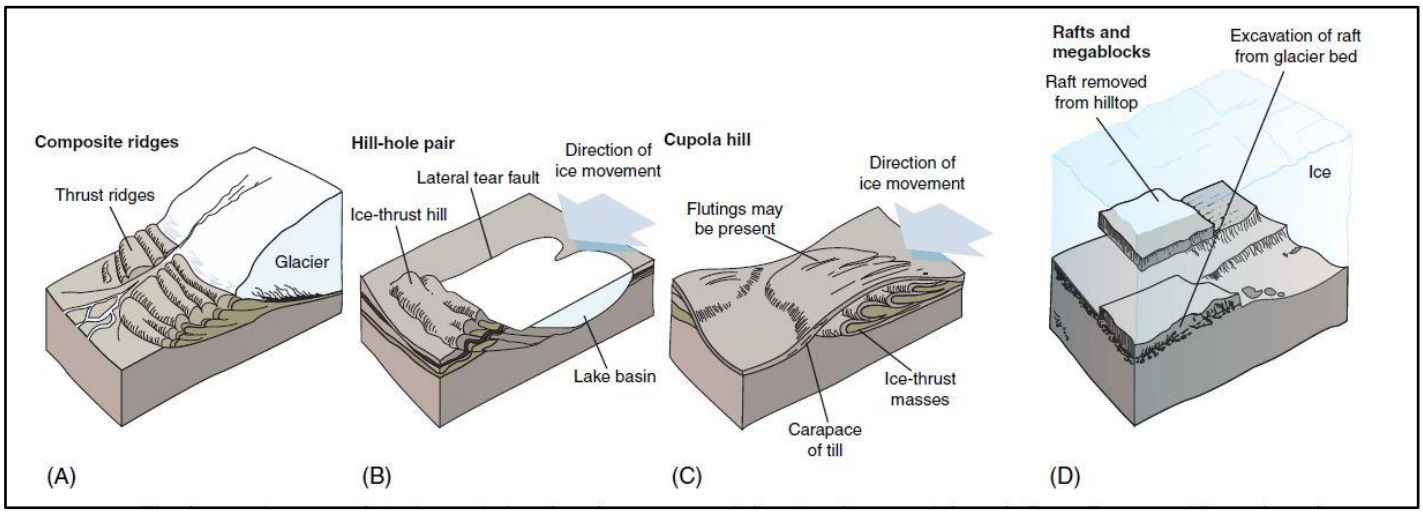

Figure 1.10: Main types of glaciotectonic landforms and their characteristics as defined by Aber et al. (1989). From Evans and Benn (2001)

The nature of deformation can be both brittle and ductile due to variation in the applied stress, temperature, and strain rate and porewater pressure. Ductile deformation like folds take place in front of an advancing glacier which can develop overfolds, or thrusting may take place in case of increasing glacier advance (Fig. 1.10 C & 1.11) (Evans, 2007). Aber et al. (1989) has defined four types of glaciotectonic landforms/structures which include: 1) Composite ridges 2) Hill-hole pair 3) Cupola hill and 4) Rafts and Megablocks (Fig. 1.10 D).

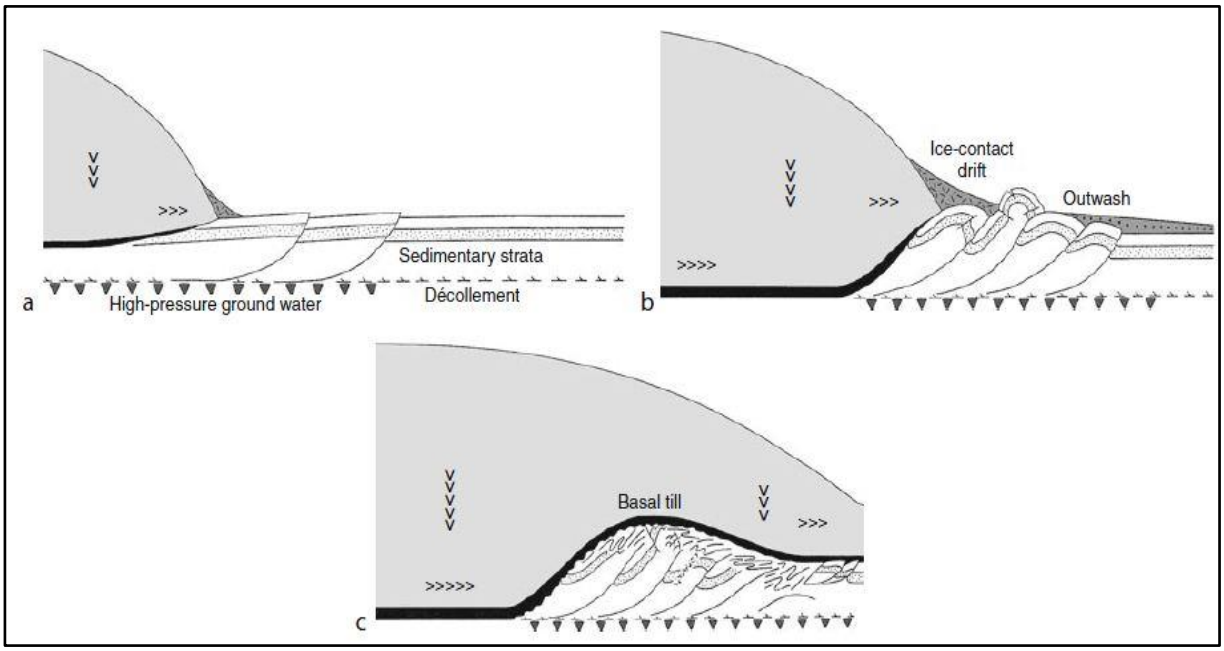

Figure 1.11: Generalized model for proglacial thrusting and subglacial modification of the thrusts during ice advance. (a) Initial proglacial thrusting (b) Building ice-marginal composite ridge, (c) Overriding and smoothing cupola hill. From Aber and Ber, (2011).

The factors that favor glaciotectonic disturbance are: (i) the slope of the proglacial area where ice advance is against a topographic obstacle, (ii) the presence of weak subsurface layers or decollement planes enhancing failure (iii) the nature of ice/sediment contact in the proglacial area, where partial burial of the glacier prior to advance would lead to lifting of sedimentary strata underneath (mega blocks) and (iv) subglacial and proglacial drainage, as failure is encouraged by high porewater pressure in proglacial and submarginal sediments and rocks (Aber et al. 1989).

There are various glaciotectonic and erosional features documented in SW Barents Sea (Andreassen et al. 2004; Rafaelsen et al. 2002; Rafaelsen et al. 2007; Winsborrow et al. 2010). Glacial groves which are linear depressions, centimeters to meters in length produced by removal of rock or sediments by erosive action of glacier (Dobhal, 2011) are also common on the seafloor in the study area. Megascale glacial lineations (MSGL) occur on the seafloor as well as on the subsurface in the study area (Andreassen et al. 2004; Rafaelsen et al. 2002; Andreassen and Winsborrow 2009). Deryabin, (2012) have reported glaciotectonic features along with its relationship with fluid flow migration and shallow gas accumulations from SW Barents Sea.

1.7 Hydrocarbon Migration and accumulation

The generation and accumulation of hydrocarbons in the subsurface is a long and complex geological process. For the presence of hydrocarbons a working petroleum system is mandatory. A working petroleum system consists of the following geological elements and processes:

1. Mature Source rock

The source rock contains the organic matter called Kerogen which when subjected to burial and heat (thermal maturation) for sufficient amount of time will produce oil and gas. Organic shales are the most common type of source rocks.

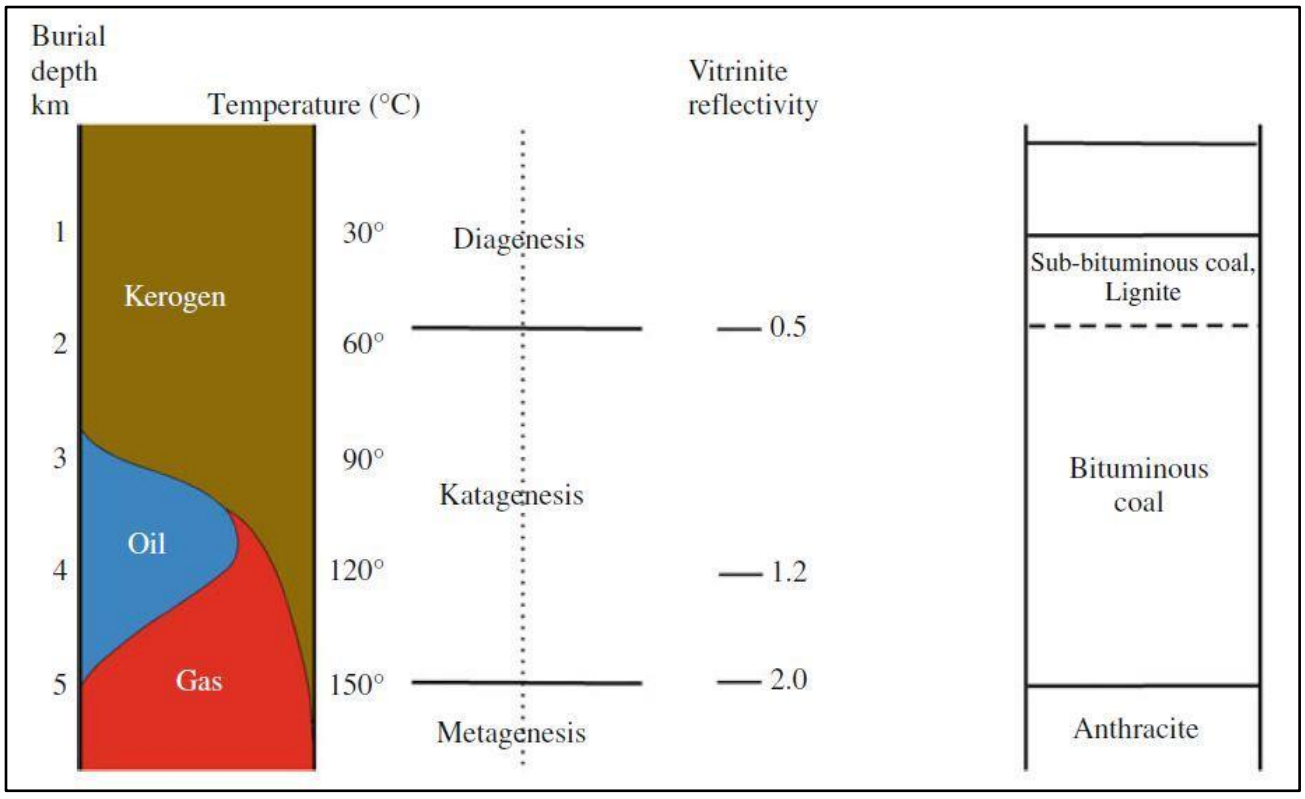

Figure 1.12: The source rock maturation is function of temperature and burial depth which can be measured as vitrinite reflectivity. Maturation is also function of time. The oil and gas window can be determined provided temperature and depth are known. From Bjørlykke (2010).

The source rocks in the Barents Sea ranges from upper Devonian-Lower Carboniferous, and Upper Permian to Upper Triassic shales (www.npd.no). Source rocks ranging from Carboniferous to Cretaceous in the Barents Sea region have been reported (Henriksen et al. 2011, b; Ohm et al. 2008).

2. Reservoir rock

The reservoir rocks should be porous enough to hold the hydrocarbons within it as well as permeable enough to allow the movement of hydrocarbons in it. Common reservoir rocks are sandstones and carbonates. The Triassic sandstones in the Sassendalen Group of both continental and marine environment act as a reservoir rock in the study area

3. Cap rock

Cap rock should be impermeable in order to seal the top of reservoir so that any hydrocarbons may not leak out of the reservoir rock. Common types of sealing lithologies are shales and evaporites. Cap rocks cannot be found at various stratigraphic levels in Barents Sea (Fig. 1.4).

4. Traps

Trap is a set of geological conditions that helps in accumulation of hydrocarbons. The trap can be structural, stratigraphic or combinations of both. In the Barents Sea both types of traps exists. The traps are mainly stratigraphic with structural rotated fault blocks (Henriksen et al. 2011, b).

5. Migration

In order for hydrocarbons to accumulate within the reservoir in a trap, the hydrocarbons should migrate from the source to reservoir. The main driving force for hydrocarbon migration is buoyancy, hydrodynamics and overpressure (Selley, 1998; Judd and Hovland, 2007). The term primary migration used is for the expulsion of hydrocarbons from the source rock whereas secondary migration refers to movement of hydrocarbons onward once it is out of the source rocks. The hydrocarbons continue to migrate updip via permeable rocks, fractures and faults until encountered by a trap. If the sealing lithologies fail, the hydrocarbons may escape further upward into surface or into another trap (Fig. 1.13).

Hydrocarbon gas can be generated either during digenesis by methanogenic bacteria at around 50^{o} C or during catagenesis which refers to the thermogenic generation of gas above 50^{o} C till 150^{o} C. The gas that is generated after 150 ^{o}C, the process is referred to as Metagenesis (Fig. 1.12). Most of the source rocks started to generate oil in the deepest basins by Middle Triassic and reached high level of maturity by Early Cretaceous. The source rocks are in post-

mature state in most of the Barents Sea areas except some structural highs (Henriksen et al. 2011, b).

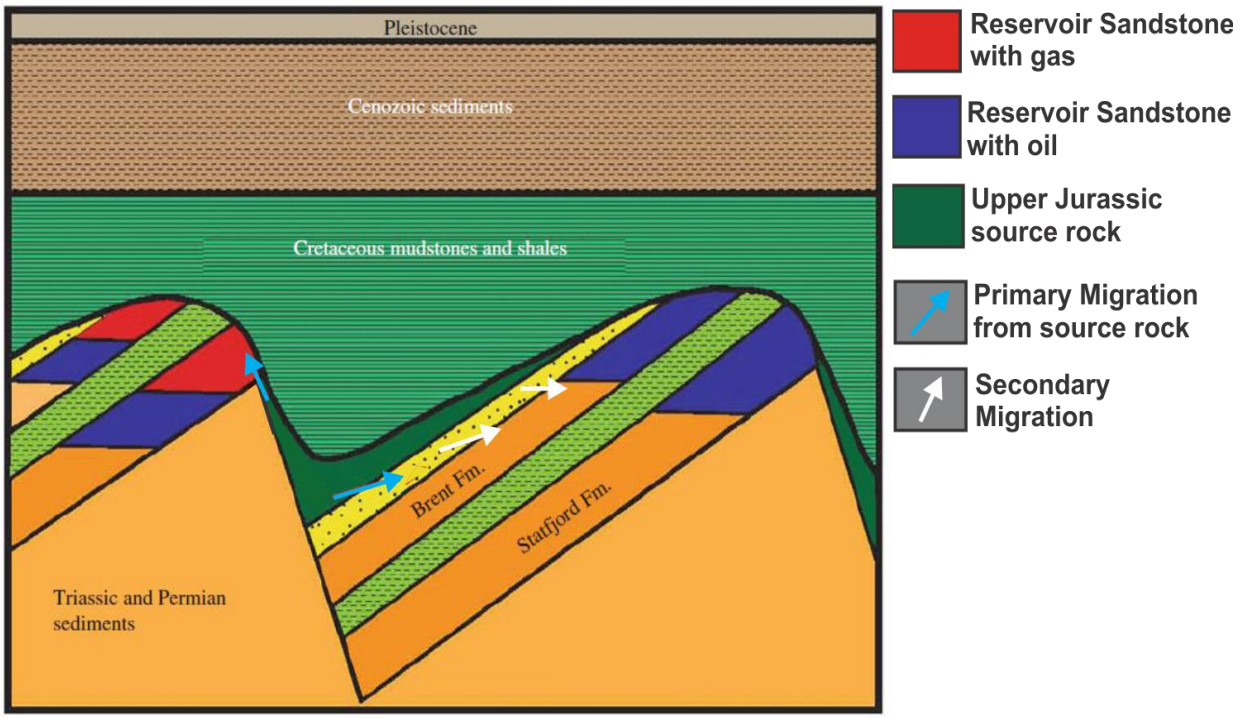

Figure 1.13: Graphic illustration of primary migration (indicated by cyan arrow) from upper Jurassic source rock into reservoir sandstone from North Sea. Secondary migration of oil (marked by white arrows) via the yellow sandstone carrier bed can also be observed. (Modified after Bjørlykke 2010)

The rate of fluid flow within a reservoir rock is determined by Darcy's Law which states that the amount of fluid flow in a medium depends on its permeability and the pressure difference between two ends of the system. The fluid will flow until it is encountered by an impermeable medium which will seal the fluid flow, in such cases the fluid will flow again if the sealing lithology fails due to overpressure forming a seal bypass system in form of fractures, faults, intrusions or gas chimneys (Cartwright et al. 2007).

Presence of gas in SW Barents Sea has also been reported by Andreassen et al. (2007a). The hydrocarbons can be detected in seismic data by presence of bright spots, flat spots, phase reversals, velocity pull down and acoustic masking (Figure 1.14) which are referred to as direct

hydrocarbon indicators (DHI) (Sheriff, 2002). Bright spots are anomalously polarity reversed high amplitudes on top of gas (Andreassen et al. 2007a) (Fig 1.14 B).

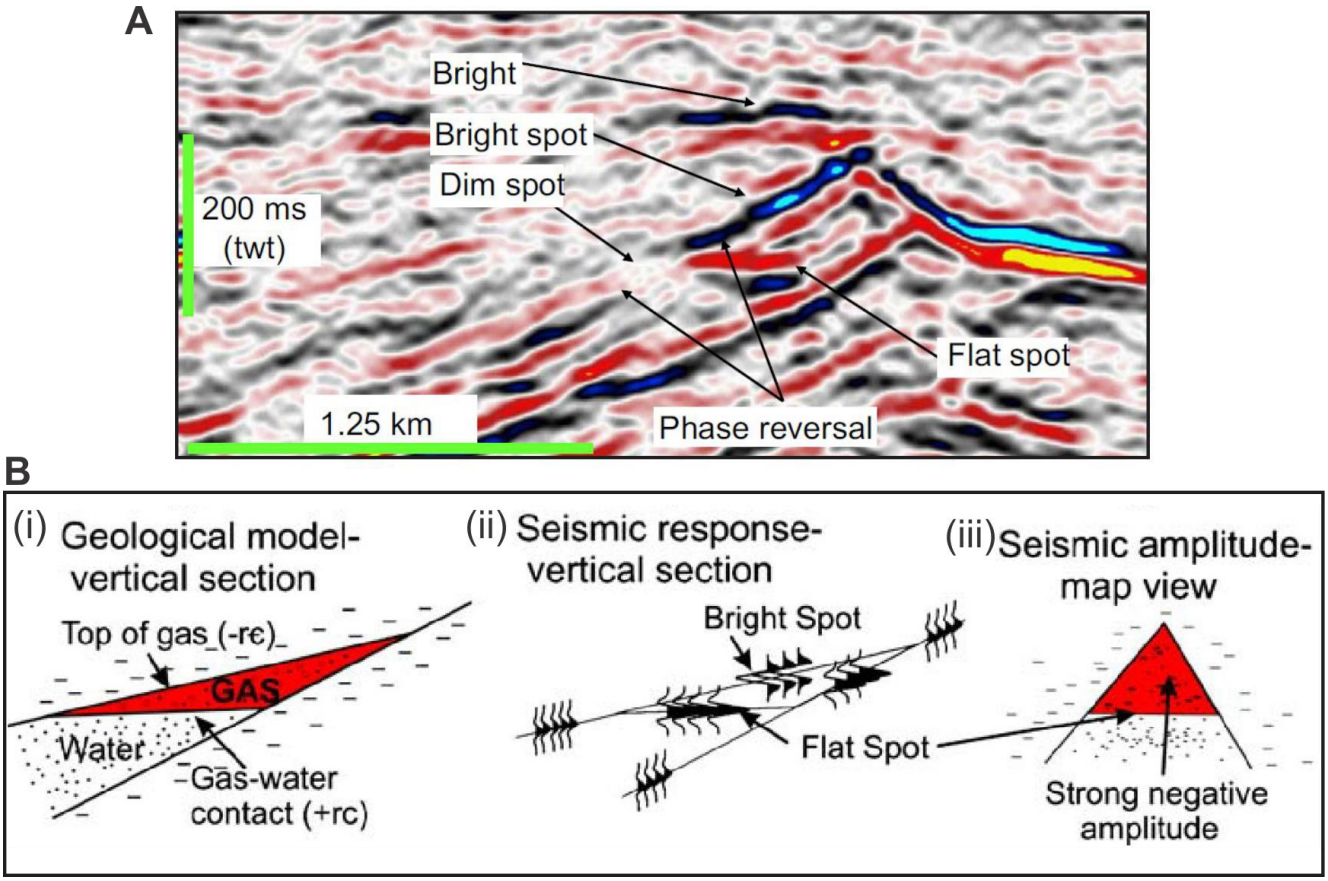

Figure 1.14 A) Appearance of direct hydrocarbons indicators such as bright spots, flat spot, dim spot and phase reversal on seismic section. From Løseth et al. (2009). B) Geological model and the seismic response to presence of hydrocarbons. From Andreassen et al. (2007a)

2 Data and Methods

2.1 Data Type

In the study following data was used:

- 3 Dimensional Seismic data.
- 2 Dimensional Seismic data.
- Bathymetric data

2.2 Seismic Data

Regional 2D lines (3.1 & 3.4) were used for regional profiles for a larger overview of the studied features and for correlation with published results. The total of six 3D surveys are used in this study (Fig. 2.1) amongst which NH0608 and SG9804 were available in the university database while ST10020 were provided by Statoil and HFCW11, HFC09 and HFCE11 by TGS.

ST10020 has coverage down to just below URU. The survey is located in Bjørnøyrenna Trough and covers about 800 Km^2, north of Loppa High. The data was acquired by Fugro-Geoteam AS in 2010. 2 airguns of 4200 cubic inches volume were used in the survey with a pressure of 2000 psi. The streamer length in the survey was 5.4 Km which consisted of 432 groups with 10 hydrophones on every group. The streamer was towed at 8 m below the water surface.

NH0608 is located over the northern tip of Nordkapp banken area (Fig. 2.1) and covers parts of south of Swaen Graben and Bjarmeland Platform. It was carried out for Norsk Hydro Production AS in 2006.

SG9804 is located on the tip of Nordkapp banken and covers approximately 990Km^2 which include parts of Swaen Graben, East Loppa high and West part of Bjarmeland Platform. The survey was carried out for Saga Petroleum ASA in 1998. The dominant frequency in the glacigenic part of the survey is about 40 Hz (Rafaelsen et al. 2002).

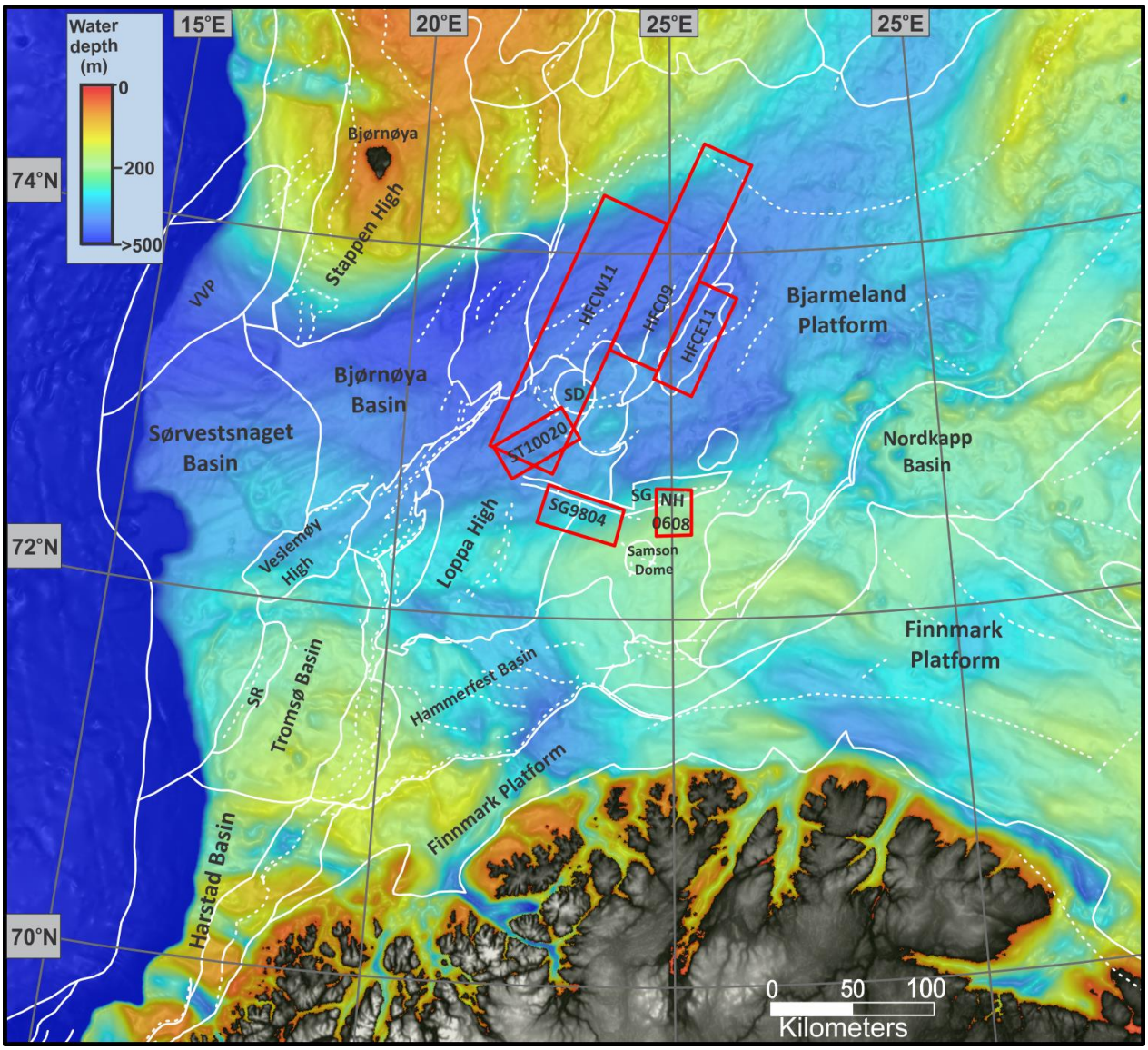

Figure 2.1: Main structural elements and fault boundaries (dashed lines) shape files from www.npd.no on IBCAO bathymetry raw data from Jackobssen et al. (2012) in study area. 3D surveys are marked by red rectangles. VH: Veslemøy High; VVP: Vestbakken Volcanic Province; SR: Senja Ridge; SG: Swaen Graben; SD: Svalis Dome.

2.3 Seismic Resolution

Seismic resolution is the ability to distinguish between two separate features on seismic data. The resolution in seismic data is both in vertical as well as horizontal direction since seismic waves travel vertically and spread spherically therefore the reflection across an acoustic impedance contrast is not just from a single point but from an area with some diameter.

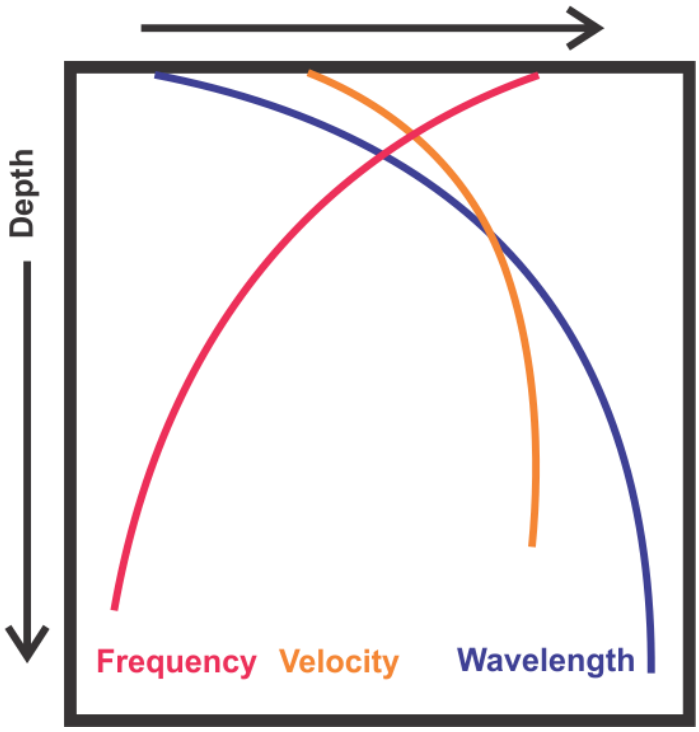

Figure 2.2 showing relationship between velocity, frequency and wavelength with increasing depth modified after Brown (1999).

Vertical resolution of a seismic data is a function of seismic interval velocity (v) and signal frequency (*f)* (Fig. 2.2). Vertical resolution of seismic data is 1/4 λ (Yilmaz, 1987) where λ is the dominant wavelength. Since λ=velocity/frequency the vertical resolution can also be calculated as follows:

Vertical Resolution= V/4*f.*

Generally the vertical resolution of seismic data decreases with increasing depth. This decrease is due to the fact that velocity increases with depth, whereas the higher frequencies are attenuated as seismic wave travels into the subsurface (Brown 2004).

Horizontal Resolution of seismic data is the minimum distance between two lateral features that can be identified separately. It is determined from the width of Fresnel Zone on unmigrated seismic section (Fig. 2.3). Fresnel zone is a function of velocity and frequency. It generally decreases with depth due to increase in velocity and decrease in frequency (Badley, 1985).

Fresnel zone is

$$rf = V/2 \ (t/f)^{1/2}$$

Where rf is the radius of the Fresnel zone, V is average velocity, t is two-way travel time and f is the dominant frequency in hertz. In 3D seismic surveys the Fresnel zone is reduced due to 3D migration techniques hence the horizontal resolution of 3D seismic data equals ***1/4 λ***.

The dominant frequency in the surveys NH0608, HFC and ST10020 is assumed to be 50 Hz (Andreassen, Karin, Comments) with a velocity of 1750 m/s in glacigenic sediments. The resolution calculated can be seen in table 1.

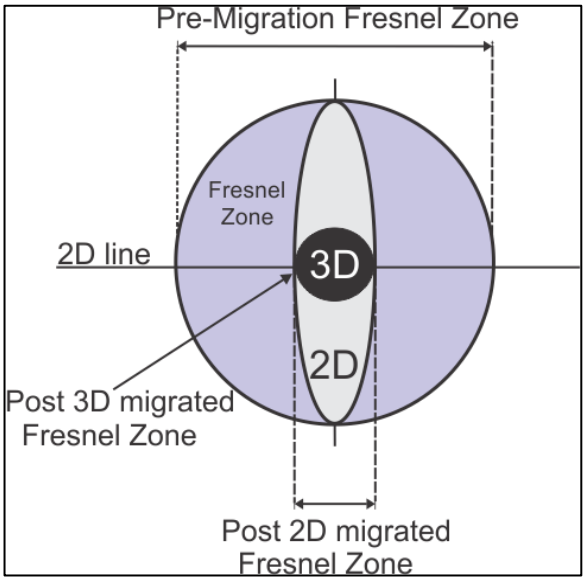

Figure 2.3 showing the size of Fresnel zone before migration and collapsed Fresnel zone after 2D and 3D migration, modified after Brown (2004).

Survey	Vertical Resolution	Horizontal Resolution
SG9804	10.94 m	10.94 m
NH0608	8.75 m	8.75 m
ST10020	8.75 m	8.75 m
HFC	8.75 m	8.75 m

Table 1: Vertical and Horizontal resolution for the surveys used in this study.

2.2 Bathymetric Data

Bathymetric data from International Bathymetric Chart of the Arctic Ocean (IBCAO) was used. The latest version 3.0 (Jakobsson et al. 2012) was downloaded from www.ibcao.org . The data is Digital Bathymetric Model (DBM) type compiled with all multibeam, dense single beam and land data added at 500 x 500m grid. The data is in Geographic Coordinate System with WGS 1984 as Horizontal and Mean Sea Level as vertical datum.

2.3 Artifacts

Artifacts in seismic data do not represent real structures and are either caused by seismic acquisition or seismic processing. The interpreter needs to be critical in analyzing seismic data so that any artifacts are not mistaken for real structures.

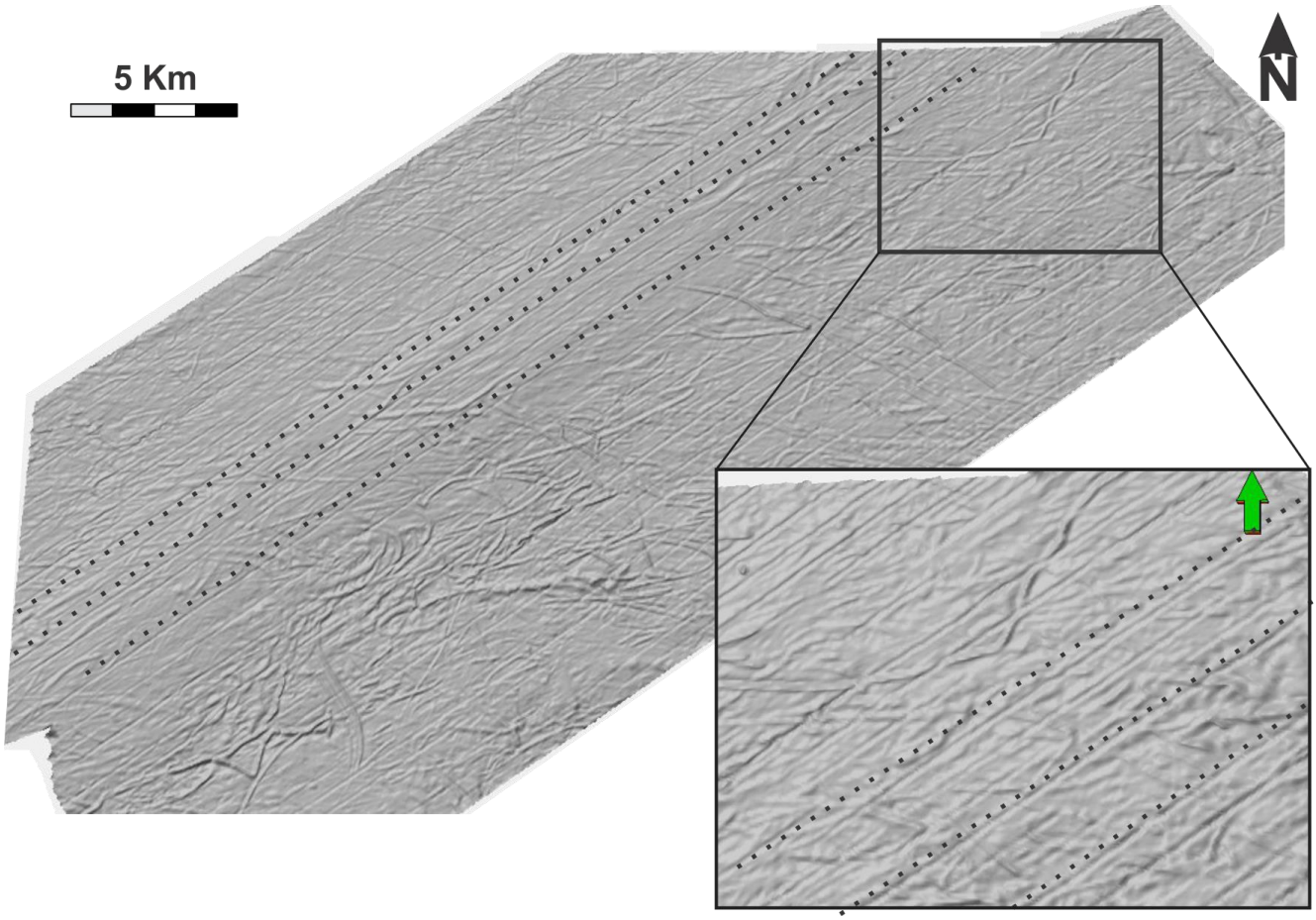

Figure 2.4: The inline acquisition footprints on seafloor surface from survey ST10020 parallel to inline as indicated by dotted black line, the zoomed view of the surface can be also seen in the figure.

The most common occurring artifact in 3D seismic surveys is the acquisition geometry footprint (Fig. 2.4) during acquisition described by Marfurt et al. (1998) as systematic noise

that correlates with the acquisition geometry. It is due to difference in towing depth of streamers or uneven geometry between inlines. It is easy to recognize the acquisition footprints on seismic data as one can easily see minor time shifts on seafloor image resulting in parallel ridges and grooves features (Bulat, 2005). The acquisition footprints (Fig.2.4) were present in all the surveys used in this study.

2.4 Interpretation tools

Various softwares that were used for interpretation and visualization of seismic and bathymetric data, as well as making figures are listed as follows:

- Schlumberger Petrel 2011.2
- ESRI Arc Map v10.0
- CorelDraw X5

Schlumberger Petrel 2011.2 seismic-to-simulation software was used for interpreting and visualizing seismic data. The software was run on a 64-bit operating workstation provided by the institute of Geology, University of Tromsø. Seismic data can be visualized and interpreted in 2D and 3D views by using various attributes for understanding and enhancing the features present in the data.

ESRI Arc Map v10.0 is a part of Arc GIS software suite. The program was used for generating bathymetric images from the IBCAO bathymetry data. The software was also run on 64-bit operating workstation. Different layers like slope map, water depth map and elevation above sea level map were overlaid for enhancing the features in it. The software was also used for digitizing and georeferencing images and results from previous publications.

2.5 3D Seismic Attributes

Seismic attributes not only enhances the geological features but also aid in identifying them. The attributes used during this study are volume based and were used on whole seismic cube as well as in predefined window.

Structural Smoothing

The structural smoothing volumetric attribute performs smoothing on the 3D cube by the application of the Gaussian weighted average filter. It smooths the seismic reflections and enhances its continuity as well as improves signal to noise ratio (Fig 2.5 B). Hence this volumetric attribute aids in interpretation of the reflectors.

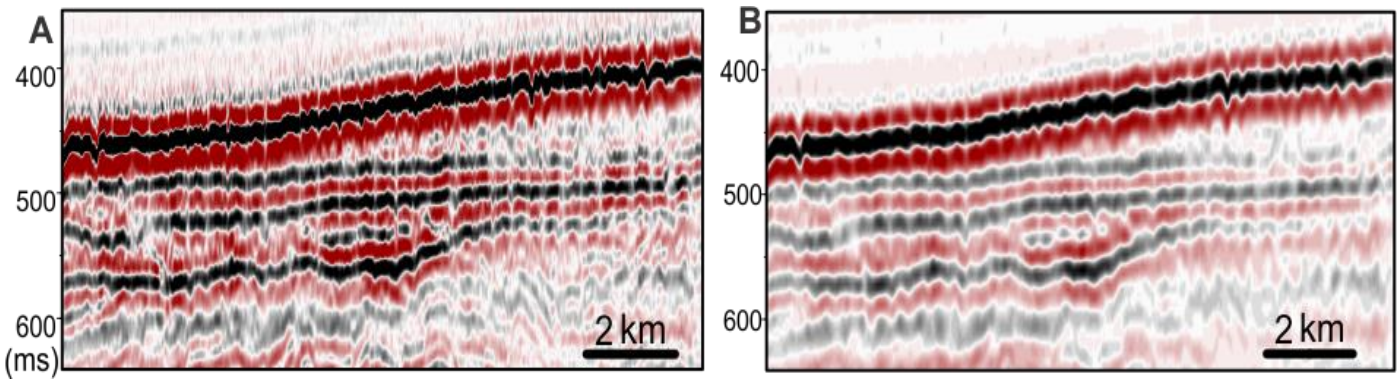

Figure 2.5: A) Normal seismic section before structural smoothing B) Seismic section after structural smoothing from the survey SG9804

Variance Attribute

The variance volumetric attribute (Fig. 2.6 B) is an edge detection method which estimates the local variance in the signal. The parameters for variance cube which can be changed are inline and crossline range as well as vertical smoothing in range of 0-200 milliseconds. The volumetric attribute was here used to enhance geological features like faults and channels.

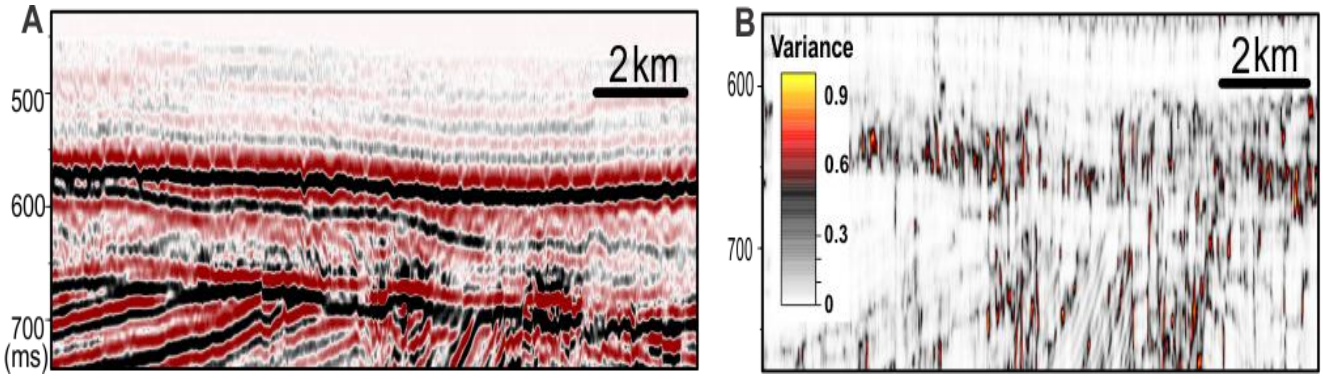

Figure 2.6: A) Normal Seismic section from a seismic cube. B) Seismic section from a variance cube from the survey ST10020

Root Mean Square (RMS) Amplitude

RMS Amplitude computes the Root Mean Squares on an instantaneous trace samples over a specified window (Petrel 2010). The RMS attribute is performed on a surface and a volume can be given either to scan traces above or below the given surface. It is a useful attribute for identification of geological features like channels, gas accumulations and isolated sediment blocks

3 Results

The main focus of this study was to study the ice stream dynamics on the Barents Sea shelf and glacio-tectonic features. Other aspect of the study was also to find if there is any relationship between erosion and fluid flow migration. To meet the required objective, key horizons were interpreted in the glacigenic part of the study area but only the horizons that have the features of interest will be documented. Before documenting the results from these horizons, a brief introduction will be given to the stratigraphy in the study area. The horizons will then be documented in their respective relative chronological order starting from the youngest (seafloor) to the oldest (URU).

3.1 Relative Stratigraphic Correlation in the study area.

The study area (Fig. 2.1) is located on formerly glaciated southern Barents Sea shelf (Andreassen et al. 2004m 2007b, 2008; Vorren et al. 1988; Rafaelsen et al. 2002). There is a thin glacigenic sediments package on the continental shelf area with the thickness varying between 0-300 m (Vorren et al. 2011). The surveys SG9804 and NH0608 are located on the Nordkappbanken area (Fig. 2.3 & 3.1) whereas the surveys ST10020, HFC09, HFCE11 and HFCW11 are located in the Bjørnøyrenna (Bear Island Trough) (Fig. 3.1 & 2.1).

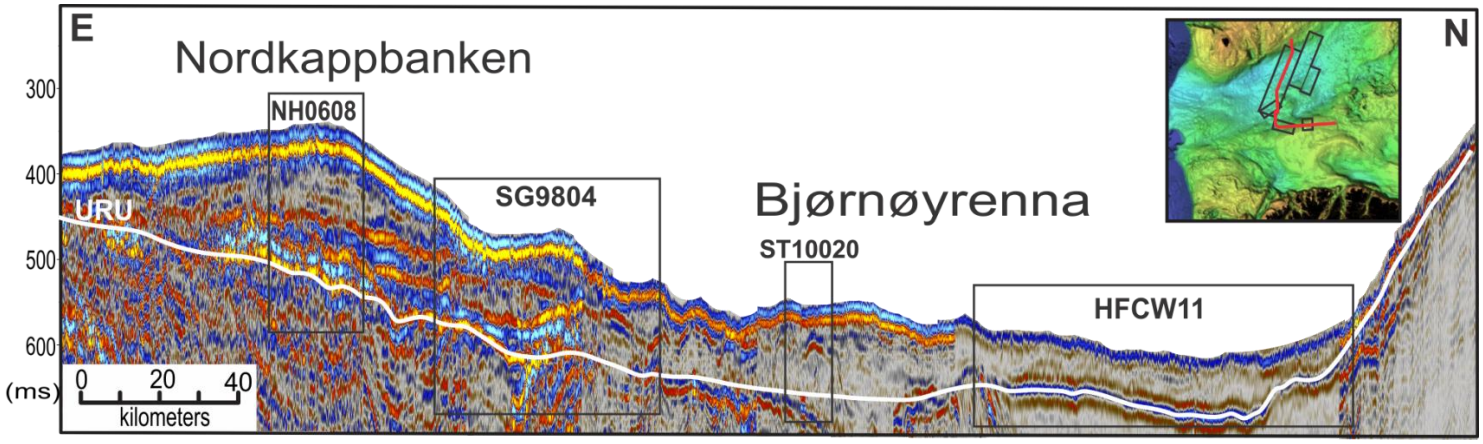

Figure 3.1: 2D composite seismic line showing the location of surveys. URU (upper regional unconformity is marked by white line. Location of composite line can be seen in top right figure marked by red line.

There is no chronology available from any well data over the seismic surveys used in this study; however chronology from surrounding areas had been used in some of the previous study over the area (Rafaelsen et al. 2002, Sættem et al. 1992a, Mattingsdal, 2008). A shallow

borehole (7222/09-U-01), which is located close to the survey SG9804, has been correlated to 2D seismic data (Sættem et al. 1992a; Hald et al. 1990). This work has been used as the basis for the correlation of 3D survey SG9804 by Rafaelsen et al. (2002) which is further extended in to the surrounding 3D surveys where possible in this study.

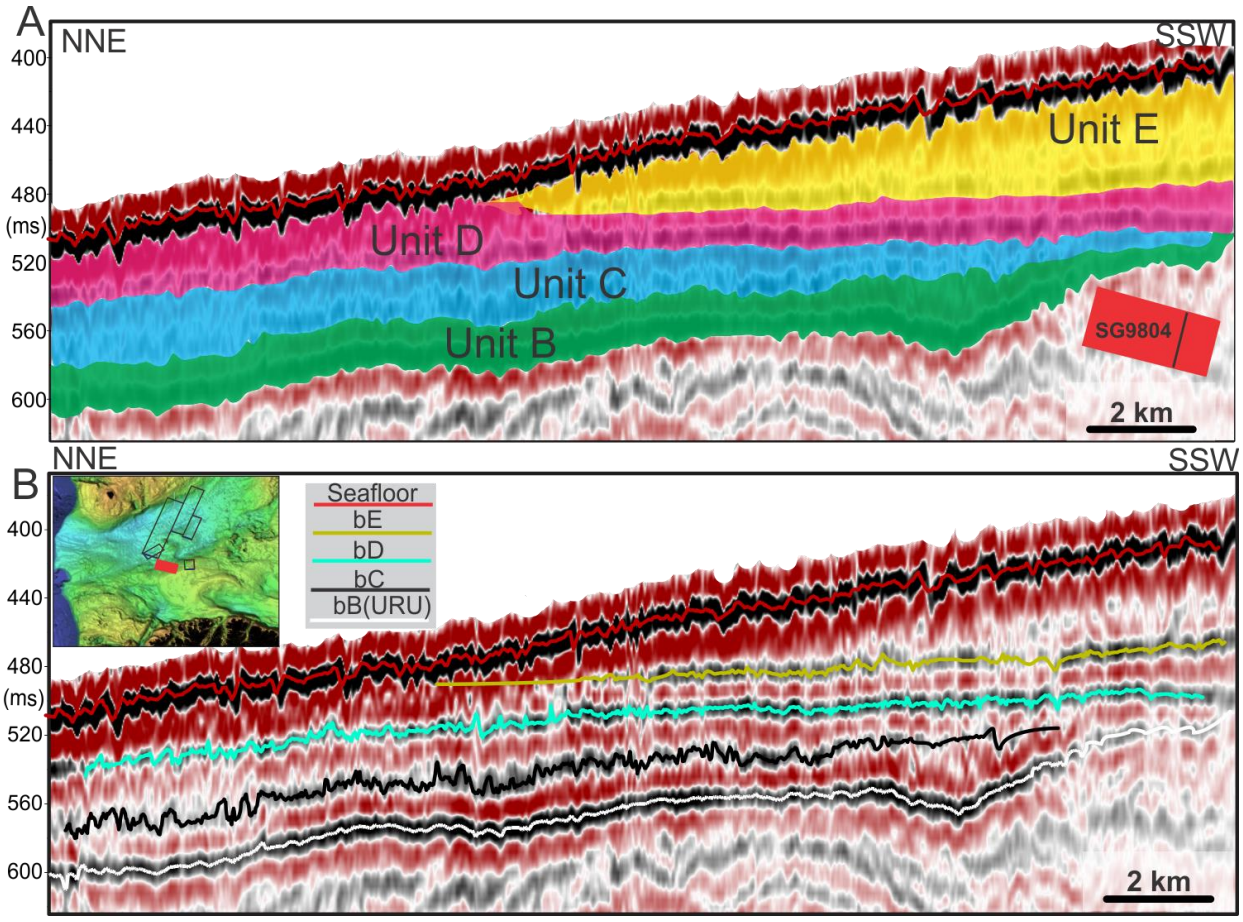

Figure 3.2: Stratigraphy from 3D survey SG9804. A) Interpreted stratigraphic units. B) Interpreted seismic horizons within the survey SG9804. The location of seismic line and survey (marked by red rectangle) can be seen in the inlet figure in A and B respectively.

SG9804 is also used in this study and all the surfaces (bE, bD, bC and bB (URU)) described by Rafaelsen et al. (2002) are interpreted (Fig. 3.2). Based on 2D seismic data and shallow borehole data (7222/09-U-01), relative age relationship in this survey can be found in the table 2 and 3.

The horizons from SG9804 are correlated to NH0608 using 2D lines (Fig. 3.4). The horizons interpreted in the subsurface in the survey NH0608 are bE, bD and URU (Fig. 3.3). bE corresponds to the upper surface of the outer Bjørnøyrenna sedimentary wedge (obsw-01)

of Ruther et al. (2009) which is dated to radiocarbon ages ranging from 17,090 to16, 580 cal yrs BP. This surface corresponds to horizon bE in the survey SG9804 which is inferred to have a date of 18 ka (Rafaelsen et al. 2002). In this study, the age assigned by Ruther et al. (2009) to bE is used, since it specifically targeted the Bjørnøyrenna sedimentary wedge.

The horizons in the surveys of ST10020 and HFC cannot be correlated to these surfaces however, based on 2D regional lines these, the horizons in these surveys should be relatively younger (less than 17ka) than the horizon bE and obsw_01.

Horizons/units	**Units in Sættem et al. (1992a)**	**Corresponding ages and their units**	
E	b5	5E	22-18 ka (Vorren et al. 1989, 1990)
bE			
D	b4	4E	c. 28 ka (Vorren et al. 1989, 1990)
		B4	<27320 ^{14}C years BP (Hald et al. 1990)
		I	Solheim & Kristoffersen (1984)
bD			
C	b2?	D_2	200-120 ka (Sættem et al. 1992b)
bC			
B			
bB			
A	b1		Younger than URU (< c. 800 ka)

Table 2: Relationship between the present seismo-stratigraphic units defined from 3D data and earlier work based on 2D seismic data. Modified from Rafaelsen et al. 2002.

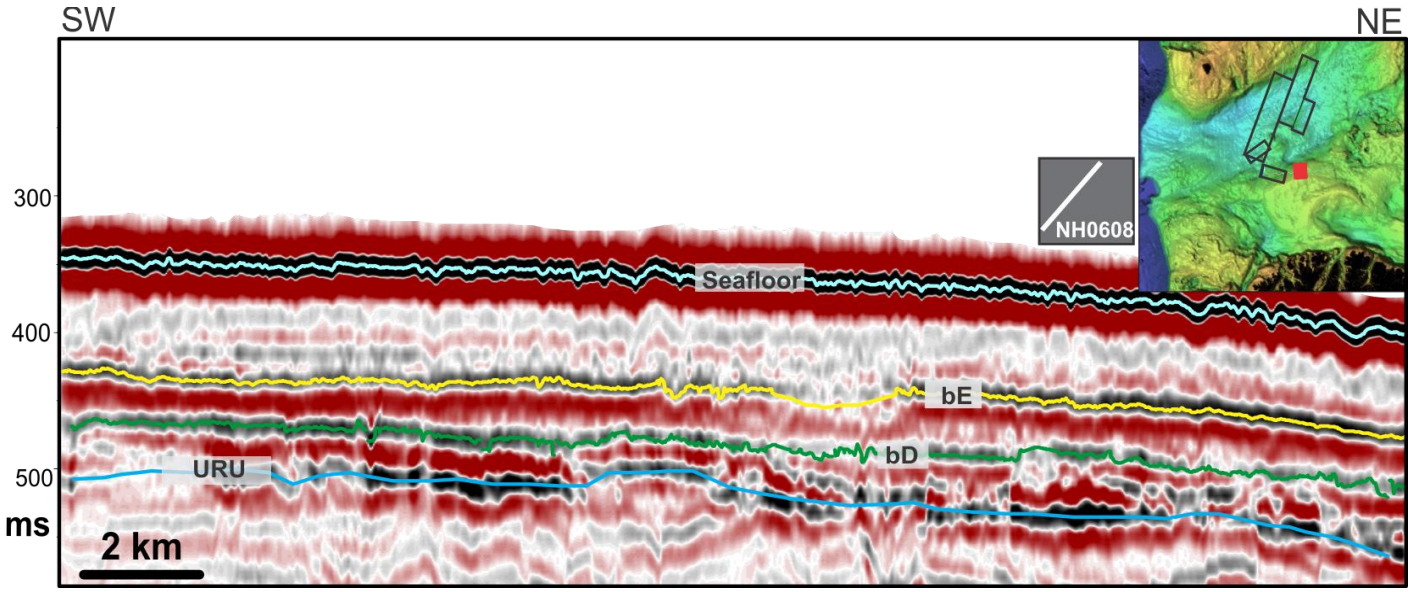

Figure3.3: Seismic profile across survey NH608 showing stratigraphy within the survey. The location of the line and survey (marked by red rectangle) can be seen in the inlet figure.

The horizon *bE* and *bD* from the survey SG9804 can be well correlated to horizon *obsw_01* and *obsw_02* respectively in the survey NH0608 using 2D line (Fig. 3.4).

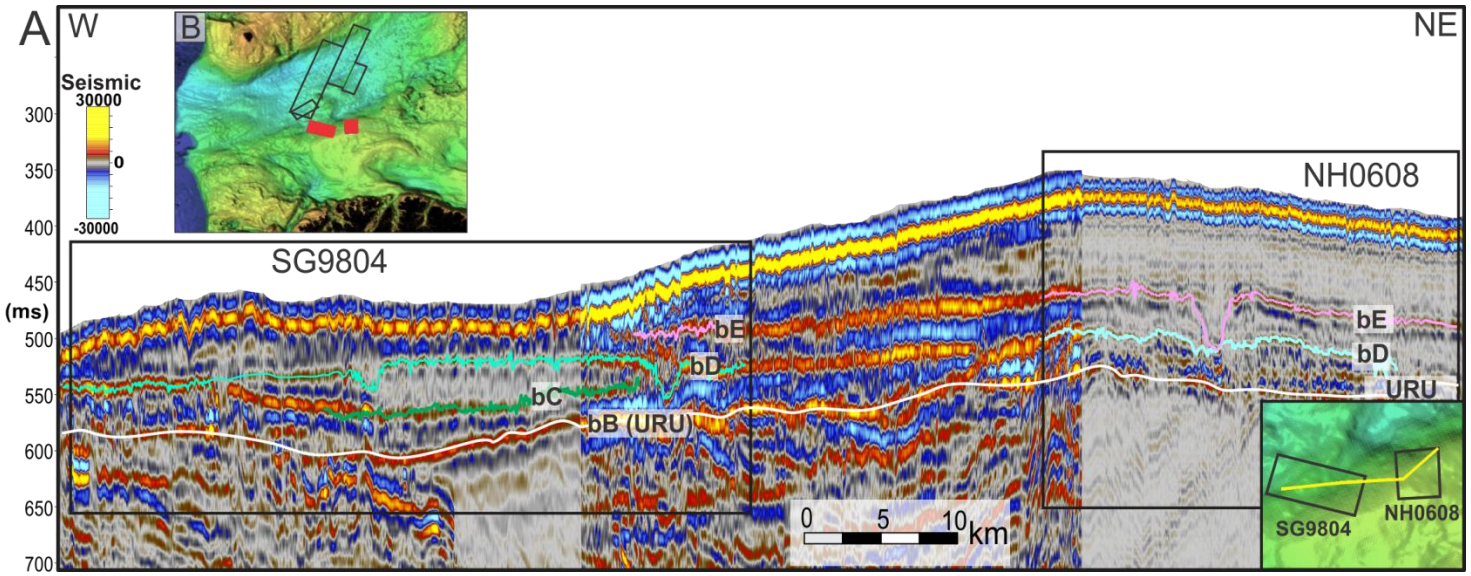

Figure 3.4: A) Composite seismic profile across survey NH608 and SG9804 showing stratigraphy within the survey. B) Location of the survey SG9804 and NH0608.The location of composite line can be seen in the inlet bottom right figure.

Based on 2D regional lines and previous work (Sættem et al. 1992 b; Rafaelsen et al. 2002; Ruther et al. 2009), the relative correlation is established in the following table:

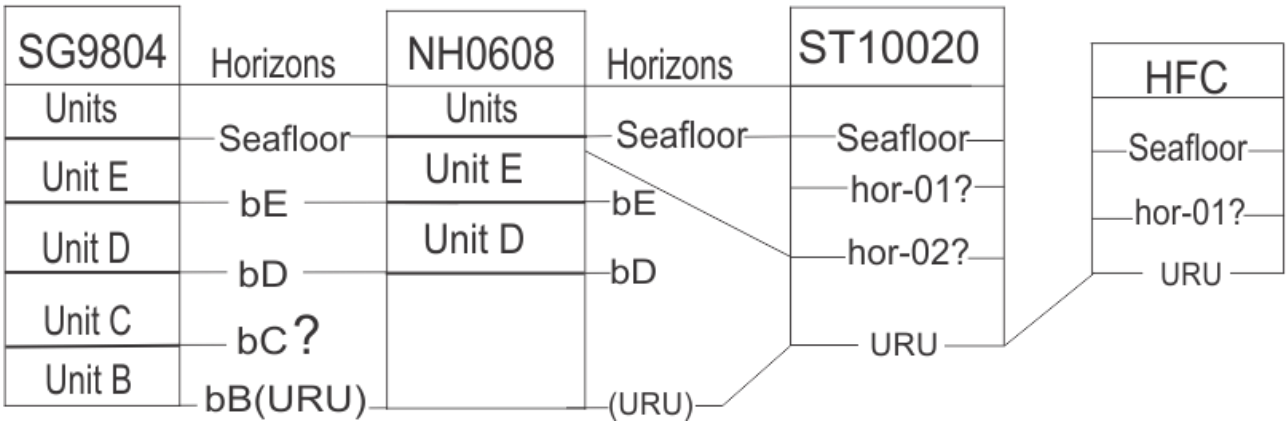

Table 3: Relative correlation in the study areas. The subsurface horizons (hor-01 & 02) in survey ST10020 are inferred to be relatively younger than horizon bE in the survey SG9804. Hor01 in HFC survey seems to be youngest of all in the subsurface horizons interpreted over the study area.

3.2 Common Morphological Elements on the seafloor in the study area.

An introduction will be given in this section to the elements that occur commonly on seafloor in study area in this section. Some of these elements can be seen on IBCAO bathymetry (Fig.3.5) and are mapped by Winsborrow et al. (2009). Some of these features like megascale glacial lineations and ice berg scour marks occur on subsurface horizons as well and will be covered in detail.

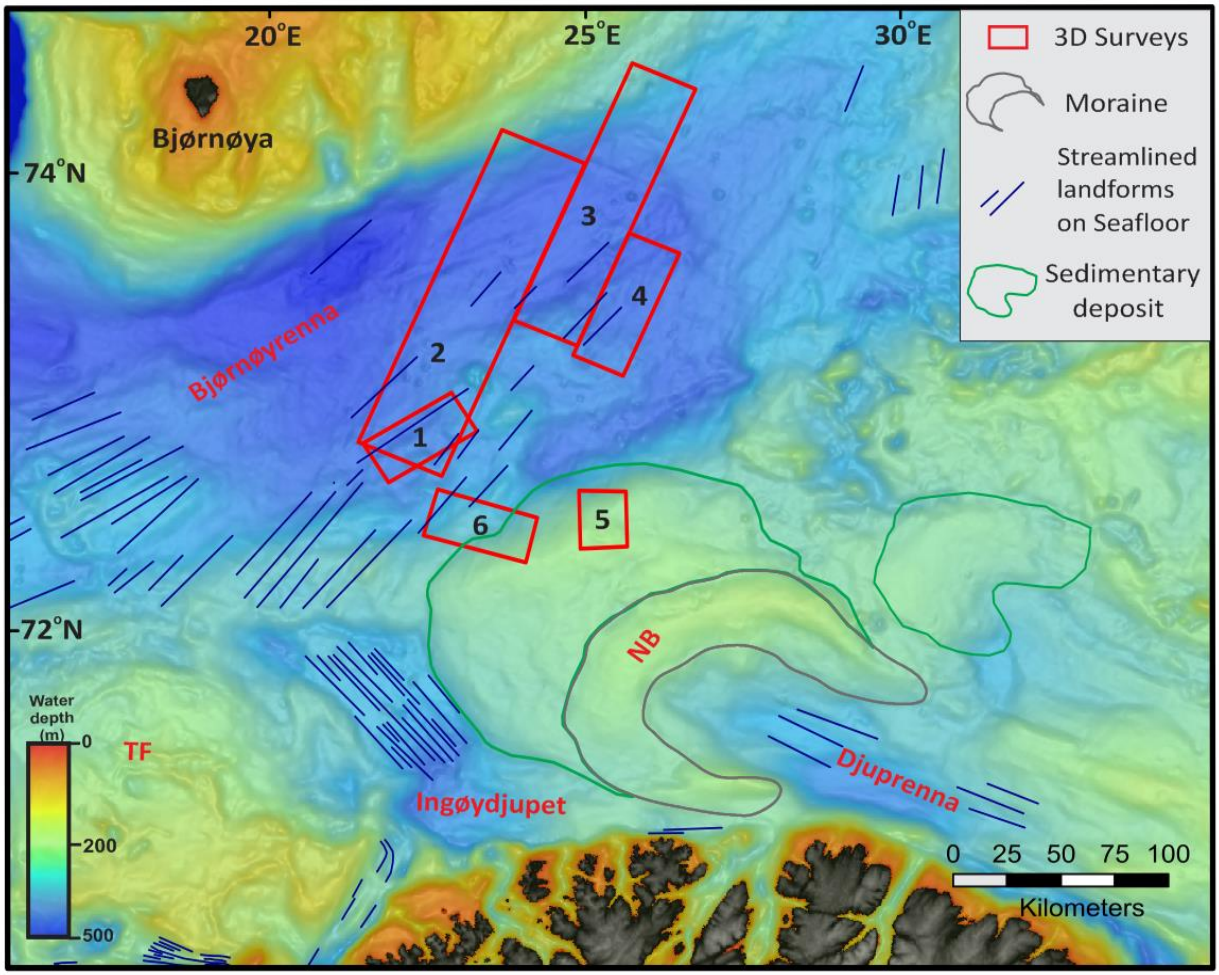

Figure 3.5: Large scale IBCAO bathymetry map (raw data from Jackobssen et al. 2012). Large scale landforms of the seabed can be seen in the map (shapefiles from Winsborrow et al. 2009). NB: Nordkapp Banken; TF: Tromsøflaket. 1: ST10020, 2: HFCW11, 3: HFC09, 4: HFCE06, 5: NH0608, 6: SG9804.

3.2.1 Ice berg plough marks

Description of elongated curved furrows

On all of the seafloor horizons in in the study area, curvilinear furrows with random to preferred orientation occur widely in the study area (e.g., Fig. 3.6 & 3.15). The furrows vary in depth, width and length. The distance between the furrows varies as well. Some of these furrows run relatively straight but most of these features tend to curve and show a random orientation (Fig. 3.6 & 3.7).

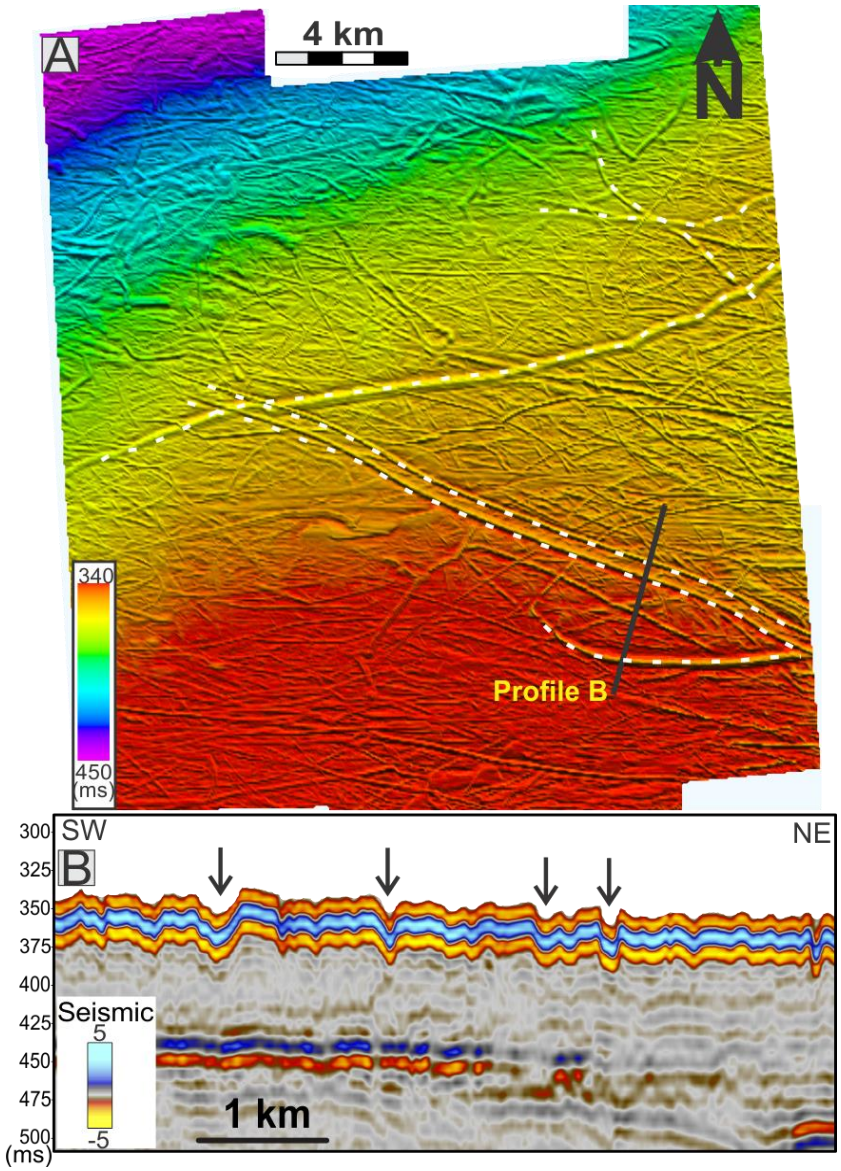

Figure 3.6: A) shaded relief time-map showing dense occurrence of elongated curved furrows from the survey NH0608 seafloor. B) Seismic profile across the furrows

The length varies from a few of hundred meters to more than 40 km in the survey HFC and 22 km in the surveys NH0608 and SG9804. NH0608 may have even longer length as the furrows is likely to continue further out of the survey. The width of these features varies from few meters to 360 m wide with some reaching up to 470 m. The relief varies from a few meters to 13 m with some up to 24 m (velocity of 1470 m/s in water). Both the width and depth within one particular furrow can vary considerably. They are either U or V shaped in cross profile with well-developed levees on the sides (Fig. 3.6 B). Some of these furrows overprint each other while some run parallel in pairs close to each other (Fig. 3.7 B).

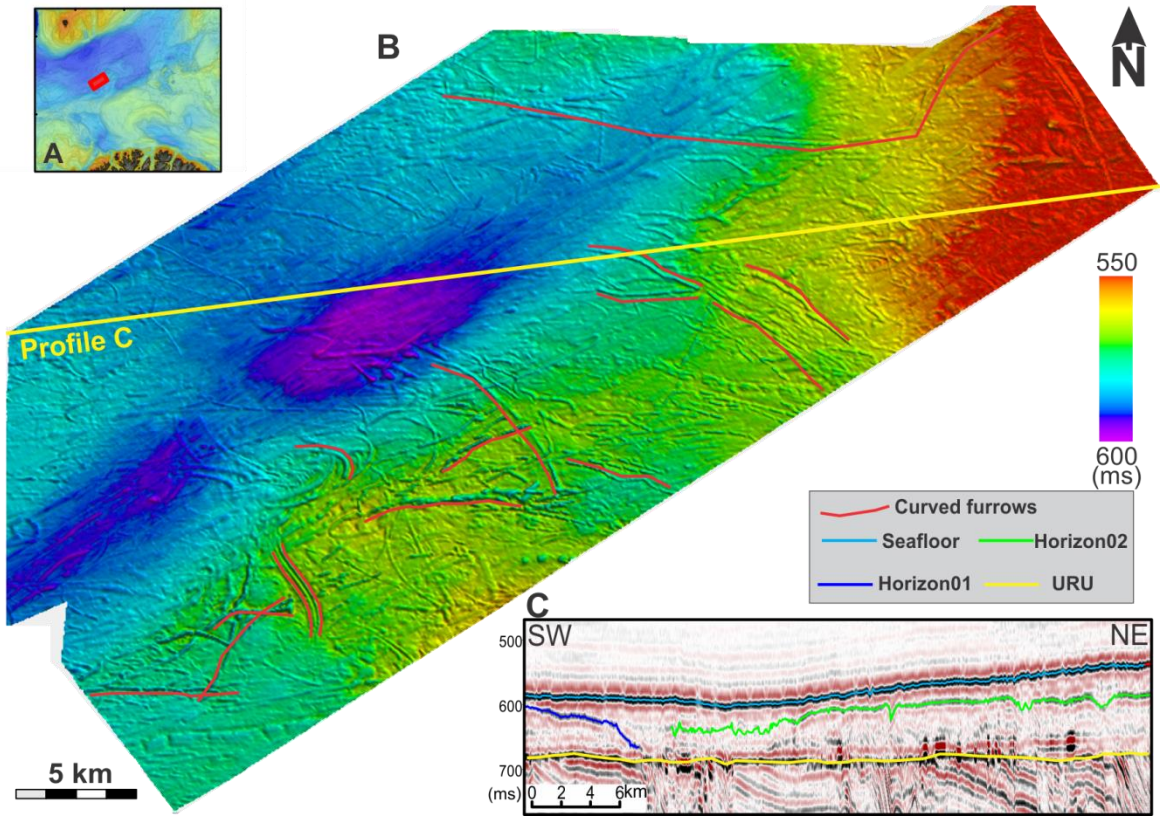

Figure 3.7: A) Location of ST10020 B) Shaded relief time- map of the seafloor horizon from ST10020 survey showing random distribution of furrows. C) Seismic profile across the survey showing the horizons interpreted in the survey.

Generally the furrows have a denser distribution in the shallow parts of the surveys compared to the deeper parts of the seafloor; however this does not apply the survey NH0608, where the entire surface has dense impressions of these elongated curved furrows.

In the survey HFC, these features do not occur widely and only a few of these features can be observed on shaded relief time-map of the seafloor. At places the furrows seems to run parallel with each other (e.g., Fig. 3.6 A). In general these furrows are abundant on Nordkapp banken area compared to the Bjørnøyrenna (Bear Island Trough). Also, the furrows that occur on HFC surveys in the Bjørnøyrenna trough are relatively longer that observed on Nordkappbanken.

Interpretation of elongated curved furrows

The curvilinear features on the seafloor as well some on some of the sub-surfaces are interpreted to be ice berg scours (Fig. 3.8) or plough marks produced by the scouring of the seafloor by ice bergs in submarine conditions (Stoker and Long, 1984). Scouring of the seafloor by icebergs is a common feature in front of marine glaciers and the ice bergs can be dragged over long distances by currents before they melt completely leaving its impression on the seafloor (Barnes and Lien 1987; Dowdeswell et al. 1993; Andreassen et al. 2008). The water depth for the occurrence of ice bergs furrows varies in the range of 100-550 m (Woodworth and Dowdeswell 1994) but these are also reported from Yermak Plateau where water depth is 850 m (Dowdeswell and Bamber, 2007).

The presence of such features is characteristic for glacio-marine environment and has been reported widely from the Barents Sea (e.g., Winsborrow et al 2010; Andreassen et al. 2008, 2007, b; 2008, Rafaelsen et al. 2002; Deryabin, 2012; Mattingsdal, 2008). The source of the ice bergs can be the terminus of large ice sheets during the major deglaciation, in this during the Last Glacial Maximum (Dowdeswell and Bamber, 2007).

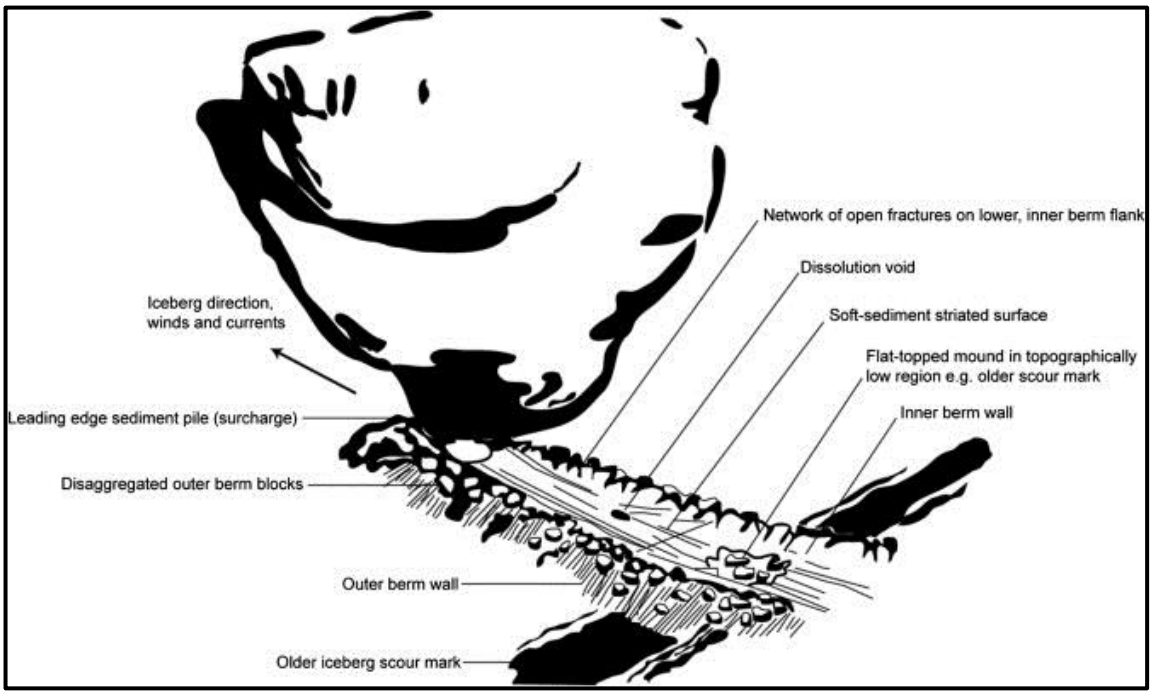

Figure 3.8: Diagram representing typical features of continental ice berg scour mark from Linch et al. (2012) (modified from Woodworth-Lynas and Dowdeswell, 1994).

The water depth in the study area ranges from about 230 m to 480 m which is well within the typical values for occurrence of ice berg furrows. The common occurrence of ice berg furrows on Nordkappbanken area can be attributed to the shallow water depth of about 230 m to 400 m. The dense appearance of furrows on the survey NH0608 is also due to the shallower water depth (about 230-340 m) compared with other surveys. However, the possibility of these areas being closer to the terminus of the ice sheet where a lot of the ice bergs may be produce and get detached cannot be ruled out. The fewer occurrences of these furrows in the HFC surveys can be accounted either for its deeper water depth (about 800 m) or these may had been produced but as it is the main trough where ice streams had been operating may have eroded these features. The larger length values of the furrows in HFC surveys indicate that the ice bergs were either large, transported over long distances by strong currents, the sediments in the area were easy to erode and or combination of all of these.

The furrows that run parallel can be part of the ice bergs with multi keels (Rafaelsen et al. 2002). The furrows with large values of relief, width and length may be indicative of large sizes of the ice bergs in addition to the nature of sediments, soft sediments will be more easily

penetrated and eroded by the ice bergs than the hard ones. The overprinting of these features suggests that multiple ice bergs operated at different times in the study area overprinting the older furrows.

3.2.2 Array of elongated curved Furrows in the survey SG9804

Description of elongated curved furrows

An array of wide furrows (Fig. 3.9 A) with well-developed ridges on the sides, on the western side of survey SG9804 can be observed on seabed. These ridges extend to approx. 10 km from north to south. The width if the furrows vary from few hundred of meters up to 1 km. At the terminal point of the furrows, curved ridges are formed. Parallel set of furrows at the west side of these furrows can be observed, terminating against the ridges (Fig. 3.9 A & B). The ridges have a steep side on the west side and more gentle slopes can be observed towards the east (Fig. 3.9, C).

The ridges as measured from bottom to top are about 7-18 m higher than the seabed (assuming velocity of 1470 m/s). Small ridges within the large furrow (Fig. 3.9E) can be observed, before terminating against a higher ridge towards the east.

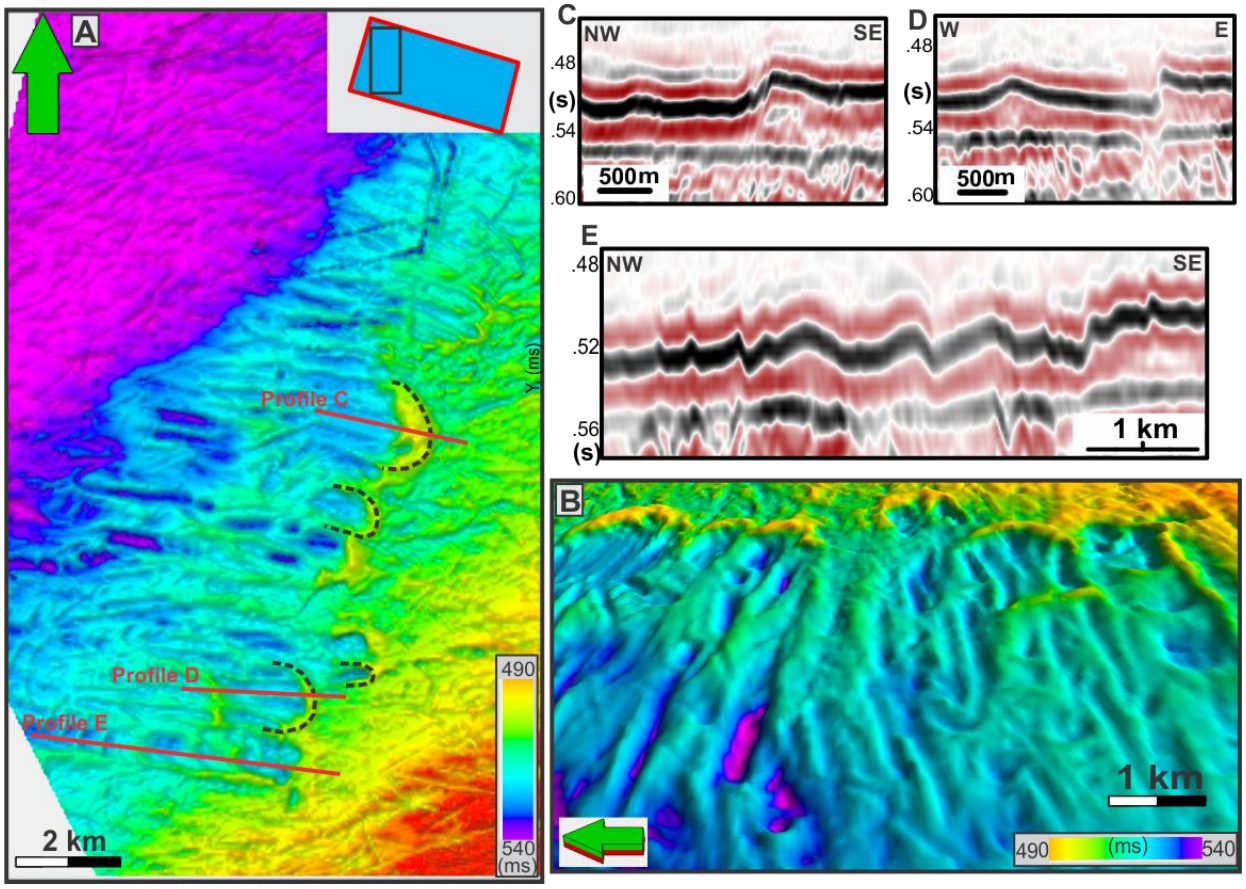

Figure 3.9: (A) shaded relief time-map from western part of the survey SG9804 as indicated by black rectangle in top right of the image. (B) 3D View of the furrows and ridges from west with10x vertical exaggeration. C), D) & E) Seismic profiles across the ridges

Interpretation of elongated curved furrows

The furrows observed before the ridges are similar in morphology to the furrows described in section 3.2.1 and hence are interpreted to be ice berg plough marks. The wider width can be accounted to an ice berg with a tabular base (Lien et al. 1989). The ridges occur at the terminal point of these furrows which may indicate that large ice bergs have been moving from east to west, this is further supported by the fact that these furrows have a steeper slope on the western side (Fig.3.9C & D). The movement of these icebergs may have been hindered by the sediments on the seafloor. As the currents acted on these ice bergs, the sediments were pushed by it creating these ridges. The smaller ridges within the plough marks (Fig. 3.9 E) may have been formed due to the dragging of ice bergs against the sediments on the seafloor.

3.2.3 Megascale glacial Lineations

Description of parallel ridges and grooves (lineations)

Large parallel grooves and ridges (lineations) (Fig. 3.10 A) can be observed in the surveys in main Bjørnøyrenna trough i-e HFCW11, HFCE11 and HFC09 as well as on some of the subsurface horizons in the survey SG9804 and ST10020. These features in the subsurface horizons will be covered in the next section.

These lineations differ in morphology from the elongated curved furrows (section 3.2.1), the features appear to be linear and have a parallel conformity (Fig. 3.10 A) .The features observed run parallel and are negative relief features (3.2.5 B). Based on the orientation and morphology, the lineations can be grouped into 3 main sets marked by white, yellow and black dotted lines. There seems to be older lineations with slightly different orientation within the set marked by yellow dotted lines but it will not be described in detail as the main focus of this study is on the subsurface horizons. Details of the seafloor geomorphology are documented by (Sommerseth, to be published).

The lineations are approximately 370 m to 1 km apart with a relief of about 10-20m (sound velocity in the water is 1470 m/s). The lineations vary in length and can be traced up to 55 km. The width of the lineations also varies between tens of meters and up to 240 m.

The lineations marked in yellow (3.2.5 A & 3.2.6 B) cross cut the ones marked in white. A cross-cutting relationship cannot be established for black lineations. The yellow marked lineations occur on a larger part of the time relief map whereas the lineations marked by white color can only be seen in the southern part. The black lineations occur on a small area only in the southeastern part of the time relief map.

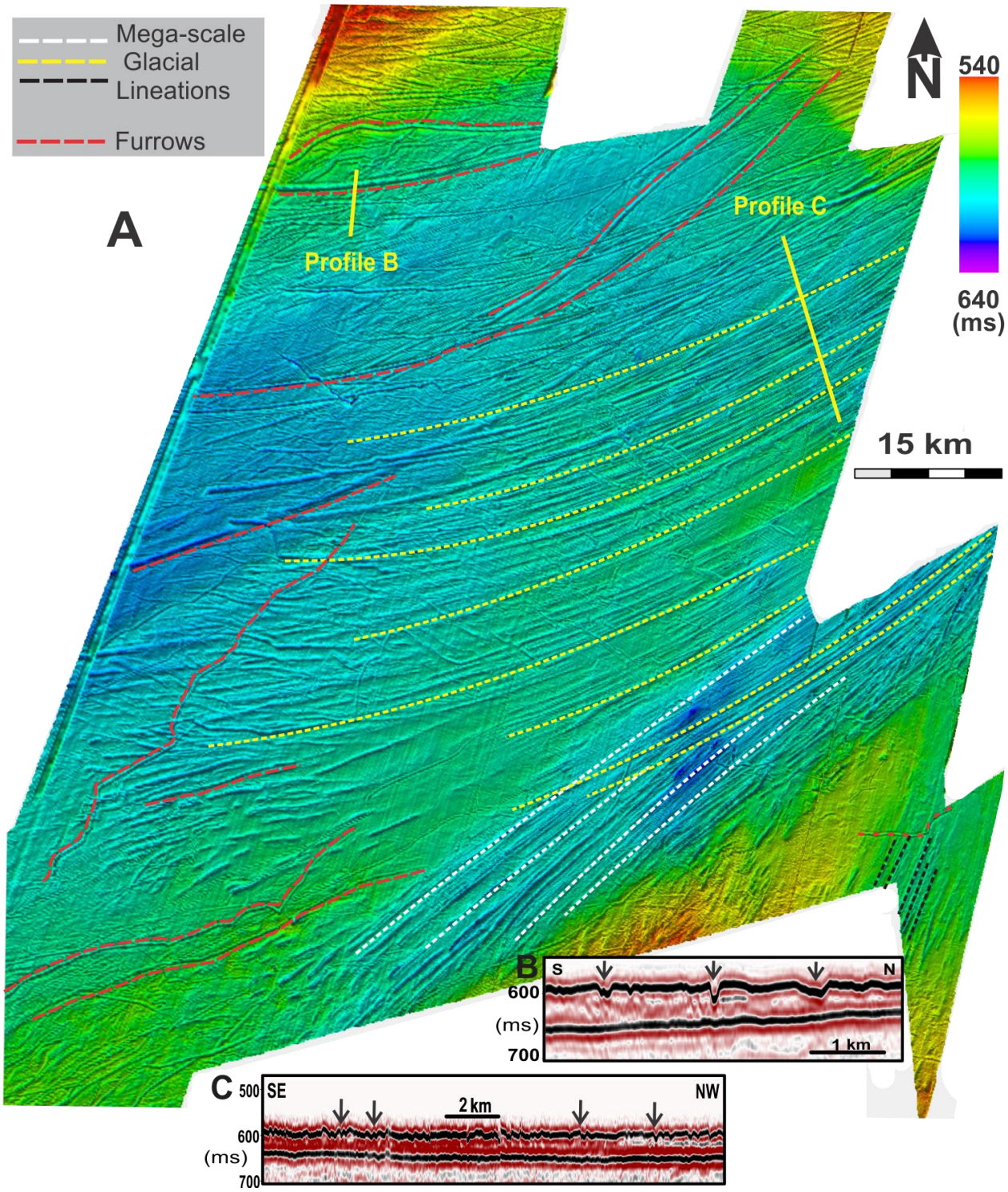

Figure 3.10: Shaded relief time-map of seafloor from surveys of HFC showing Megascale glacial lineations (MSGL) and plough marks. Profile B is across the furrows. Profile C is across elongated ridges and grooves

The lineations tend to curve in different directions, the ones marked by white dotted line (Fig. 3.10 A) curve towards west whereas the set marked by yellow dashed lines curve towards southwest. Furrows marked by red line (Fig. 3.10 A) are also present in the area, cross cutting the grooves and ridges. From the morphology and cross profile, these grooves and ridges seem to be erosional features.

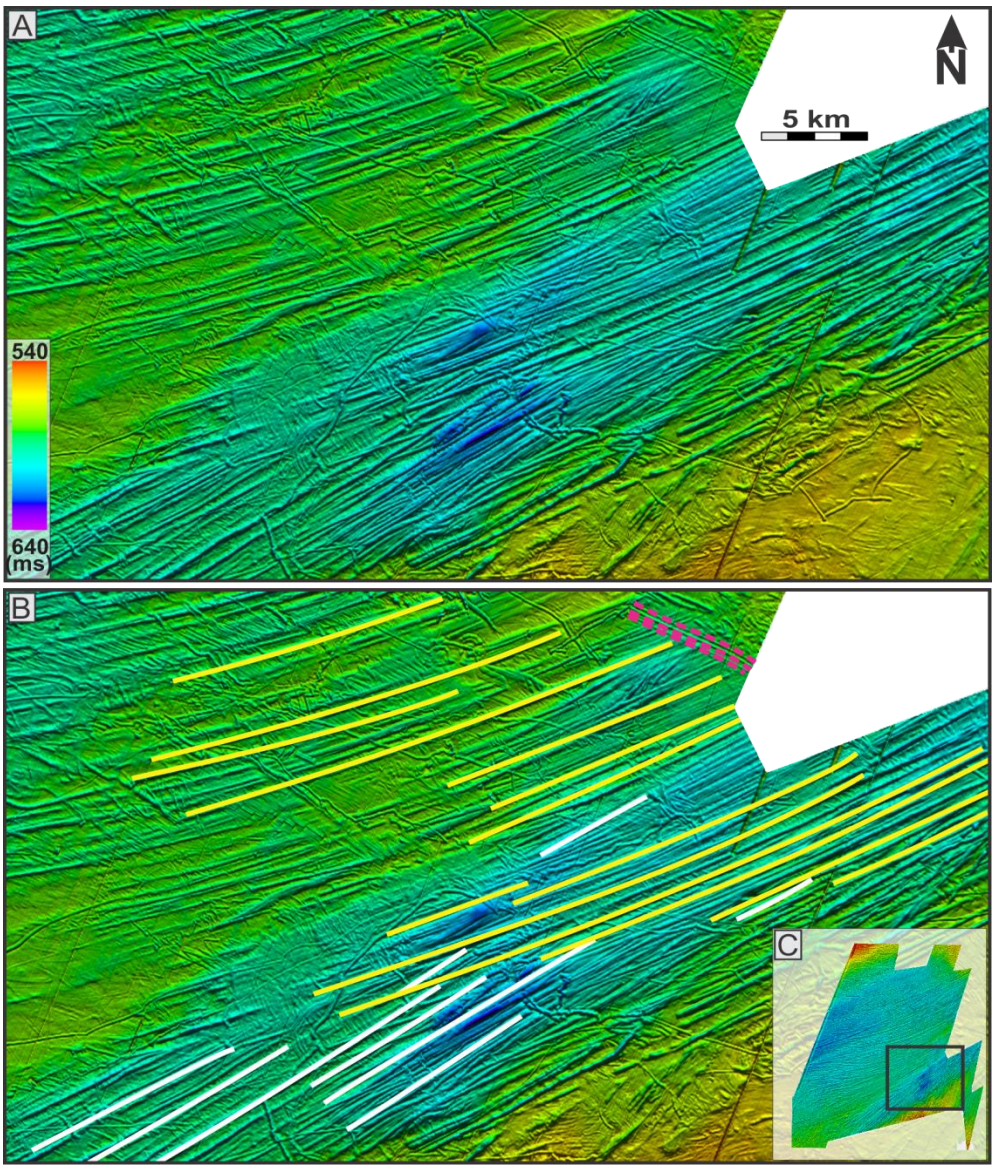

Figure 3.11: A) un-interpreted shaded relief time-map. B) Interpreted shaded relief time-map of seafloor from survey of showing Megascale glacial lineations (MSGL) marked by solid lines and parallel plough marks marked by dotted pink lines. C) Location of the surface in the survey.

Interpretation of parallel ridges and grooves

Based on the morphology and glacial history of the study area, the lineations observed are morphologically similar to landforms interpreted to be mega scale glacial lineations (Clark, 1993; Stokes and Clark 1999). These features are formed by subglacial processes at the base of ice steams and often produce distinctive subglacial bedforms in response to the deformation caused by fast flowing grounded glacier (Clark et al. 2003; Andreassen et al. 2008) which appear as large-scale parallel streamlined ridges and grooves and such features formed by paleo-ice streams were first reported by Clark (1993). The ice streams which produce such features are large (>29 km wide and >150 km long) rapid flowing corridors of ice within an ice sheet where ice movement has a typical velocity of 100-800 m/year than surrounding part of ice sheet where typical movement is around 5 m/year (Andreassen et al. 2007b). These ice streams accounts for the majority of ice and sediments within an ice sheet (Bennett 2003) and dominate the mass balance and stability of continental ice sheets (King et al 2009).

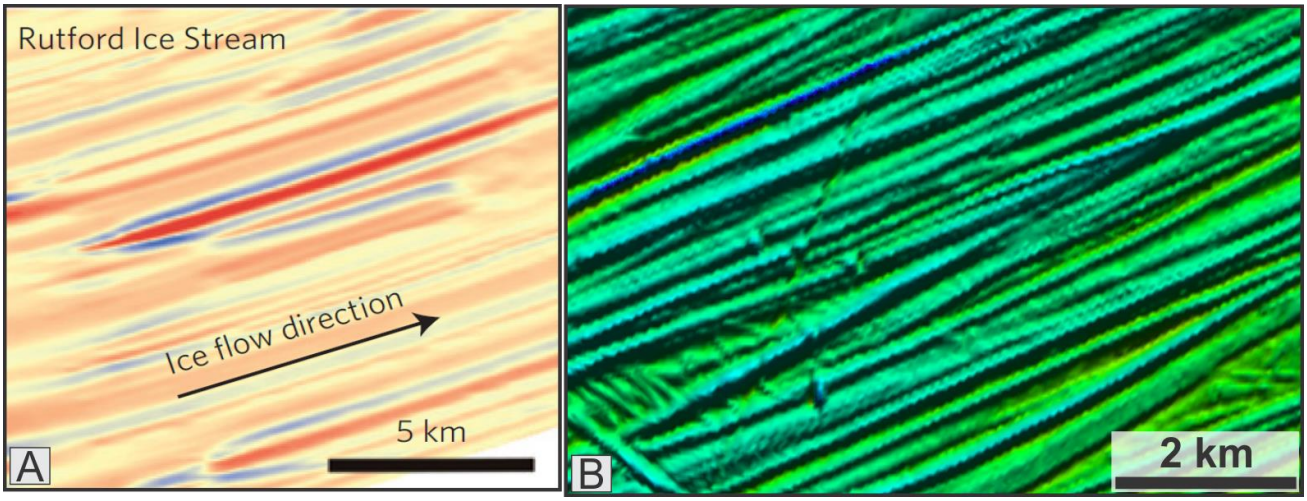

Figure 3.2.7: comparison between MSGL beneath Rutford Ice stream (Fig. A) in Antarctica from King et al. (2009) and MSGL from seafloor shaded relief time-map (Fig. B) from the surveys HFC in study area.

The ice streams are dynamic and are able to switch on and off, accelerate, decelerate, widen, migrate and change flow direction over short time scales (Conway et al. 2002; Catania et al. 2006; Stokes et al. 2009). The potential controls on ice streams location have been discussed in detail by Winsborrow et al. (2010b). Similar landforms have also been reported by various authors from the southwest Barents Sea (Andreassen et al. 2008; Andreassen et al. 2007b; Rafaelsen et al. 2002) and ice streams in west Antarctic (King et al. 2009, Catania et al. 2006). The landforms reported by King et al. (2009) are from the satellite data under active

present day Rutford ice stream from west Antarctica (Fig. 3.2.7 A). These features are formed in response to deformation in areas of fast flowing grounded glacier (Clark et al. 2003; Andreassen et al. 2008).

The lineations in such landforms are very long topographic corrugations having reliefs typical up to tens of meters, are hundreds of meters wide, several kilometers long and length to width ration (elongation ratio) exceeding 10:1 which indicates a rapid flow of ice streams (Stokes and Clark, 199; 2001, 2002, Fowler 2010). The presence of the lineations depicts a warm-based glacier. The orientation of these parallel lineations is useful indicator of the paleo-ice streams direction and can be useful to determine the source areas and location of these ice streams (Clark 1993).

Based on their parallel conformity and orientation they can be grouped into three sets represented by white and yellow and black colors. Each set is inferred to be formed by one particular ice stream. Paleo ice streams have been reported by several authors from the study area (Andreassen et al. 2004; Andreassen et al. 2008; Andreassen et al. 2007; Rafaelsen et al. 2002; Vorren and Laberg, 1997).

In the study area, the three different sets of MSGLs may indicate that three different ice streams or the same ice streams changed its orientation of flow three times. The ice stream represented by white dashed lines was older than the ice stream represented by yellow dashed lines as it crosscuts the former. The curving nature of the lineations suggests that the ice streams have been bending in Bjørnøyrenna trough which acted as loci for fast flowing ice.

The occurrence of yellow lineations over a small area can either be indicative of width of the ice stream but here it is more likely that the lineations produced by this ice stream may extend further but as it is being over printed by the yellow lineations, it may have eroded. Also, on the basis of crosscutting relationship, the yellow lineations are younger than the white lined lineation.

3.2.4 Pock marks

Description of circular depressions

Circular to sub-circular depression (Fig. 3.12) can be observed on the seafloor of surveys HFCW11, HFCE11 and HFC09 (Fig. 2.1 and 3.1). These features vary in size and approximately range from about 170-300 m in diameter. The depth of these depressions range from 11 m to 30 m (assuming sound velocity in the water is 1470 m/s). The depressions occur randomly on the deepest part of HFC surveys. Although their occurrence is random on the seafloor, at places its association with furrows can be observed, these occur either within the furrow or where the furrow terminates (Fig. 3.13A). On seismic profiles (Fig. 3.13 B) these features are u-shaped and almost run down till URU.

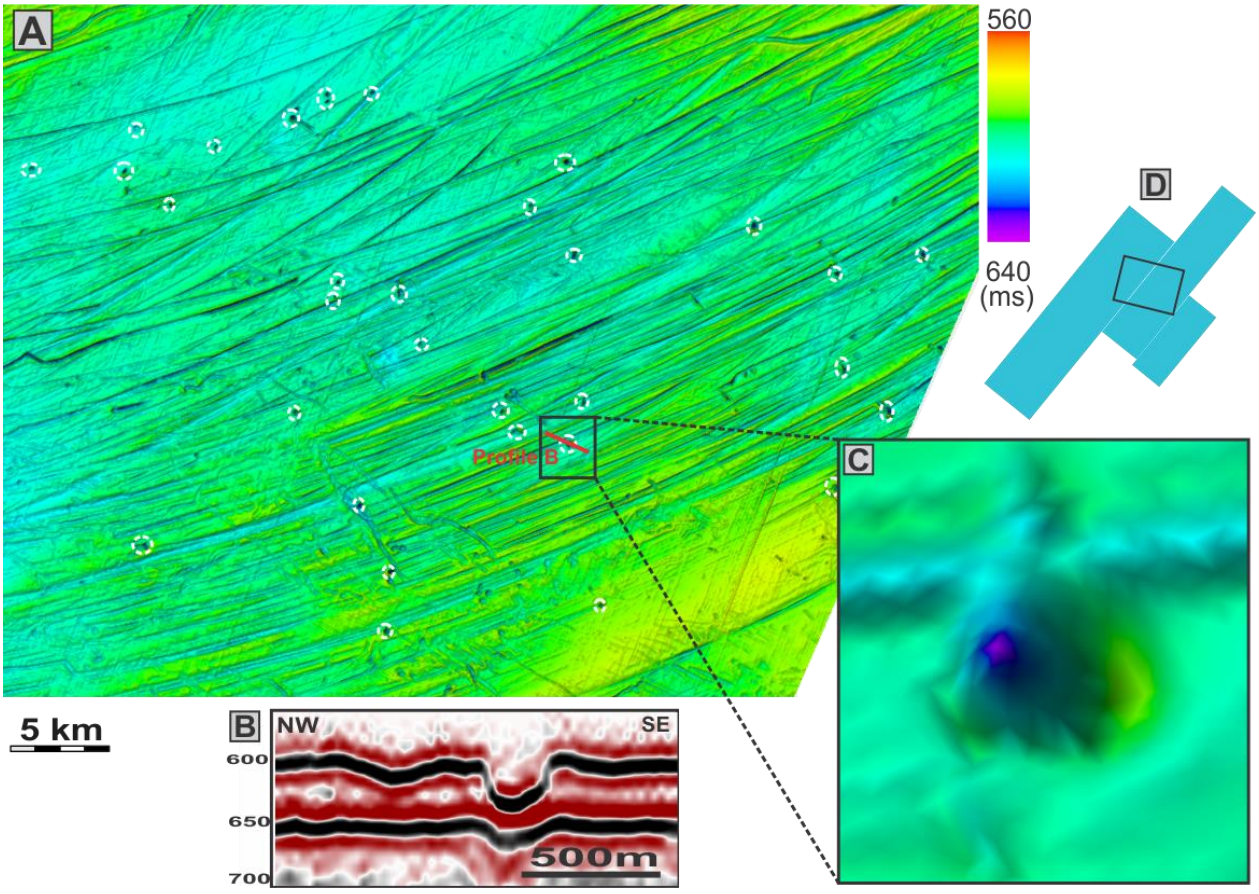

Figure 3.12: A) Shaded relief time-map showing circular depression (marked by white circles) on part of the time map indicated by a rectangle in Fig. D. B) Seismic profile across the circular depression showing vertical stacking of the pockmarks in cross profile. C) Enlarged view showing morphology of the circular depression

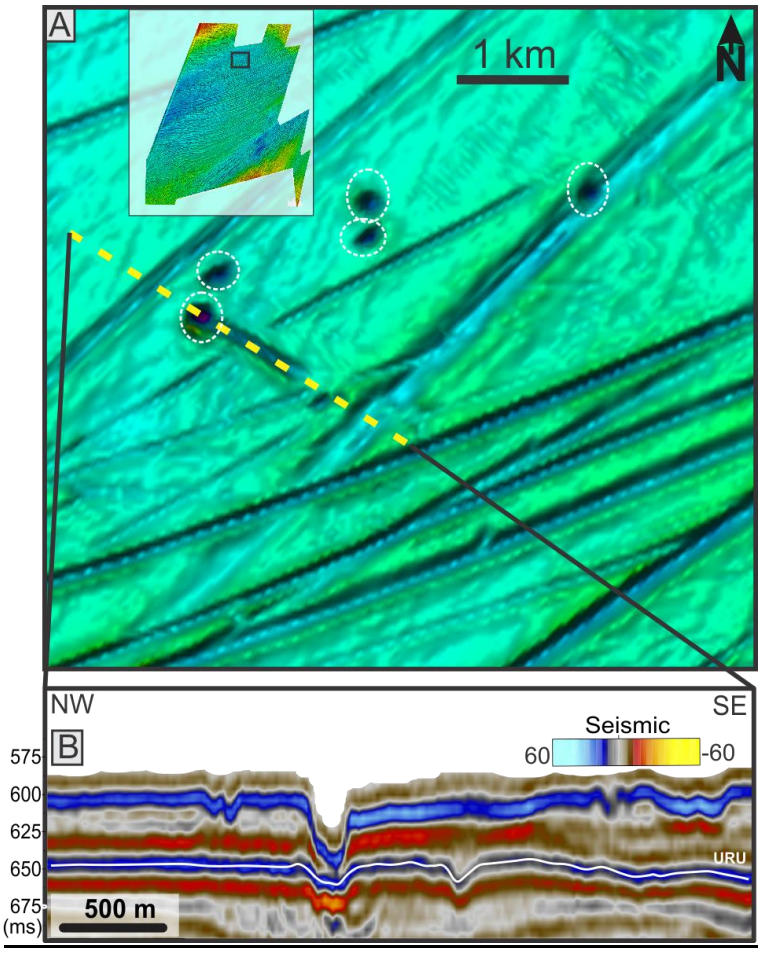

Figure 3.13: A) Shaded relief time-map showing association of circular depression (marked by white circles) with ice berg furrows. B) Seismic profile across the circular depression showing vertical stacking of the pockmarks in cross profile. The location of the time relief map can be seen in the top left enclosed figure in A.

Interpretation of circular depressions

The genesis of the circular depressions can be accounted to various geological processes such as grounded icebergs, glaciotectonism, meteorite impact and volcanism. Here these circular depressions are interpreted to be pockmarks which are formed as a result of fluids expulsion from seabed causing sediments removal (Hovland, 1981; Hovland and Judd, 1988; Judd and Hovland. 1992; Lammers et al. 1995).

Although the genesis of these depressions from other geological processes cannot be neglected, the interpretation here is based on the facts that these depressions are randomly distributed over the seafloor and the typical shape of the depressions and its subsurface expression (Hovland et al. 2002) as characterized by vertical stacking of pockmarks (Fig 3.12 B & 3.13 B).

Pock marks are also widely reported from the study area by Chand et al. (2012). The pock marks seem to be related to the faults in the subsurface. As this data is limited to URU, it cannot be documented but extensive faulting in the subsurface can be seen on 2D regional lines. These features are formed after the deposition of glacigenic sediments, which is most likely during the deglaciation as it intrudes the glacigenic sediments. The occurrence of these features in the deepest part may be associated with thin sediment cover, which can be easily eroded by the escaping fluids. Also the lithology of the sediments cannot be ignored; soft sediments like clay are more easily eroded than hard sediments.

3.3 Results from subsurface horizons.

3.3.1 Megascale glacial Lineations

In all of the surveys internal reflectors within the chaotic glacigenic seismic package can be mapped. The interpretation for these horizons was limited only to areas with high interpretation confidence. All the interpretation was gridded into shaded relief time-maps. A total of two horizons (bE, bD) were present in the subsurface in the survey NH0608, two horizons in ST10020 (hor-01 & hor-02) and one (hor-01) in the survey HFC. Horizon (bE, bD & bC) were present and mapped in survey SG9804 as well. The description and interpretation of these surfaces is given in the following section.

Description of parallel ridges and grooves on Horizon01 in survey HFC

The horizon is characterized by a weak to moderate peak in the glacigenic part below the seafloor. The horizon cannot be followed throughout the HFC surveys (Fig. 3.14 B). The horizon was mapped on the peak in areas with good reflections and confidence level in interpretation.

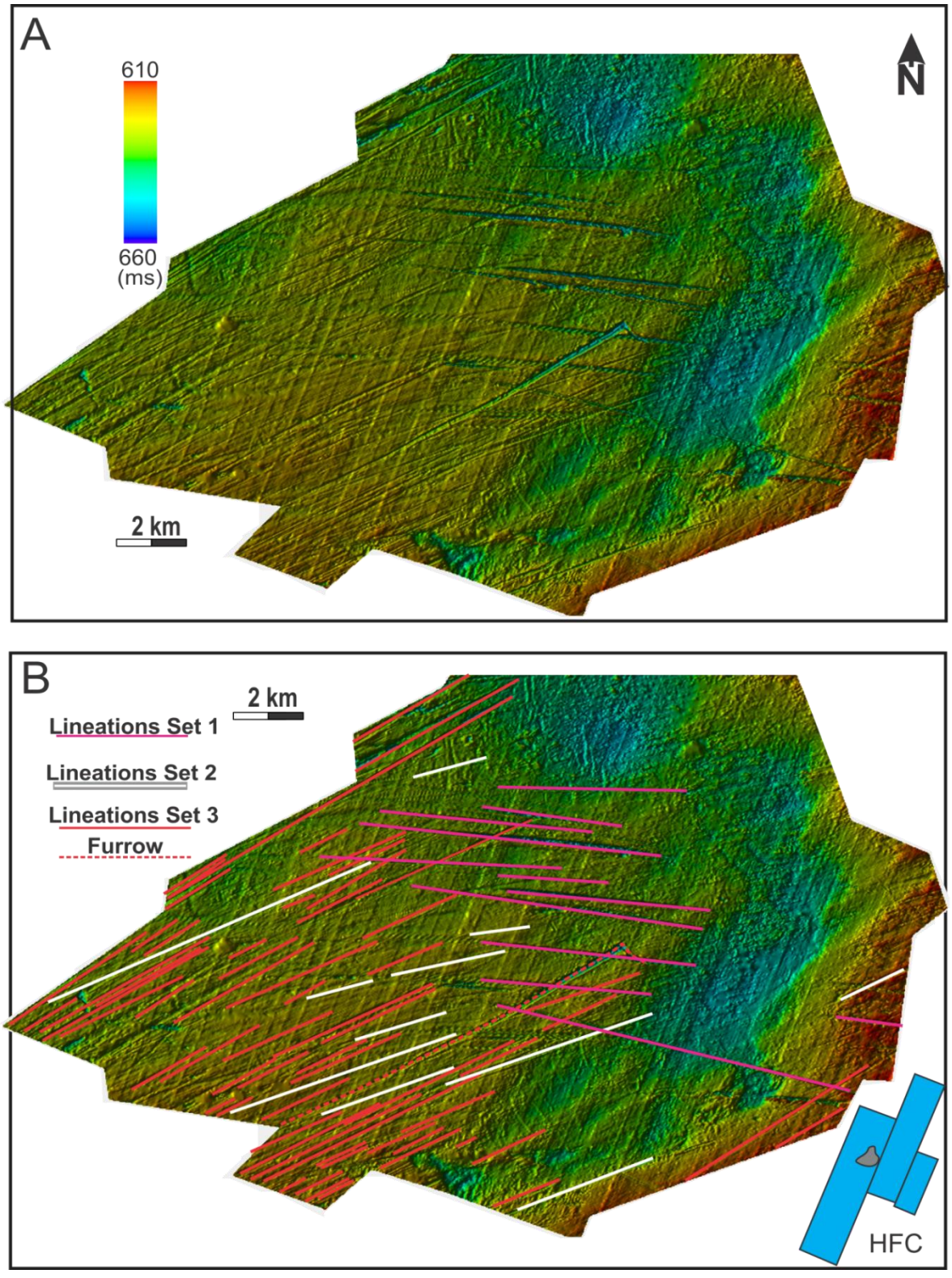

Figure 3.14: A) Un-interpreted shaded relief time-map of Horizon01 in HFC. B) Shaded relief time-map of Horizon01 in the surveys HFC.. The dashed blue line shows a furrow on this horizon. The limit of interpretation of the horizon01 is represented by a polygon in the surveys in the right lower corner of the figure.

Parallel to semi parallel lineations were on shaded relief time-map of this horizon. Based on orientation three types of these lineations can be observed on this surface. The lineations marked by red lines (Fig. 3.14 B) are oriented in north-east and south-west direction. On seismic profile it is difficult to separate the lineation from each other in most places as the reflector is very irregular in nature, however at places the relief of these lineations seems to range from 1.75 to 3 meters deep (velocity of 1750 m/s). These lineations are densely spaced than the other lineations on this surface. The length of the lineations cannot be determined accurately as the whole surface cannot be mapped due to chaotic nature of the reflector, however the length of these lineations vary between 4-12 km in the interpreted area. These lineations overprinted by the lineations marked by magenta color (Fig. 3.14 B). The red lineations are quite parallel and do not vary in its orientation throughout the surface.

The lineations set marked by magenta (Fig. 3.14 B) lines have an orientation from east to west with slight inclination towards southwest. The relief of these lineations is well developed but these lineations are not present throughout the surface and can be seen only in a limited area. The length of these lineations is from 2 to 8 km with width varying between 70-200 m. The relief of these lineations ranges from 2.5-22 m. The morphology of some of these lineations differs with respect to each other as some of these are more pronounced with greater widths and relief. These lineations with high relief and width values seem to overprint all other lineations, whereas the same lineations set but with smaller relief and width are being overprinted by the lineations set marked by red lines.

A lineation set marked by white color (Fig. 3.14 B) with an orientation of northeast and southwest can be observed. It tends to be more oriented towards east and can be observed only a few places. The lineations have length ranging from 1.5-9 km. The width and relief of these lineations is 70-130m and 1.5-3m respectively. The lineations are being overprinted by all other lineations present on this surface.

A furrow that runs mainly in north-south direction can be seen marked by red dotted line. It can be followed up to 11.5 km on the surface with a relief and width of 13 m and 280 m respectively. The relief and the width of the furrow decrease down towards the south.

Absence of lineations can be observed in the deeper part of shaded relief time-map (Fig. 3.14 B).

Interpretation of parallel ridges and grooves on Horizon01 in survey HFC

The lineations are interpreted to be mega scale glacial lineations (MSGL) formed by a fast-flowing ice stream (section 3.2.3). From different orientations of these lineations it can be inferred that different ice streams had operated in this area. The lineations marked by black and white lines can be indicative of a single ice stream which might have changed its position slightly at various time periods. The white lineations are being overprinted by all other lineations; hence it is the oldest with respect to other lineations sets.

The magenta colored lineations seem to be overprinted by red lineations and some cases it overprints it, it is difficult to conclude the relative age. On the basis of the morphology of the lineations, I interpret some of these wide and deep lineations to be ice berg scours marks (marked by red dotted line in Fig. 3.14 B)(section 3.2.1) which overprints the black lineations and hence these are younger whereas these magenta colored lineations with small relief and width are being overprinted by the black lineations and it can be hence concluded that the black MSGLs are the youngest on this surface.

The furrow marked by red dotted line (Fig. 3.14 B) is interpreted to be produced by scouring action of the base of an iceberg (section 3.2.1). The decrease in relief in width can be indicative of the direction of the ice berg i-e the ice berg generated in the north and tend to die towards the south as its width and relief decreases.

The absence of lineations in the deeper part of the survey may due to the erosion of these areas after the formation of the lineations hence it's not visible now.

Description of parallel ridges and grooves on Horizon01 in survey ST10020

The horizon was mapped on peak in the northern side of the depression (Fig. 3.15 C) and on lower zero crossing at places in the southern side due to interference with the seafloor. A big depression like feature can be seen in the time relief map (Fig. 3.15 A). The depression cannot be mapped throughout the survey. It is about 7 km wide with a length of 14 km in the mapped area. The depression is discussed further in section 4.2.2.

On the western side of the depression linear ridges and grooves like features are observed (Fig. 3.15 B) which runs parallel with each other. The relief of the linear grooves and ridges vary from 4-8 m (assuming velocity of 1750 m/s in glacigenic sediments). These features can be followed from 1.8-3.7 km while their width varies between 60 m to 140 m.

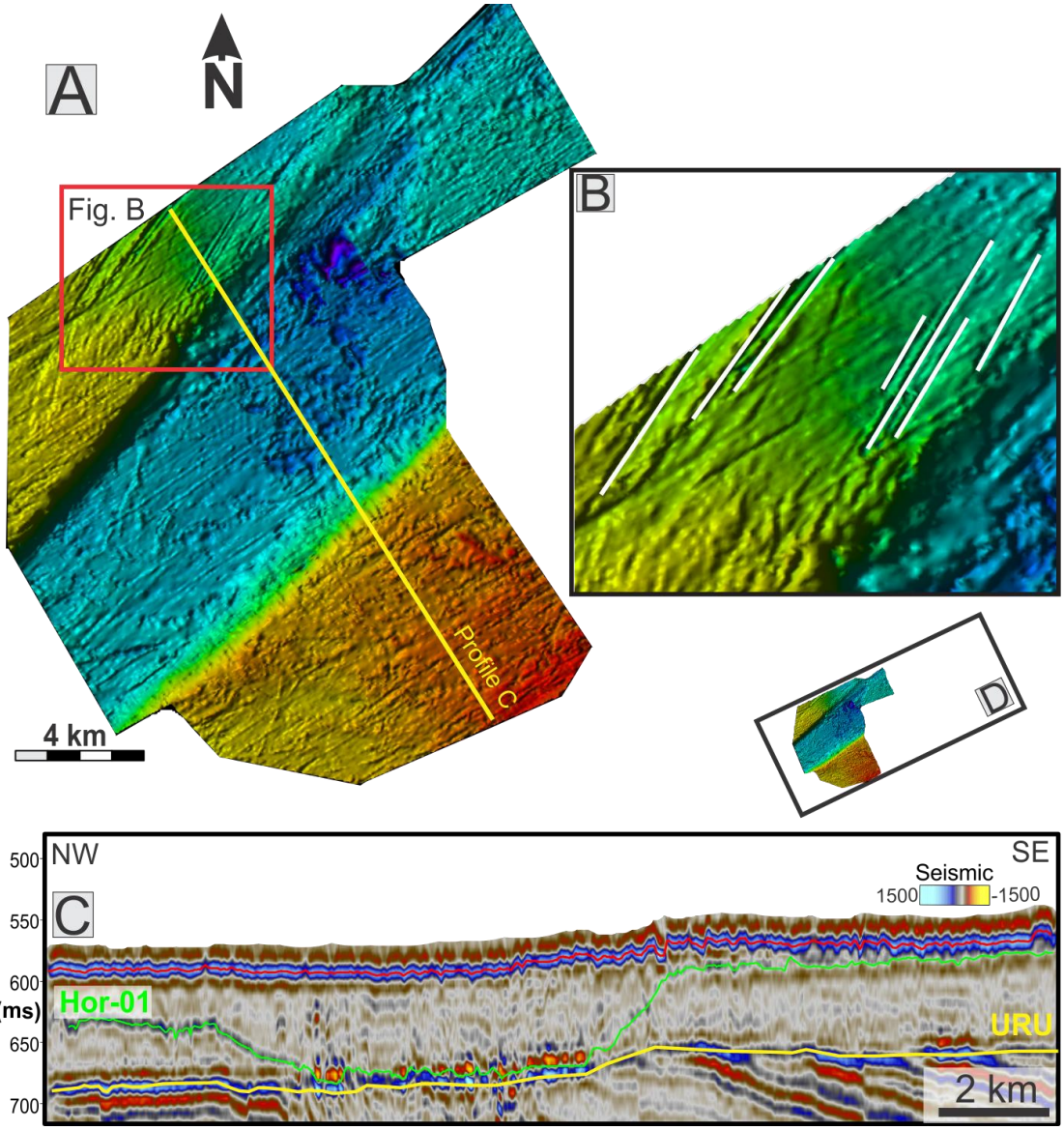

Figure 3.15: A) shaded relief time-map of Horizon01 B) enlarged view of the lineations on the relief map marked by a red rectangle in Fig. A. C) Seismic profile across the lineations. D) Extent of interpretation within the survey ST10020

Interpretation of parallel ridges and grooves on Horizon01 in survey ST10020

Based on the morphology and their parallel conformity, the linear ridges and grooves are interpreted to be megascale glacial lineations (section 3.2.2). Looking at the 2D regional

lines and some arbitrary lines within the survey, horizon01 seems to be part of horizon02 and the depression observed here is actually part of some reflectors under these reflectors but could not be observed due to the resolution limitations (section 2.3) of the data. This will be highlighted further in the discussion part.

Description of parallel ridges and grooves on Horizon02 in survey ST10020

Linear ridges and grooves like feature can be seen on horizon 02 (Fig. 3.16 A). The lineations are not developed extensively. These features are relatively parallel to each other and appear only in the shallow part of the survey. They also tend to curve towards south-western side. The longest lineation can be followed to about ~ 11 km. The relief of the lineations is from 7 to 3.5 m while the width ranges from 80 to 220 m.

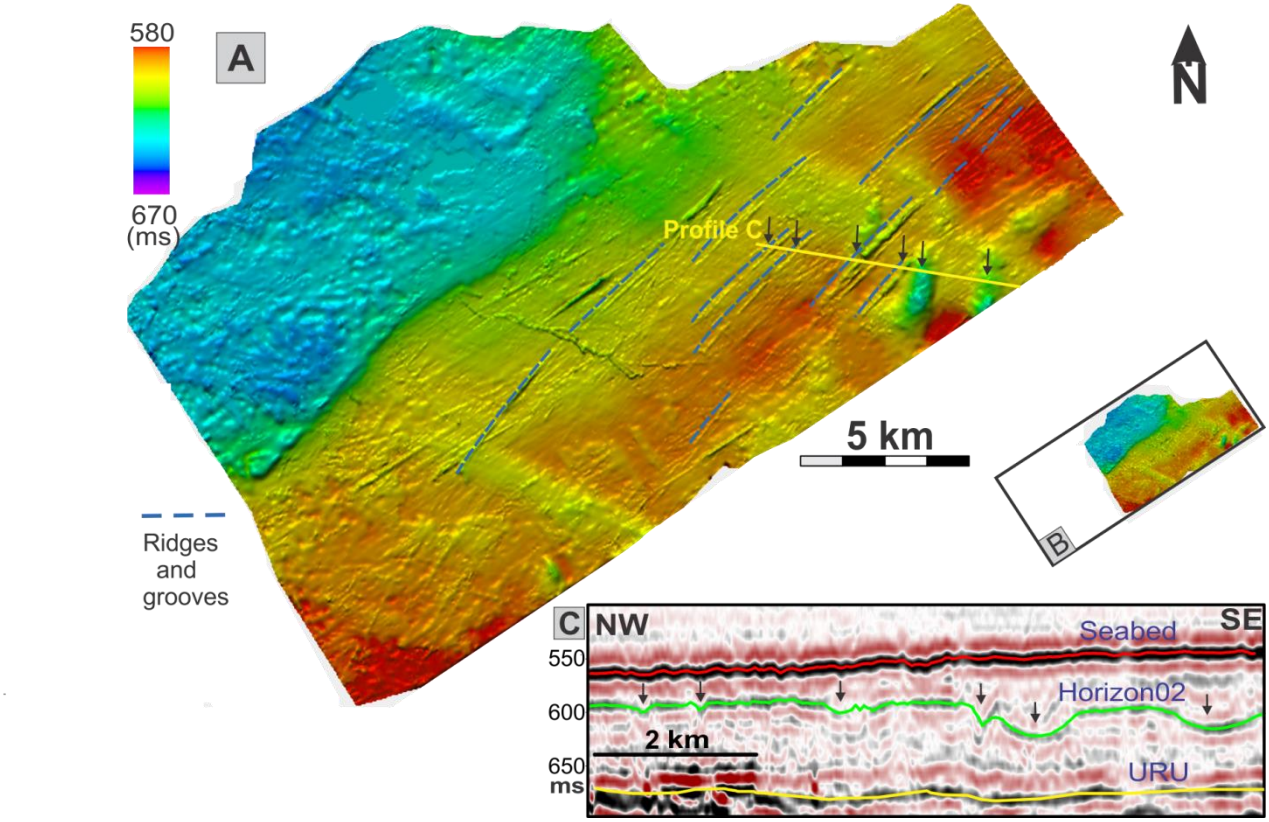

Figure 3.16: A) shaded relief time-map of Horizon02 B) Extent of the interpretation in the survey C) Seismic profile across the lineations. The lineations are marked by black arrows in the figure.

Interpretation of parallel ridges and grooves on Horizon02 in survey ST10020

Based on the morphology, the ridges and groves like feature are interpreted to be mega scale glacial lineations (MSGL) which are subglacial bed forms (section 3.2.3). The curve nature of the bed forms may indicate that the paleo ice stream was gradually bending and changing its direction over this part of the study area.

Description of parallel ridges and grooves on bE in survey NH0608

The survey is located on the Nordkapp banken area (Fig. 1.1). The horizon01 within the survey NH0608 is under the seafloor is characterized by a strong peak (Fig. 3.17 C). The horizon interpretation was limited to the areas of high confidence and hence was not interpreted in the eastern part of the survey due to chaotic reflections (Fig. 3.17 B). The horizon is shallow in the southern part of the survey and its depth increase towards the north (Fig. 3.17 A).

Two sets of elongated ridge-groove features appear on the surface (Fig. 3.17 A). They are parallel and well developed on the northwestern part of the horizon. Orientation of the white ridge-groove feature is southwest to northeast whereas the one marked by red lines has an orientation from south-southwest to north-northeast. The red lined lineations have a relief of 1.5-10 m with width of 100-200 m. The length of these lineations ranges from 3-9 km. The relief of red lineations ranges from 2-3.5 m. The width of these lineations is from 80-90 m while the length varies in range of 2-7 km. Observation also suggests that the red lined lineations overprints the white lineations.

Interpretation of parallel ridges and grooves on bE in survey NH0608

Elongated ridge-groove feature is interpreted to be megascale glacial lineations formed by fast-flowing ice streams (section 3.2.3). Two different orientations of these lineations can be indicative of two ice streams or two different streaming events of the same ice stream as the orientation does not vary drastically and ice streams can change its orientation over a period of time that were active at different times. According to the observation, the red lined lineations seem to have a younger origin as it overprints the white lineations.

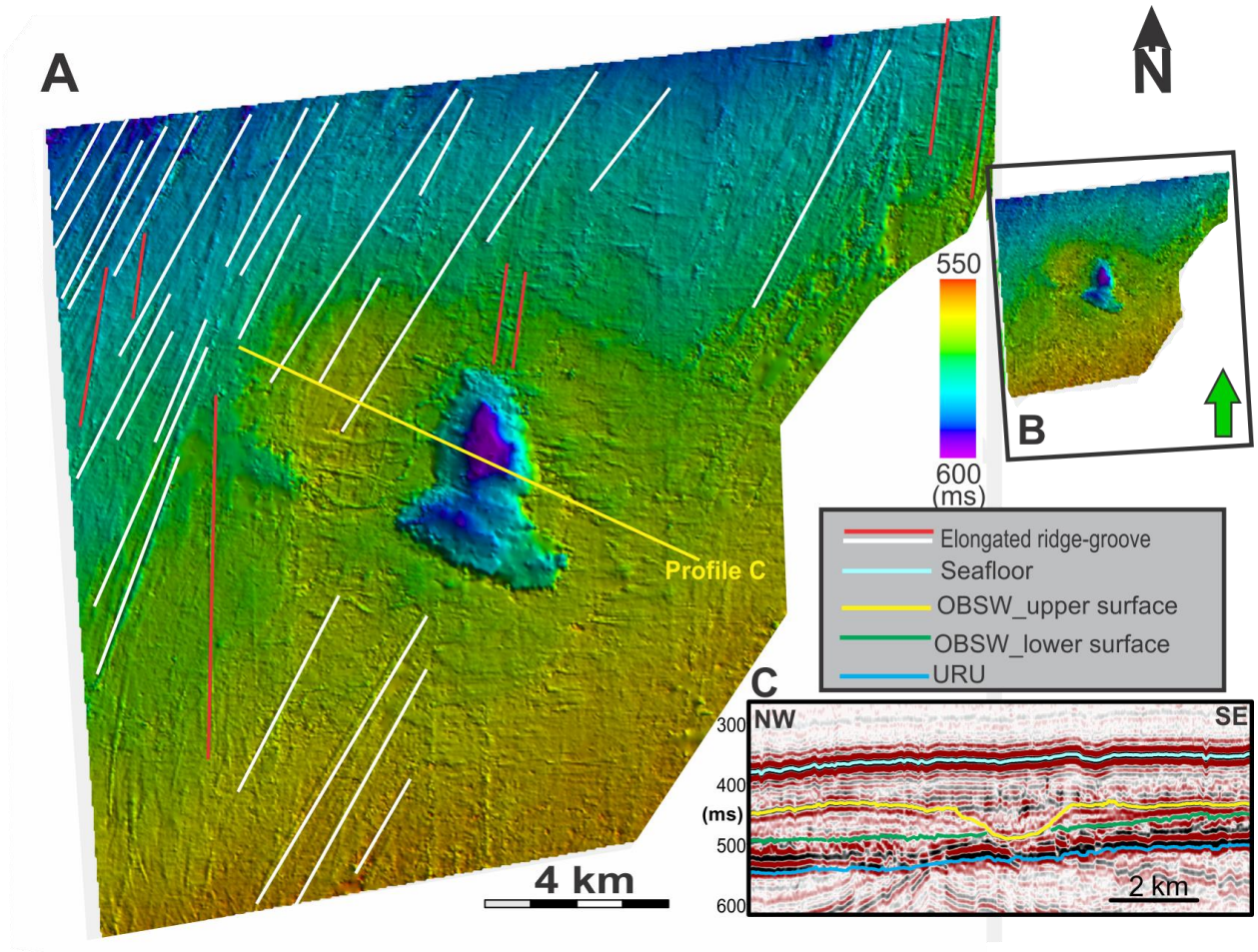

Figure 3.17: A) shaded relief time-map of interpreted horizon horizon01 with a large depression. B) The limit of interpretation of the horizon within the survey NH0608 can be seen in the top right corner. C) Seismic profile across the survey showing the horizons interpreted.

Description of parallel ridges and grooves on Horizon bE in survey SG9804

The horizon is marked by a moderate peak under the seafloor in the glacigenic sediments (Fig. 3.18 C). The horizon is present only in the eastern part of the survey and terminates against the seafloor towards the west (Fig. 3.18 D). The wedge might continue further towards the west but cannot be seen on seismic profile as the wedge thins out towards west. The probable extent of the horizon is represented by the line in Fig. 3.18 D. The horizon is relatively straight but slight dip towards northeast with the shallow parts in southern part (Fig. 3.18 A)).

On two way travel time relief map set of linear furrows and ridges with different orientation can be observed (Fig. 3.18 B). Although the seismic signature of the lineations

cannot be well observed for all of the lineations but some of these linear features appear to have a V-shape on seismic profile (Fig. 3.18 C). The lineations with well-developed seismic signature have depth ranging from 3-5.5 meters (assuming velocity of 1750 m/s). The length of the lineations varies from 2-20 km with width ranging from 50-200 m. The lineation set represented by white lines has orientation in southwest-northeast direction whereas the lineations marked by yellow lines have an orientation in north-south direction. The lineation set represented by white lines is well developed throughout the horizon. The lineations marked by yellow line can only be seen in few places in the southern part of the horizon. The yellow marked lineation set also cross cut the lineations marked by white lines.

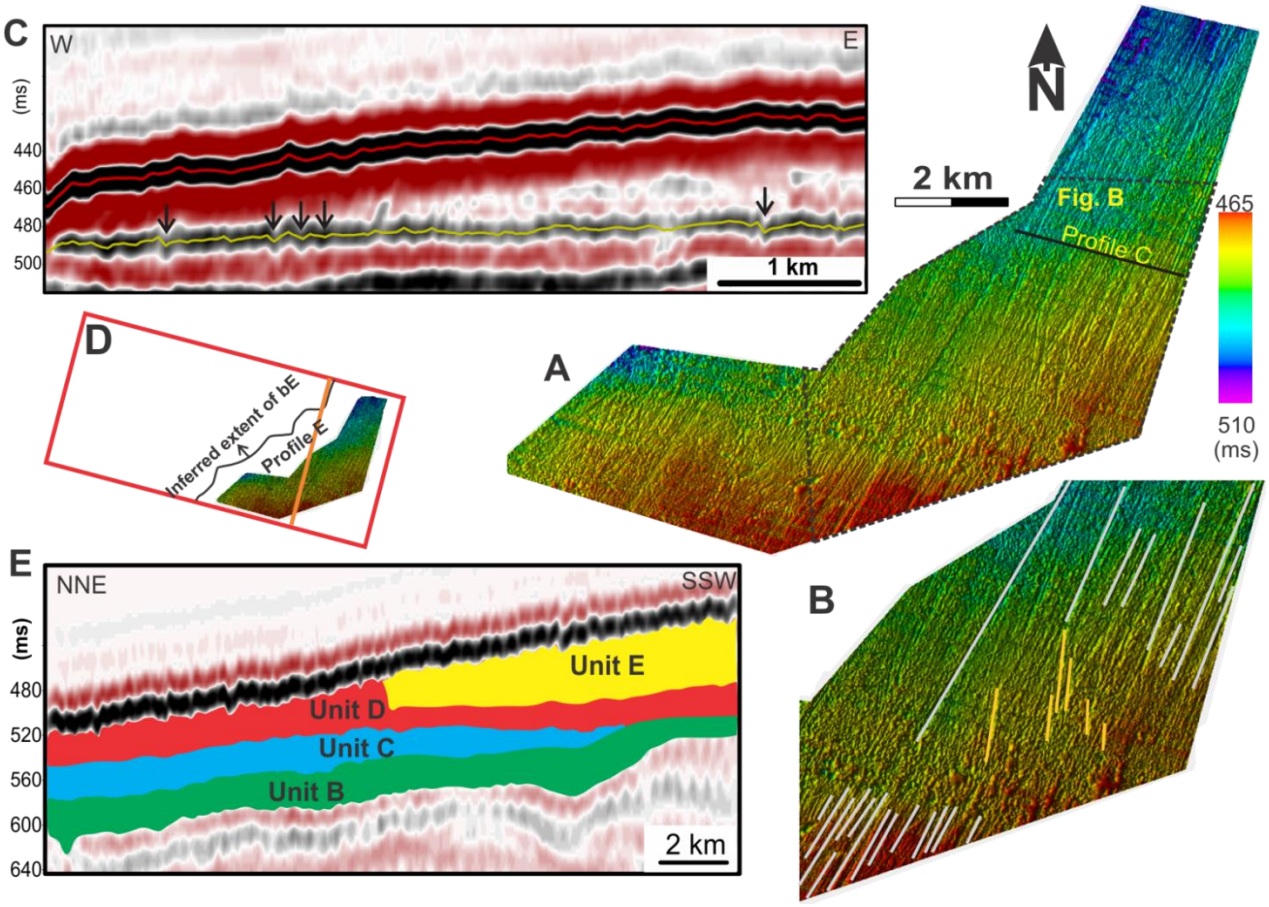

Figure 3.18: A) shaded relief time-map of horizon bE in survey SG9804. B) Interpreted sets of lineations represented by white and yellow arrows. C) Seismic profile across the linear features. The appearance of the lineations is marked by black arrows. D) Extent of the interpretation of the horizon bE in 3d survey. The possible extent of the surface can be seen by a polyline. E) Seismic profile showing the stratigraphy from 3D survey.

Interpretation of parallel ridges and grooves on Horizon bE in survey SG9804

The lineations are interpreted to be mega scale glacial lineations (section 3.2.3) formed by fast flowing ice streams. The white lineations are older than the yellow colored lineations as the later cross cuts the former. These two different orientations also indicate that there may have been two ice streams or it could be the from the same ice stream that had been active during different time period over the study area.

Description of parallel ridges and grooves on bD in survey NH0608

The horizon is characterized by a moderate to strong peak (Fig. 3.19 A). The horizon was interpreted on the peak in 3D survey. The horizon cannot be followed throughout the survey and was interpreted where there was a high confidence in interpretation. The surface is shallower towards the south and get deeper in the north (Fig. 3.19).

On shaded relief time-map linear ridges and grooves (lineations) (Fig.3.19 B) were observable. The lineations have an orientation of north-south. The lineations can only be observed in the southern shallow part of the survey as these diminish towards the north. The relief of the lineations varies between 1.5 – 6m. The width of the lineations ranges from 120 – 270 m while it can be followed from 2 to 9 km.

Interpretation of parallel ridges and grooves on Horizon02 in survey NH0608

The lineations are interpreted to be megascale glacial lineations as discussed in section 3.2.3. Its presence in the shallow parts only may be indicative of the extent of the grounding zone of the ice stream. The north-south orientation of the lineations indicates the direction of the ice stream that had been active over the study area.

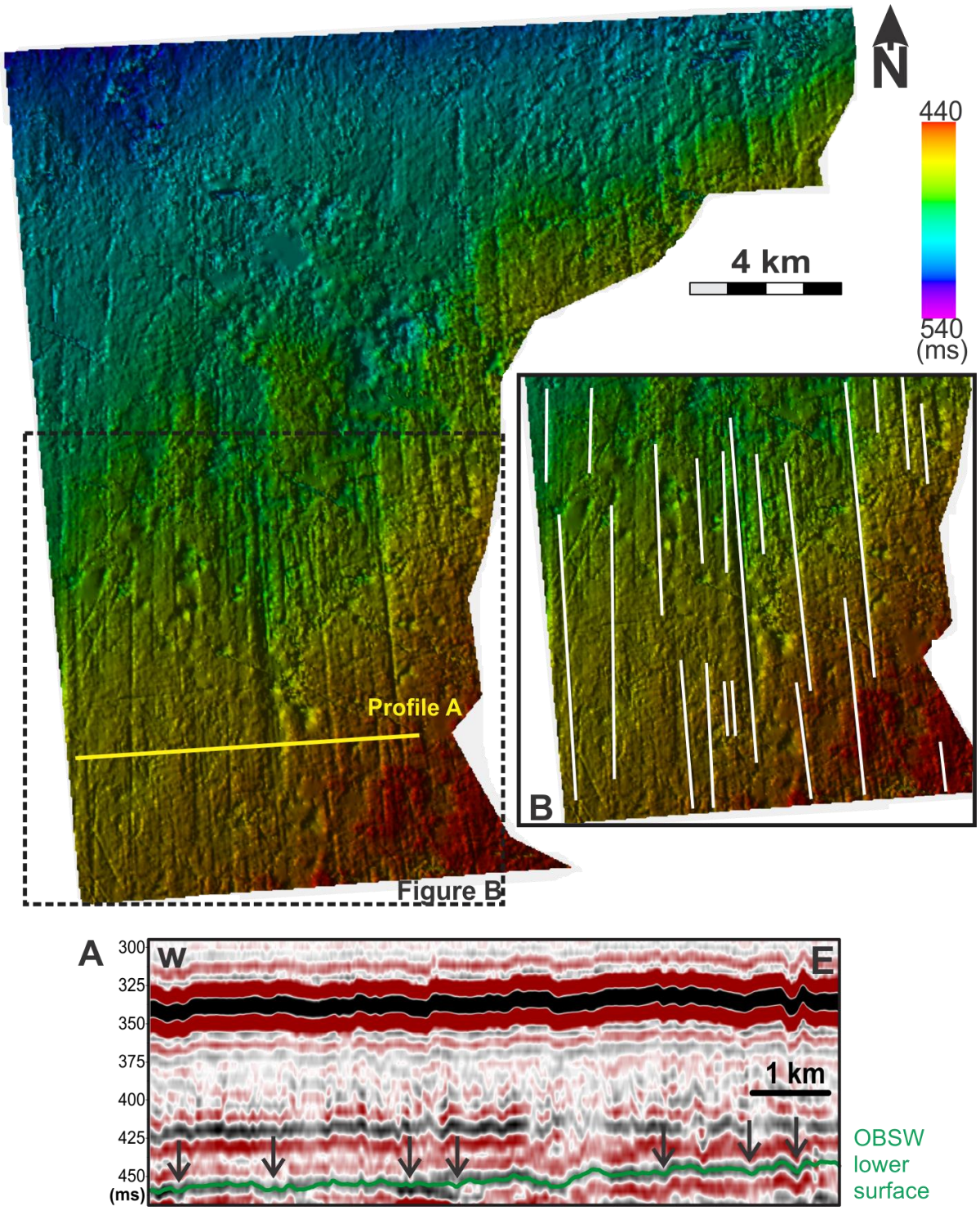

Figure 3.19: shaded relief time-map of Horizon02. A) Seismic profile across the linear features. Seismic signature of these features is indicated by black arrows B) mapped lineations on the surface. The location of the image is represented by dotted lines.

Description of parallel ridges and grooves on Horizon bD in survey SG9804

The horizon is marked by moderate to strong peak under the horizon bE (Fig. 3.4). The horizon was interpreted throughout the 3D survey. The horizon is relatively flat with various depression and dips slightly towards the west (Fig. 3.20 A).

On shaded relief time-map of horizon bD, at least two sets of linear ridges and grooves (lineations) can be observed (Fig. 3.20 A). The lineations on seismic profile cannot be differentiated into individual lineation but some of more pronounced lineations seem to have a V shape on seismic profile. On time relief map it seems that the lineation shallows on both sides as it terminates.

The lineations marked by white lines (Fig. 3.20 B, C & E) have an orientation of north-east and south-west while the lineations marked by blue lines (Fig. 3.20 E) have an orientation of south-east and north-west and tend to curve slightly. The relief of both lineations set range from 2.5-7.5 m for the lineations that can be distinguished on seismic profile; hence there may be some lineations with relief less than 2.5 m. The width of the lineations ranges from 50-150 m while the lineations are 1-12.5 km long.

The lineations marked by white line are better developed on the surface than the one marked by blue lines. Also the white marked line overprints the black marked lineation set.

Interpretation of parallel ridges and grooves on Horizon bD in survey SG9804

The lineations are interpreted to be form of subglacial bed forms, mega scale glacial lineations (MSGL). The lineations may have been caused by the same ice stream which changed its orientation and operated at different time period. The white marked lineation set is younger than the blue marked lineations as it overprints the later, hence the youngest orientation of the ice stream is represented by the white lines. Also the non-existence of the blue lined lineations throughout the survey could possibly due to erosion by the white lined lineations which were produced by a later ice streaming event.

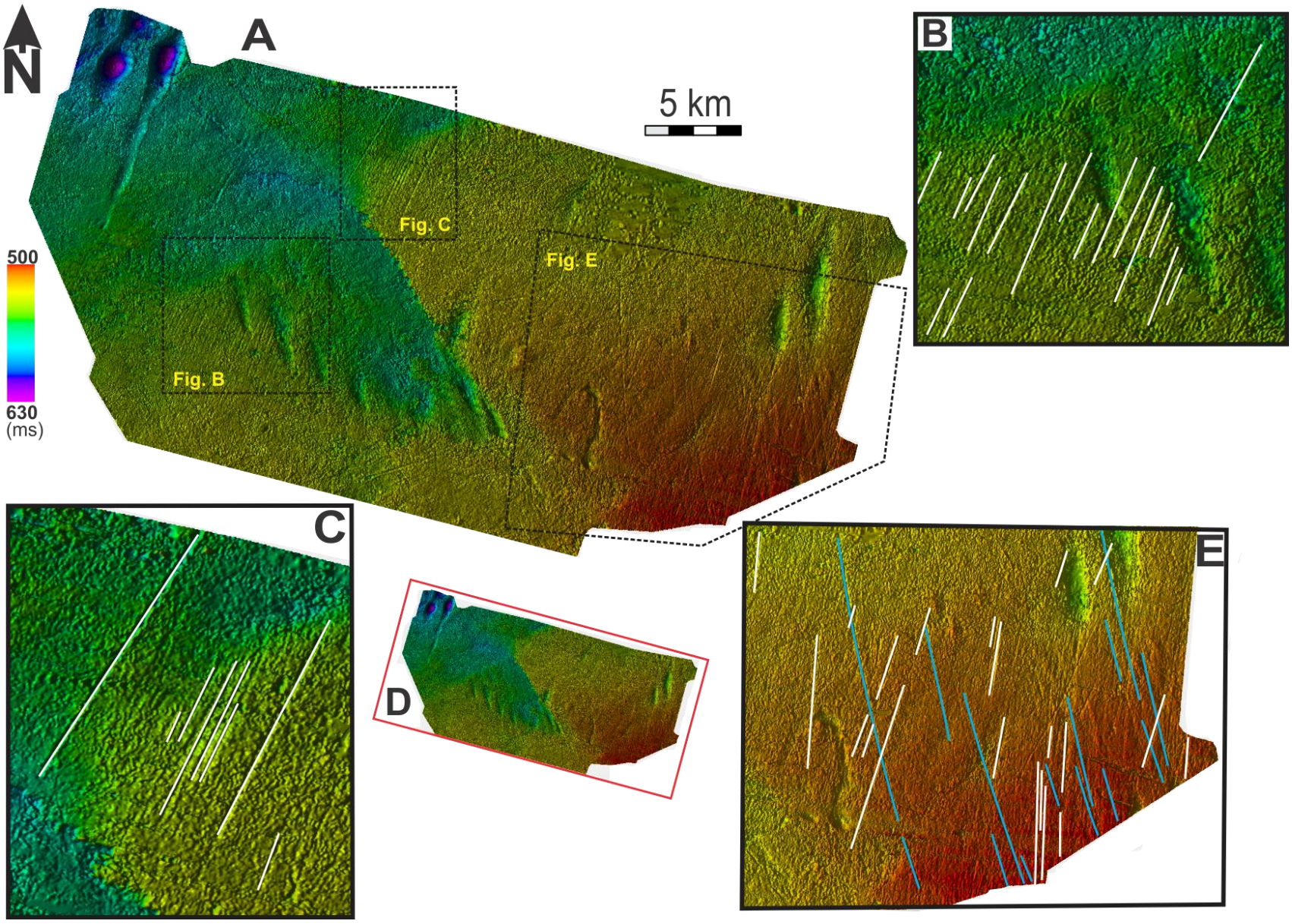

Figure 3.20: A) shaded relief time-map of Horizon bD. B), C) and E) showing the lineations on the surface. The location of each figure can be seen as dotted polygons in fig. (A). D) Extent of the interpretation of Horizon bD in survey SG980

3.3.2 Channel like feature

Description of channel like feature on horizon02 in the survey ST10020

A channel like depression (Fig. 3.21 B) is observed in the central part of the survey ST10020. It emerges in the shallow part and terminates as it reaches towards the north-western deeper part. The channel can be followed up to a distance of ~6.5 km. The channel is variable in depth and rages from 1.75 m to 7.8 m (assuming velocity of 1750 m/s). On time slice from variance cube high values of variance can be seen within the channel like feature (Fig. 3.21 A).

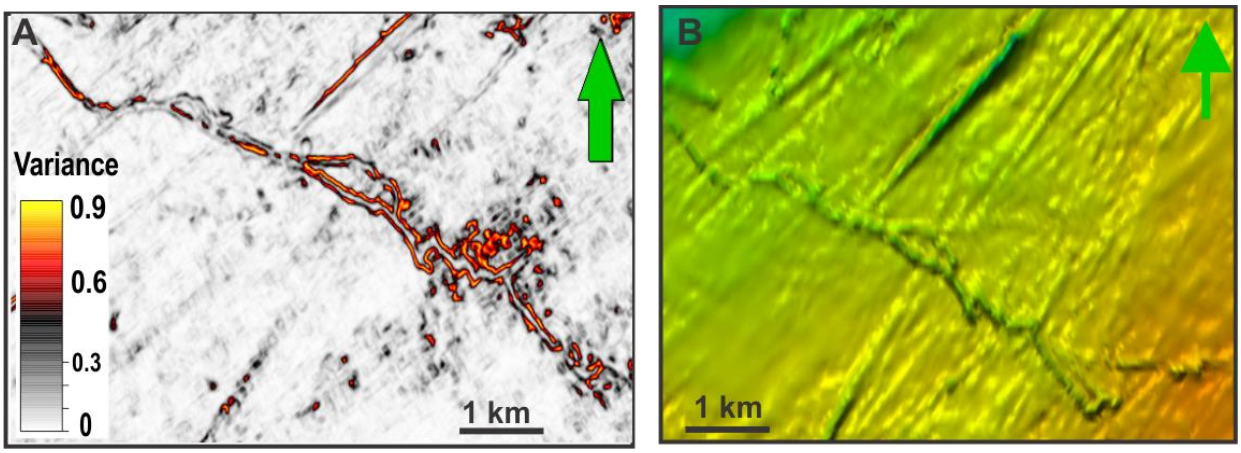

Figure 3.21: (A) time slice from variance cube at t= 612 milliseconds (B) Channel like feature from twt time map of horizon 02.The location of the channel on time relief map can be seen in Fig. 3.22 A.

Interpretation of channel like feature on horizon02 in the survey ST10020

On the basis of variance time slice and surface morphology, the channel is interpreted to be melt water channel that may have been produced due to melting of ice. The high values of the variance time slice may indicate presence of glacio-fluvial sands within the channel as glacio-fluvial sands is common a common sedimentary infill in such features (Ó Cofaigh, C., 1996). These features are also described as tunnel valleys which are elongate overdeepened depressions with often steep asymmetric side that cut into bedrock or glacigenic sediment and form anastomosing or net like pattern (Ó Cofaigh, C., 1996) . The occurrence of such features is common in subglacial landforms (e.g., Smith et al. 2009; Andreassen et al. 2008). The channel is younger than the glacial lineations as it cross cut the lineations (Fig. 3.22 A).

3.3.3 Depressions (Glaciotectonic features)

In all the seismic data used in this study, depressions on shaded relief time-map were observable on some of the subsurface horizons. The results having these depressions will be discussed in the following section.

Description of slightly elongated depressions in the survey ST10020

Two depressions (Fig. 3.22 A & B) appear in the north-eastern part of this horizon. The depressions appear to be linear in shape with elongation in north-south direction. They also appear to be wide in the center and narrow as they shallow. One depression is well imaged while the second depression on the edge cannot be mapped completely due to lack of data but it seems that both the depressions share the same morphology. The length of the well imaged depression is 3 km while the width is 980 m. Some roughness can be seen at the edges of the depression. Lineations can be seen on the sides of these depressions (Fig. 3.22 D).

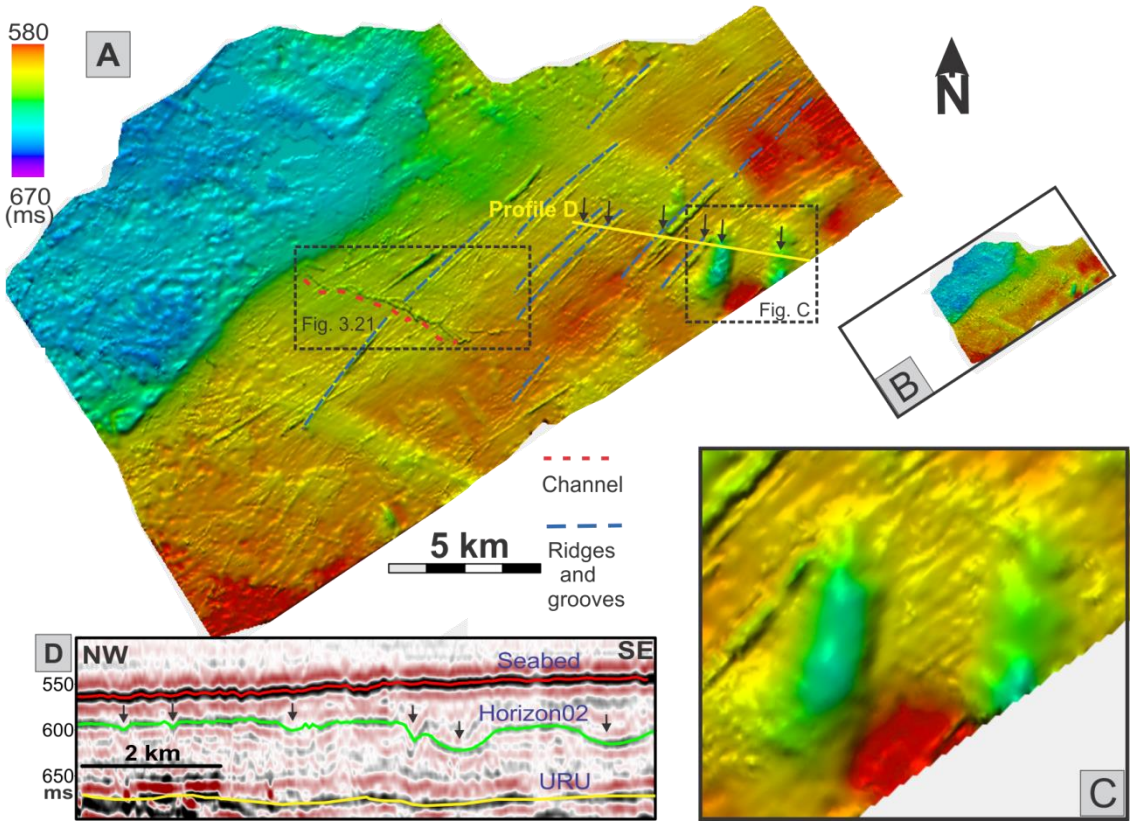

Figure 3.22: A) shaded relief time-map of horizo02 B) Extent of the interpretation of horizon02 in the survey. C) Zoomed view of the depressions D) Seismic Profile across the depressions and linear ridges and grooves marked by arrows on the seismic. The corresponding features on relief time-map is also indicated by arrows

Interpretation of slightly elongated depressions in the survey ST10020

The slightly elongated depressions seem to have been formed by subglacial erosion. Erosion caused by plucking is one of the primary erosional processes (Ber and Aber 2007) that may have produced these depressions. The depressions also have similar morphology to the type II depressions documented by Rafaelsen et al. (2002) which are interpreted to be product of subglacial erosion. Since the lineations cross cuts the depressions which suggest that these depressions may have formed before the lineations.

Description of irregular shaped depression (Type C) on bE in the survey NH0608

A large closed depression (Fig. 3.23) was observed on the surface bE. The depression is irregular in its shape. It is about 5 km long and has a variable width with an average of 2.5 km. The depth of the depression is also variable; it is shallower towards the edges and t deeper in the center, reaching up to 43 m (assuming velocity of 1750 m/s).

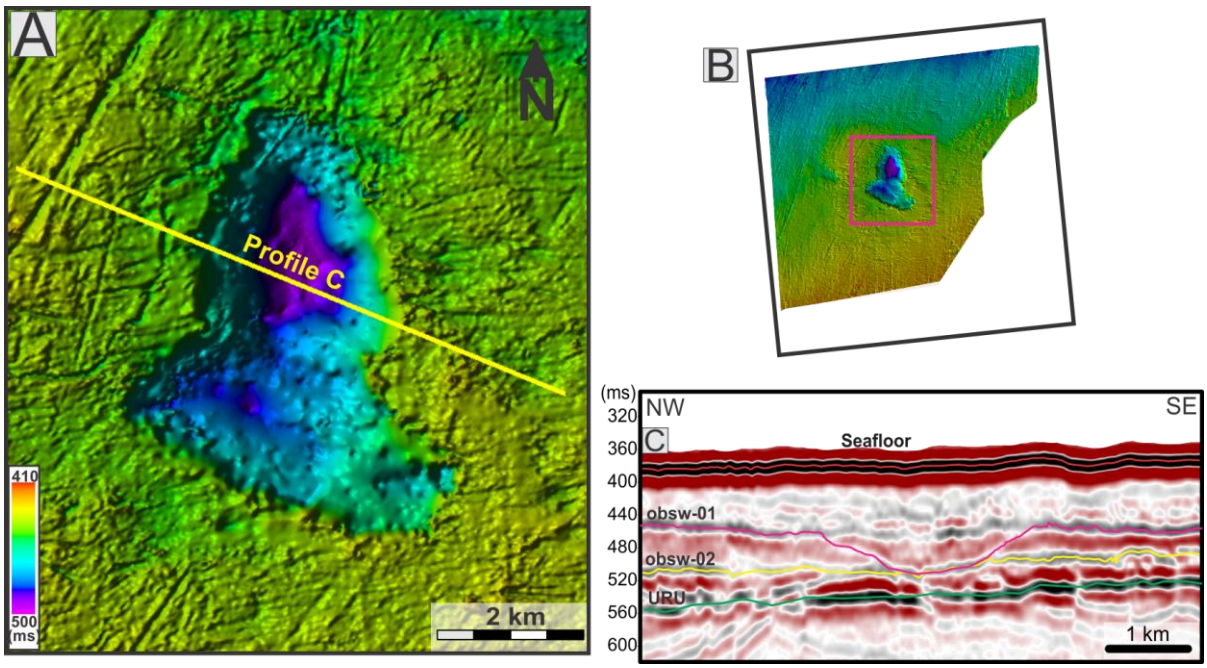

Figure 3.23: shaded relief time-map of bE in the survey NH0608. B) Location of the depression marked by a red rectangle C) Seismic profile across the depression

Interpretation of irregular shaped depression on bE in the survey NH0608

The depression is interpreted to be formed by subglacial erosion. Basal freezing has been common in glaciated south-western Barents Sea (Sættem et al. 1992a & 1996; Ruther et al. 2009). Basal freezing may have occurred here which was followed by a readvance of the glacier, plucking sediment blocks and creating the irregular depression. In addition to basal freezing fluid flow may have acted in erosion as well which will be discussed further in the discussion chapter.

Description of semi-circular depressions on bD in the survey SG9804

Two types of semi-circular depressions can be observed on this horizon. Since there is a variation in in the morphology of these depressions, hence they will be classified as type A and type B depressions.

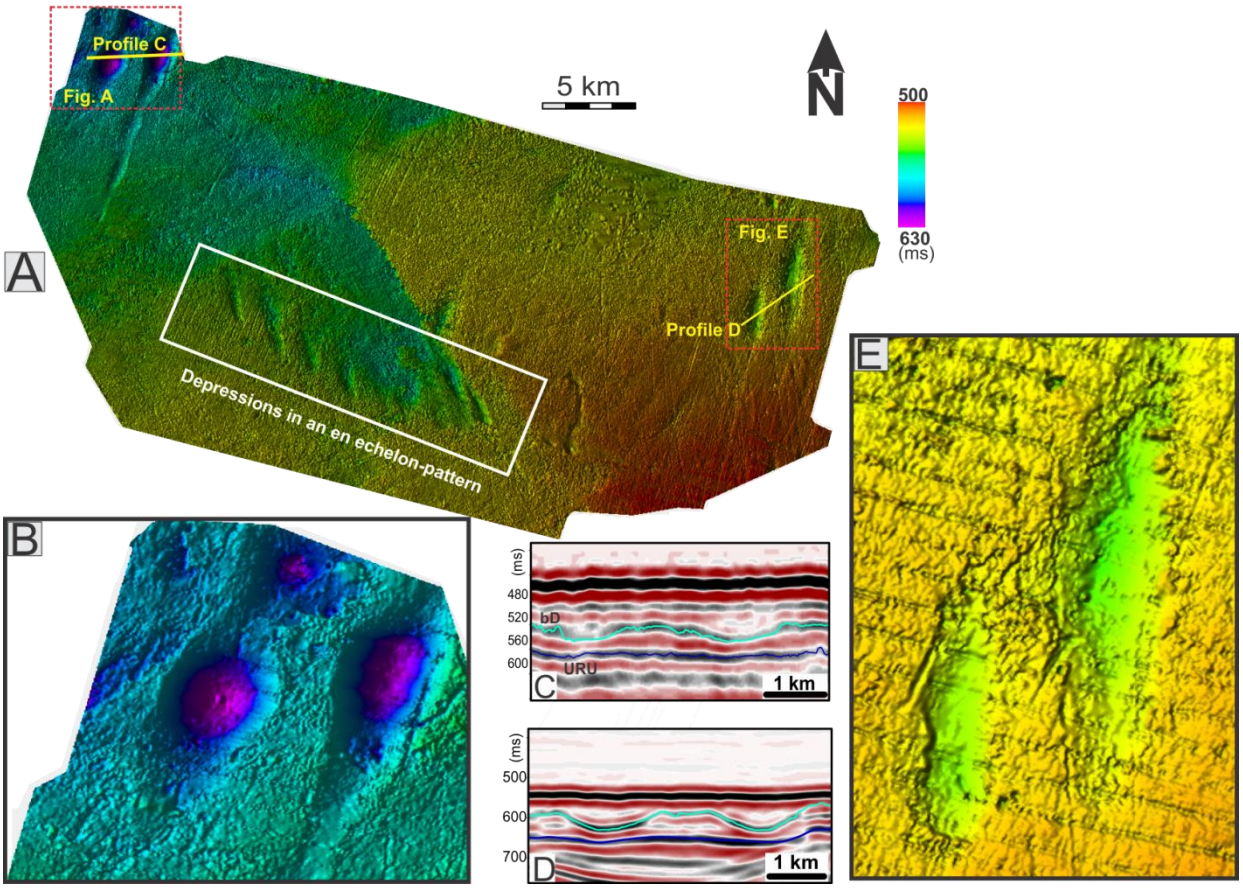

Figure 3.24: A) shaded relief time-map of horizon bD in the survey SG9804 showing different types of depressions. B) Enlarged view of type A depressions C) & D) Seismic profile across the depressions. E) Type B depressions.

Type A depression occur in the northwest of the survey (Fig 3.24 A). The depressions are wide and deep in the center and become narrow as they shallow. One of the depressions seems to continue further southward and can be followed up to a distance of 10 km. The second depression is 1900 m in its longest axis. The width of the depressions along its widest area varies between 1550-1650 m. The depth along the deepest points varies between 36-37 m.

Type B depressions (Fig. 3.24 A) occur as an echelon pattern in the southern part of the horizon as well as two parallel depressions (Fig. 3.24 E) in the northeast. These echelon pattern depressions seem to share the same size. The depressions are not as deep as Type A and some of lineations can be seen passing along the edges of these depressions. These depressions are 7-24 m deep, 1100-1250 m wide along its widest areas and vary in length from 2500-5000 m.

Interpretation of semi-circular depressions on bD in the survey SG9804

These depressions are interpreted to be formed by subglacial erosion. These are also described by Rafaelsen et al. (2002) as product of subglacial erosion. Type A depressions may have been worked by melt water which may have smoothed the edges of these depressions since lineations that occur on this horizon cannot be observed along these depressions.

Type B depressions seem to be formed after the lineations as some of the lineations cross cut these depressions. The Type B depressions in the northeast also seem to have been formed by ice movement with different orientation than the one in echelon pattern as the former has an orientation of north-south whereas the later have an orientation towards north-west and south-east. Furthermore Type A depressions are younger than type B depressions as there are no lineations over them or they may have formed at the same time as type B depressions but due to modification by melt water the lineations cannot be observed over them.

3.4 Results from URU

The horizon was interpreted in all the survey both on the peak and upper zero crossings. The results were more pronounced on the peaks; hence all the surfaces represented here will be from the interpretation on the peak of reflectors. Also only those surfaces will be documented here which showed the features of interest for this study.

3.4.1 MSGL on URU

Description of parallel ridges and grooves on URU in survey HFC

Different sets of linear ridges and grooves (lineations) can be observed on URU time relief map from the surveys SG9804 (Fig. 3.31) and HFC (Fig. 3.25 & 3.26). All the lineations observed can be assigned into groups on the basis of their orientation. At least 4 different lineations can be observed on the basis of the aforementioned criteria.

The lineation set marked by red lines (Fig. 3.26 & 3.27) has an orientation of northeast-southwest and tends to curve towards the west in the southwest. These lineations appear in central northeast part on twt relief map. The lineations are well developed and tend to die towards the west. Some of these lineations seem to reappear in the west. The lineations have a relief of 1.5-5.5 m but some of the lineations that are not detectable on seismic profile may have smaller relief than reported. The individual lineations can be followed from 5 and up to more than 25 km over the surface. The lineations are well developed on the northeast and southeast and tend towards the west. Some furrows with a different orientation marked by dotted pink color (Fig. 3.26) can be observed along these red lineations. These pink lineations overprints the main lineation set marked red color.

The yellow lineations (Fig. 3.26 & 3.28A) are very linear without any curving and have an orientation of northeast-southwest. They are mainly present in the northwest on the time relief map. These lineations seem to continue further to the southwest out of the study area.

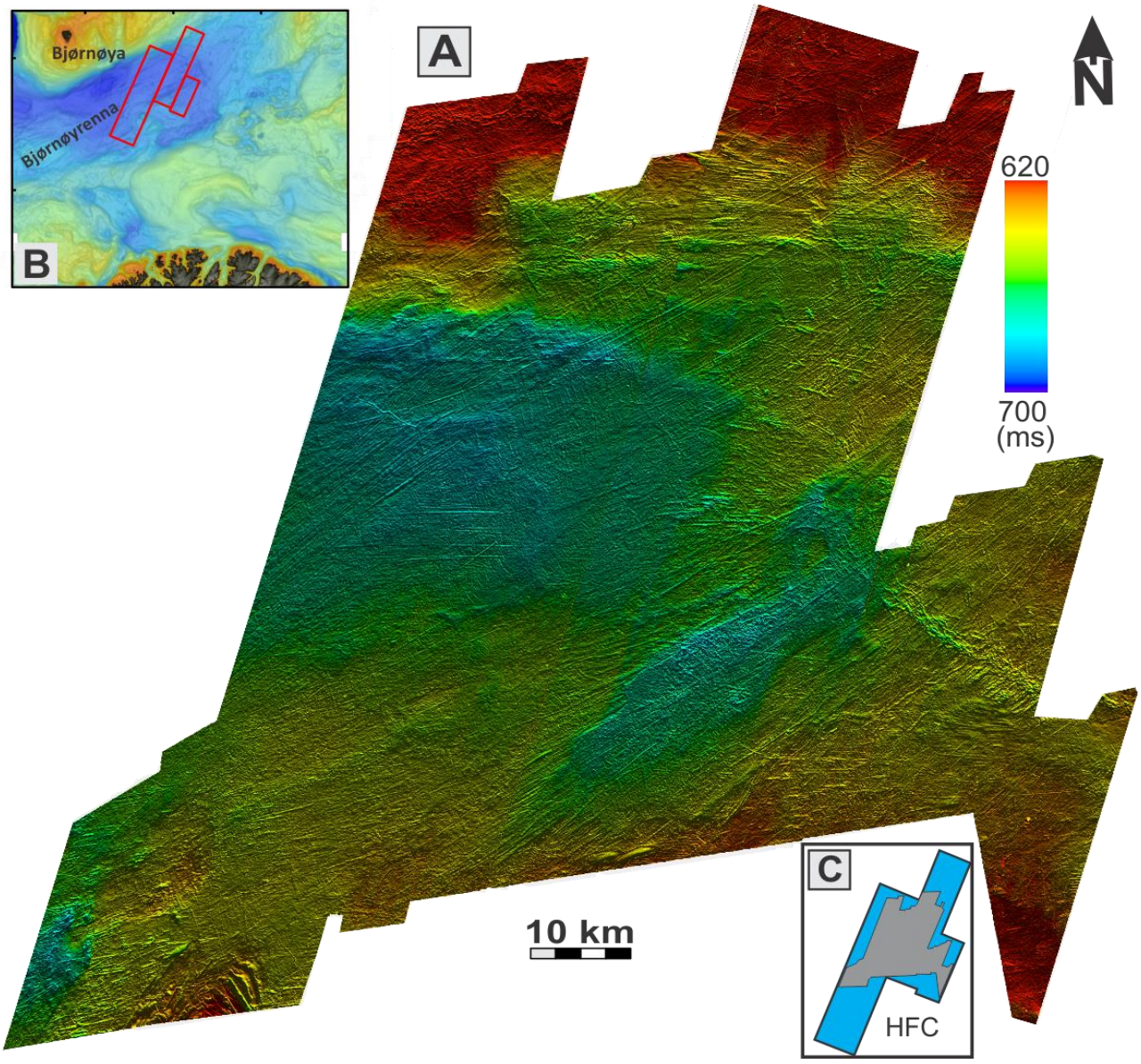

Figure 3.25: A) un-interpreted shaded relief time-map of URU in the survey HFC. B) Location of 3D surveys. C) The extent of interpretation within the 3D surveys is shown by grey polygon.

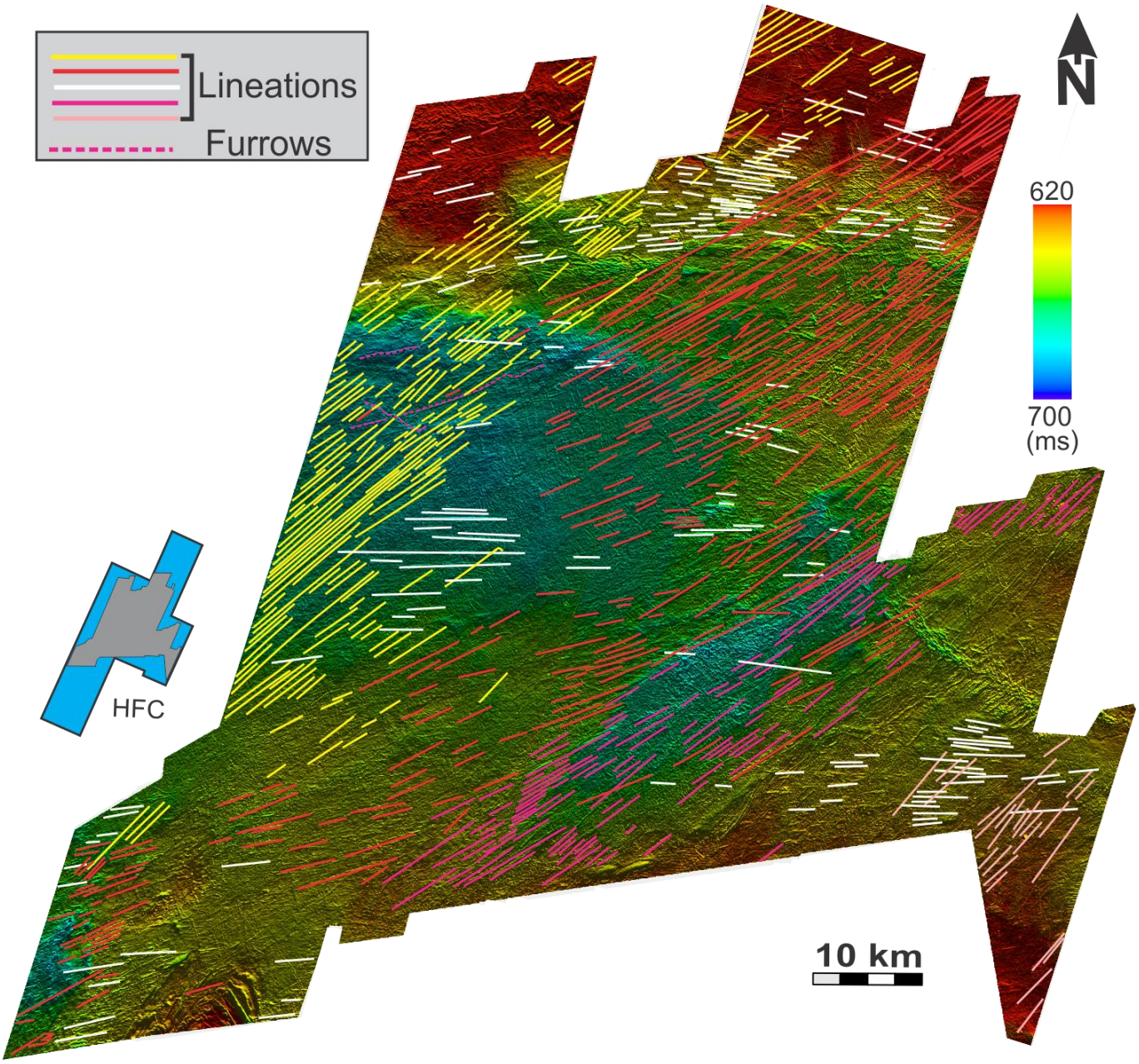

Figure 3.26: interpreted lineations and furrows on shaded relief time-map of URU in the surveys HFC. The extent of the interpretation is indicated in t lower left corner of the figure.

There are some lineations with the same orientation marked in light pink (Fig. 3.26) but it is uncertain if these belong to the yellow lineations as these are situated in the southeast and show less parallel conformity as well as these vary in the overall appearance than the yellow lineations. The relief of yellow lineations ranges from 1.5-3.5 m. The lineations are 150-230 m wide with length ranging from 5 to more than 30 km. The furrows marked by pink color (Fig. 3.28 A) overprints the lineations.

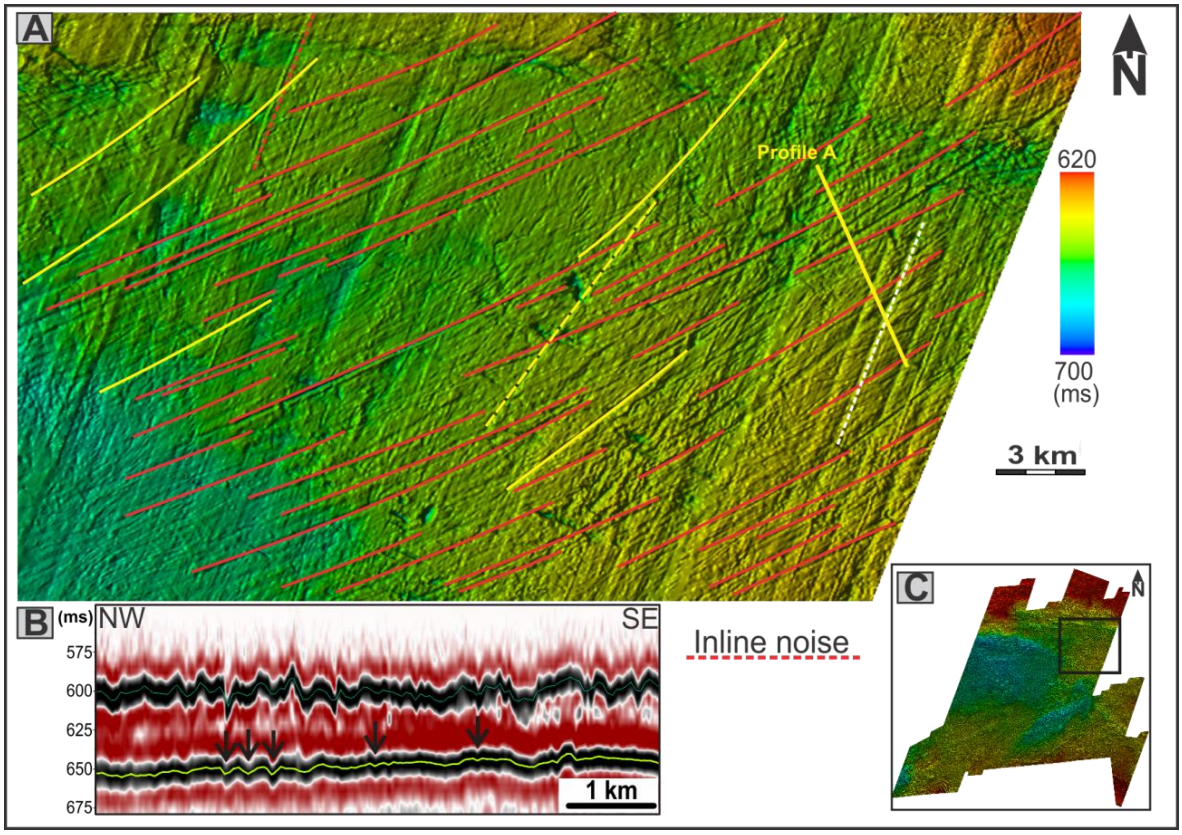

Figure 3.27: A) close view of the lineations marked by red lines on URU shaded relief time-map. B) Seismic profile across the lineations. The lineation's appearance on seismic profile is indicated by black arrows. C) The location of figure on URU shaded relief time-map.

The lineation set marked by white lines (Fig. 3.26 & Fig. 3.29 A) is only present in small parts of the study area, and best developed in the north and in the southeast. These lineations have an east-west orientation. A few lineations with such orientation can be observed at places which are believed to belong to same group. The lineations in the north are closely spaced. These lineations have a relief of 2-4.5 m and width ranging from 80-150 m, but as with other lineations smaller values can be present which are not observable on seismic profile. The

lineations can be followed from few 100 meters to more than 7 km. The lineations die out and reappear at different places. Also the surface along these lineations is not uniform and local highs can be observed (Fig. 3.29).

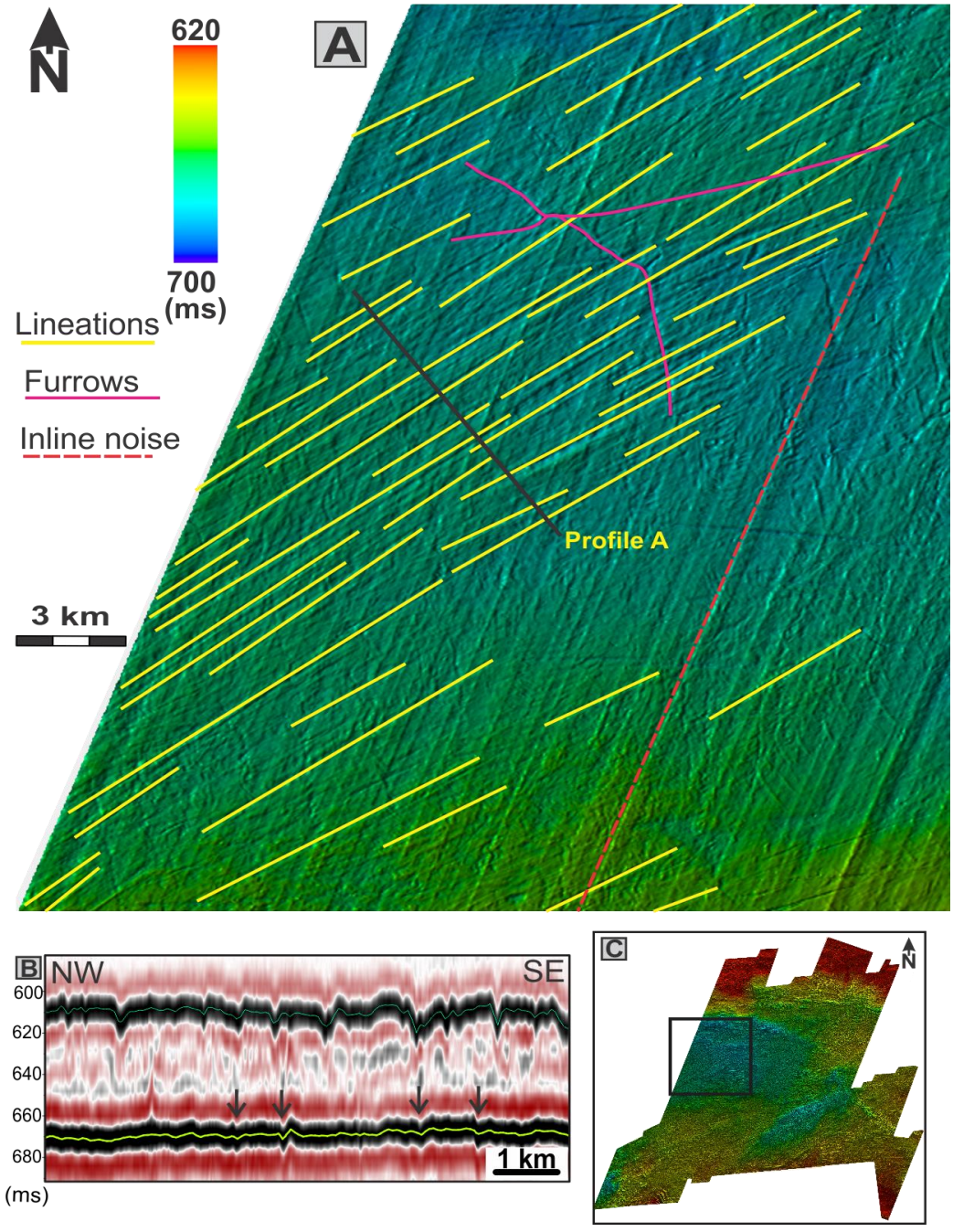

Figure 3.28: A) close view of lineations marked by yellow lines in the northwest of URU shaded time relief-map map. B) Seismic profile across the lineations. The appearance of the lineations on seismic profile is indicated by black arrows B) Location of the lineations on URU on shaded time relief-map

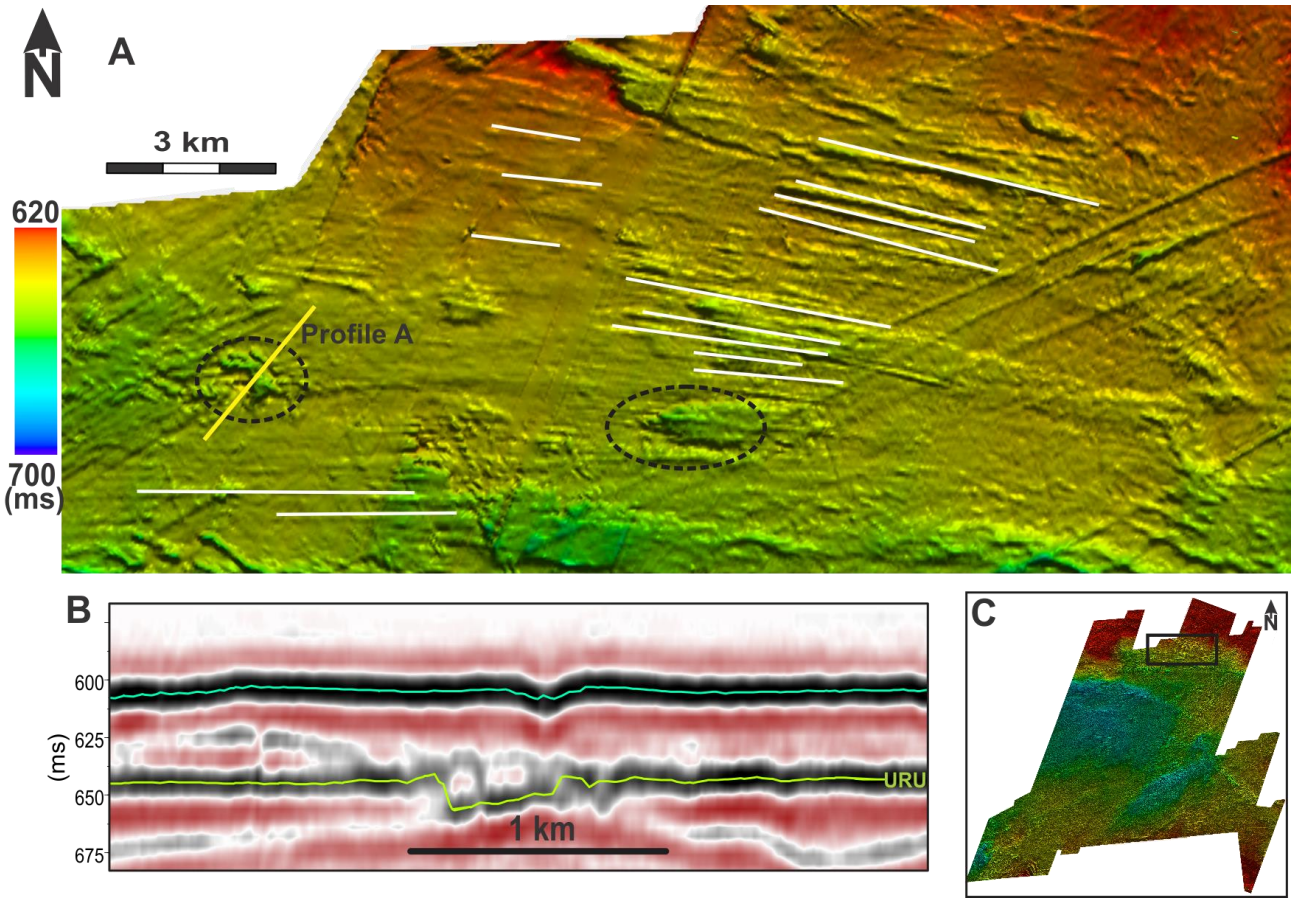

Figure 3.29: A) close view of lineations marked by white lines in the northeast of URU shaded time relief-map. B) Seismic profile across the depression observed along these lineations. Some of the depressions are indicated by dotted circle. C) Location of the lineations on URU shaded relief time -map.

A lineation set marked by magenta color (Fig. 3.26 & 3.30 A) in the southeast can be seen, having an orientation of northeast-southwest. The lineations can be followed from few meters and up to a distance of 1.5 km. The relief of the lineations ranges from 2-9 m while the width is from 70 m to 145 m. The lineations seem to diverge as it ends towards southwest. This set occurs in a depression which is obvious in twt relief map. The surface along this depression is not uniform and some highs marked by white arrow in figure 3.7 can be seen towards the end as the lineations terminate.

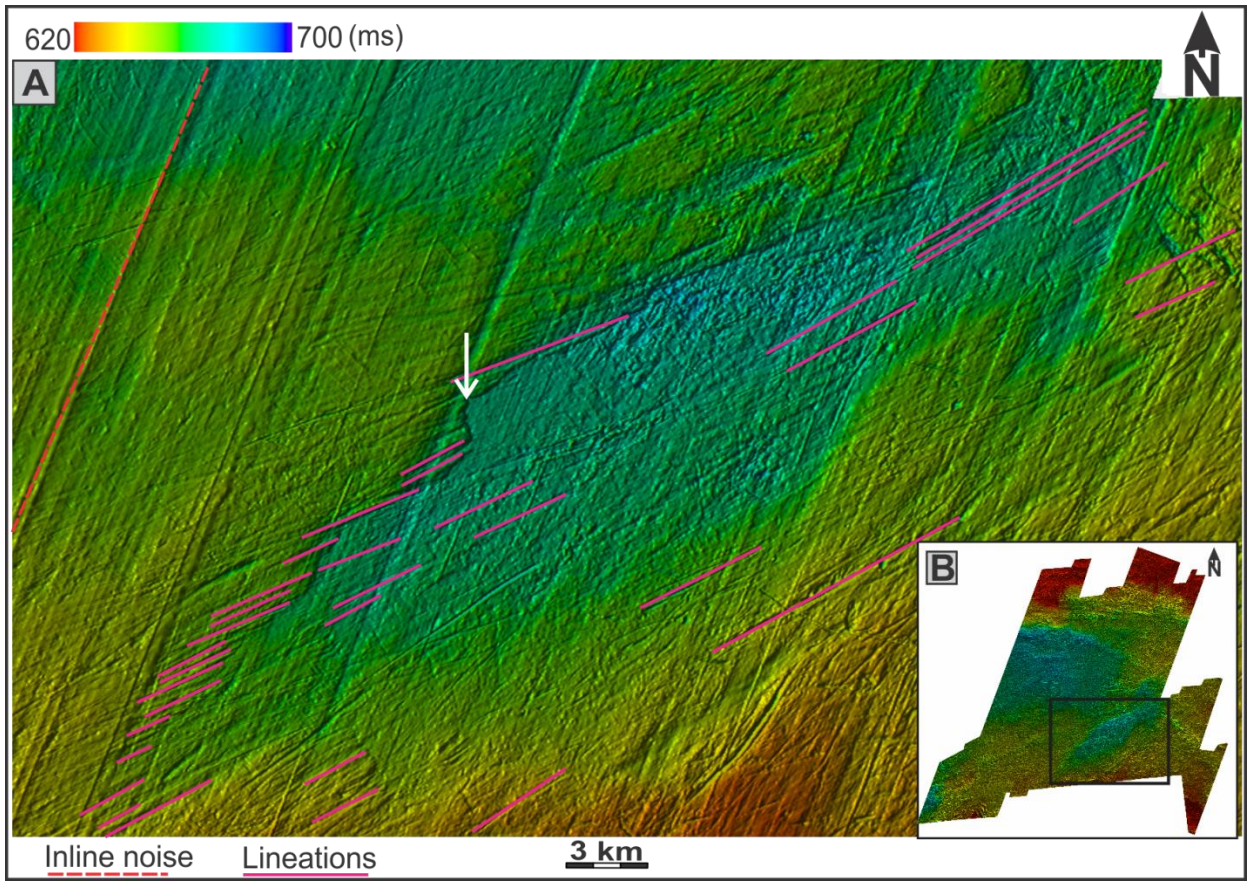

Figure 3.30: A) close view of lineations marked by pink lines in the southeast of URU shaded time relief-map. B) Location of the lineations on URU shaded time relief map. High relief areas can be seen along these lineations as indicated by white arrow.

Interpretation of parallel ridges and grooves on URU in survey HFC

Based on the morphology, the linear ridges and grooves (lineations) are interpreted to be mega scale glacial lineations (MSGL) (section 3.2.3). The different orientation of the MSGLs can be either related to switching on and off of the same ice streams with the source area shifting each time at different time intervals or it may be due to ice streams that operated at various time each with its own source area. Looking at the large scale landforms of the seafloor in southwest Barents Sea, the second explanation seems more likely. It will be further discussed in the discussion part in the next chapter.

The red lined lineations are interpreted to be the youngest since it cross-cuts other lineations. The lineations marked by white color are older as these are overprinted by the black

lineations. The white marked lineations also seems to be older than the yellow marked lineations as these are overprinted by the later. The white marked lineations also seem to be older than the lineations marked by magenta color. The light pink color lineations overprints the white lineations hence these are younger than the white lineations. Based on this the youngest lineations in the study area are shown by black lines while youngest by white lines.

The furrows are interpreted to be ice berg scour marks (section 3.2.1) and since these overprints the lineations which suggest that these are younger. Also based on this observation it can be inferred that glacio-marine conditions followed after the subglacial conditions which formed MSGLs.

The slight highs of the URU surface are interpreted to be areas where there had been less subglacial erosion as the bed rock below the URU truncates toward the glacigenic part but seems like the central part of these truncated reflectors had been eroded with respect to the sides (Fig. 3.29 B)**.**This may had been due to the nature of bed rock which resisted erosion in these areas which are now represented by relatively high relief areas than the depressions.

Description of parallel ridges and grooves on URU in survey SG9804

The horizon is marked by a strong peak (Fig. 3.31 B) in the 3D survey. Throughout the survey the reflector can be followed very well except the south-west region (Fig. 3.31 D) where it becomes chaotic due to truncation of underlying reflectors into it. The horizon was mapped on both the peak and upper zero crossings. The features were more pronounced on the peak along this horizon. The extension of the interpretation within the 3D survey can be seen in figure 3.31 D.

Three sets of linear furrows and grooves (lineations) can be observed on time relief map of this horizon (Fig. 3.31 A & C). The lineations set marked by red lines have an orientation of southeast-northwest while the lineations marked by white lines have an orientation of north-east (Fig. 3.31 C). The red marked lineations are well developed on the surface than the white lined lineations. The lineations are 1.6-9 km long with ranging from 80-160 m. The relief of the lineations ranges from 2-3.5 m. Some of the lineations may have relief smaller than this but they are not imaged well on the seismic hence it is difficult to determine accurate relief for these

lineations. The white marked lineations overprints the red marked lineations. The lineations marked by magenta lines in the main figure overprints the red lined lineations and have orientation in northeast-southwest direction (Fig. 3.31 A). A furrow marked by white dashed line (Fig. 3.31 A) can be observed with a relief of 18 m and width of 200 m. It also seems to be overprinted by the lineations observed on this surface.

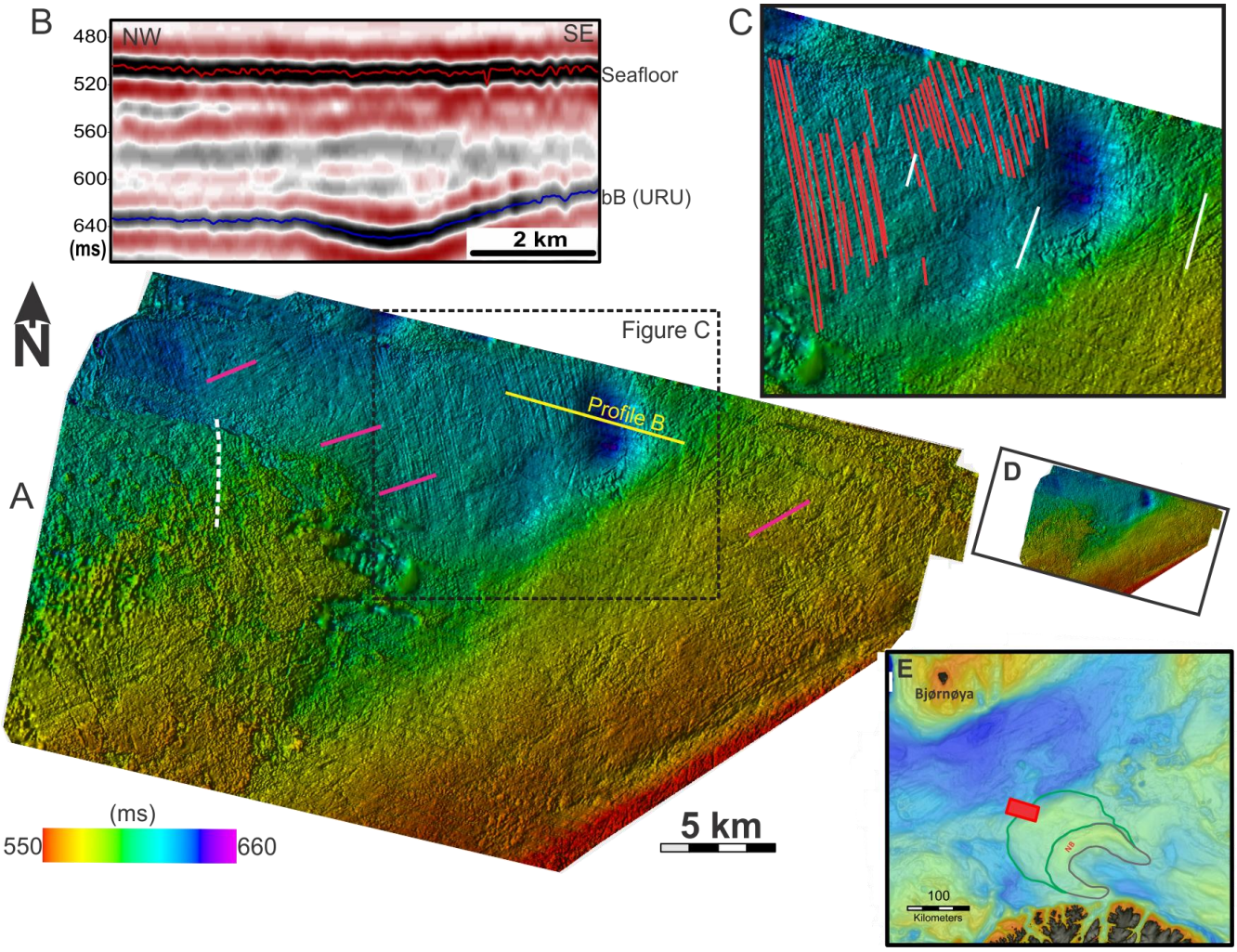

Figure 3.31: A) shaded time relief-map of horizon bB (URU) B) seismic profile across the depression on URU C) zoomed in view of the lineations on the surface D) extent of the interpretation in 3D survey E) Location of 3D survey

Interpretation of parallel ridges and grooves on URU in survey SG9804

The lineations are interpreted to be megascale glacial lineations formed under subglacial conditions (section 3.2.3). The lineations have quite opposite orientations, the magenta colored lineations have orientation in the northeast-southwest direction while the red lined lineations have an orientation in southeast-northwest direction hence these may had been produced by two different ice streams operating at different ice streams. The white lineations may be megascale glacial lineations as well but it is difficult to say anything with respect to the ice stream for it as only two of these lineation are observable on the whole surface. The possibility of erosion cannot be ruled out for these lineations.

The lineations marked by red color are younger than the lineations the magenta colored lineations as the former overprints the later. The absence of the lineations on the rest of the surface can be attributed to erosion if any lineations were present or it may not be within the resolution limit of the data.

3.2.1 Channels like Feature on URU

Description of Channel-like feature in the survey HFC

A number of channels like feature (Fig. 3.32) appear in the southeast of the URU surface in the HFC 3D surveys. To enhance the feature this area was interpreted on the lower zero crossing. The feature emerges as a single body in the shallow part in the southeast and run towards northwest developing into anastomosing like pattern. On seismic profile the channel is represented by depressions which cut into the bed rock beneath URU (Fig. 3.32 B & C). The depth of the channel varies between 10-30 m with respect to adjacent URU surface. The depth decreases towards the northwest as we move from southeast. The width of the channel like feature increases towards the northwest as it diverges into many other small channels like features. The feature is overprinted by the lineations observed on this surface (section 3.25).

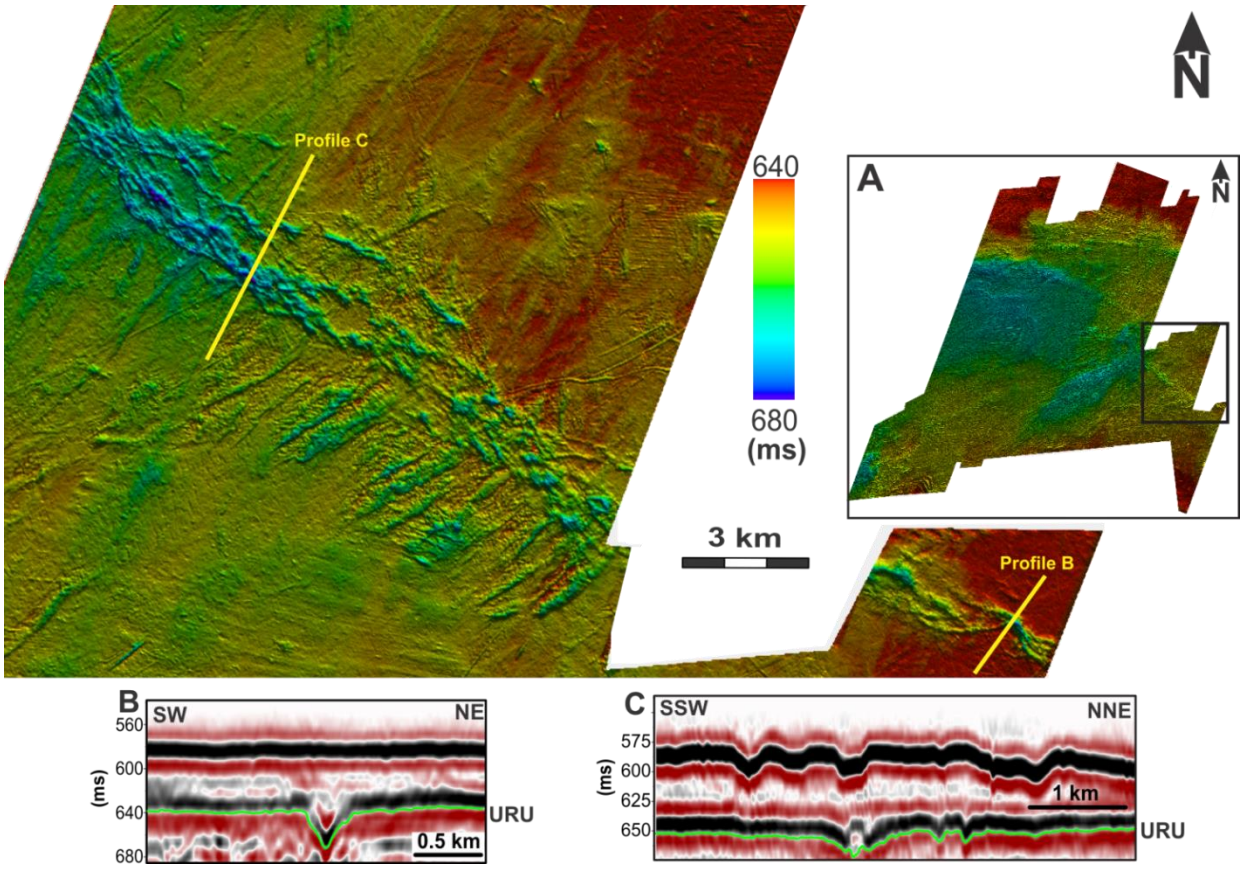

Figure 3.32: shaded relief time-map of URU showing a channel like feature. A) The location of channel on URU twt relief map. B) and C) seismic profile along the channel. The channel is also characterized by depressions on seismic

Interpretation of Channel-like feature in the survey HFC

The channels like feature are interpreted here to be a melt water channels (Section 3.3.2). Melt water channels have been reported in southwest Barents Sea by Andreassen et al. 2008 and by Wellner et al. 2006 from Ross Sea in Antarctica. The depressions cut into the bed rock which may suggest that some erosion of bed rock might have taken place along with the erosion of glacigenic sediments. The overprinting of the channel by the lineations suggests that the channel is older with respect to lineations.

4 Discussion

The main topic of discussion for this study is ice streams dynamics. Source areas for the ice will be suggested and so will also potential changes in source areas over time, based on mega-scale glacial lineations observed on buried surfaces. Also the various geomorphological elements like iceberg plough marks and channels will be discussed briefly. The glacio-tectonic features occurring in this study will be discussed as well along with its relation with fluid flow migration.

4.1 Ice streams dynamics

The morphological elements observed in the study area like MSGLs and depressions suggest that glacial erosion was a common process. The paleo-ice flow direction in the study area can be inferred from the orientation of these MSGLs. Paleo-ice streams have been identified based on glacial landforms and used for reconstruction of numerous paleo-ice sheets (e.g., Andreassen et al. 2008; Winsborrow et al. 2009; Rafaelsen et al. 2002; Dowdeswell et al. 2010). These ice streams are the controlling factors for ice and sediments within an ice sheets (Bennet 2003). The factors controlling the location of an ice stream within an ice sheet is discussed by Winsborrow et al. (2010, b). The dynamic nature of the ice steams in the southern Barents Sea is documented by various authors (e.g., Andreassen et al. 2007b; Andreassen et al. 2008; Rafaelsen et al. 2002; Ottesen et al. 2005). The hypothesis for formation of MSGLs is open to discussion with respect to either being formed by depositional process (Clark, 1993; Canals et al. 2000) or erosional processes (Tulaczyk et al. 2001; Clark et al. 2003; Andreassen et al. 2007 b). The MSGLs interpreted in this study (e.g., Fig. 3.10, 3.14, , 3.26) appear as sets of ridges and grooves, which indicate that the grooves were created by erosional processes with residual accumulation appearing as ridges (Tulaczyk et al. 2001). The presence of various orientations of the MSGLs observed on different surfaces indicate that the ice streams had been dynamic; switching on and off, changing flow trajectories and cross-cutting each other.

The MSGLs observed can be grouped into flow-sets which are defined as landforms of coherent and systematic pattern that record distinct phases of ice flow (Clark, 1993; Clark et al.

2000; Winsborrow et al. 2009). The MSGLs mapped (e.g., Fig. 3.10 & 3.25) can be grouped into flow-sets on the basis of following parameters:

1. Parallel conformity

   The MSGLs within a flowset need to have a similar orientation in comparison to its neighbors.

2. Morphology

   The MSGLs observed within the same flowsets are required to exhibit similar geomorphology.

3. Close proximity

   The MSGLs within the same flow-set are required to be closely packed, with the spacing between each MSGL observed more or less constant.

Each flow set could possibly represent a flow for a particular period. The width of each flow set can be indicative of the width of the ice stream, however glacial erosion is a common process in ice streams therefor consideration should be taken if there had been some erosion of previously formed MSGLs by later glacial erosional processes. Two end member ice stream landsystems (Fig. 4.1) are devised by Clark and Stokes (2003) for possible reconstruction of paleo-ice streams: (i) the 'rubber stamped' or isochronous (Fig. 4.1 A) imprint which is produced when an ice stream imprint is produced at the same time and represents the time activity of an ice stream when the ice stream witched off. Hence every bedform within such a flow set will be of approximately same age. (ii) the 'smudges' or overprinted, is a time transgressive imprint (Fig. 4.1 B) which is produced when an ice streams operates through several cycles of advance and retreat or continuous retreat, hence earlier imprints are modified and/or overprinted by the later flow cycles and therefore the flow sets will have different ages.

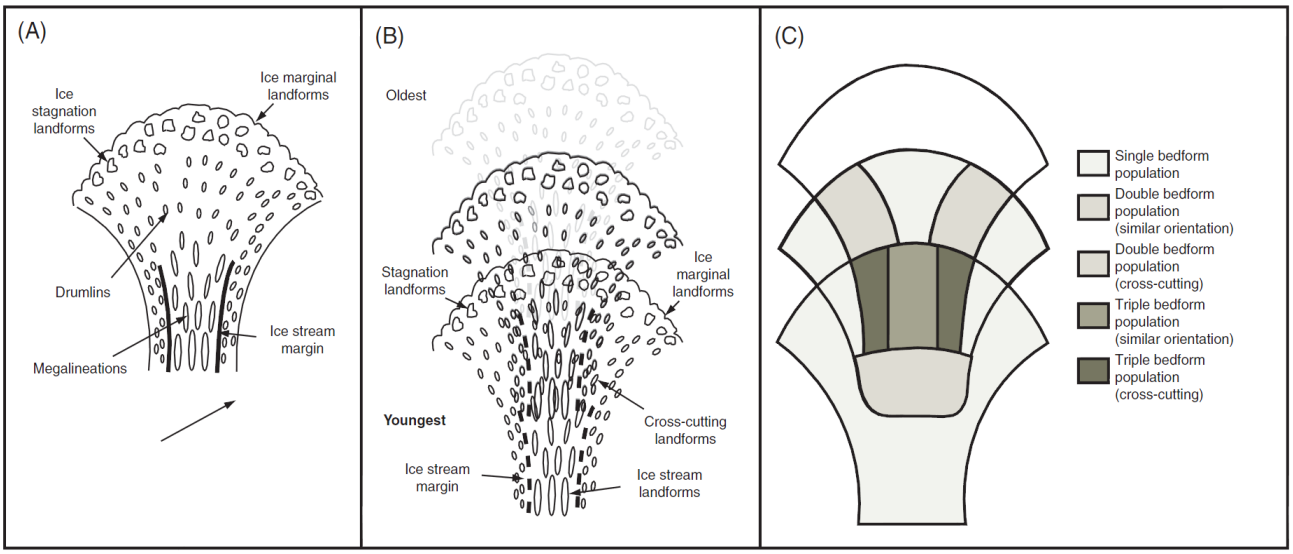

Figure 4.1: End member of paleo-ice streams imprints A) Rubber stamped imprint or imprint of ice stream shutdown. B) Smudges or time transgressive ice stream imprint. C) Schematic diagram showing the distribution of various cross-cutting bedforms imprints associated with time transgressive ice stream landsystem. From Clark & Stokes (2003).

4.1.1 Paleo-ice streams on URU

On URU surface (Fig. 3.26) in the Bjørnøyrenna trough, various orientations of megascale glacial lineations are observed and grouped into different flowsets with different colors (Fig. 3.26 & Fig. 4.2). The dominant flow set is marked by red color and has an orientation of northeast which is curving towards the western side. Based on the URU time relief map (Fig. 4.2), the source area for the ice stream is likely to have been located in the high relief northern areas like Storbanken (Fig. 4.3). The curving nature of the ice stream is coherent with the present day topography as well as URU time relief map of Bjørnøyrenna. Hence, these observations indicate that the ice stream followed the Bjørnøyrenna trough and the trough existed in the study area since URU time. Relatively this flow set is the youngest on this surface.

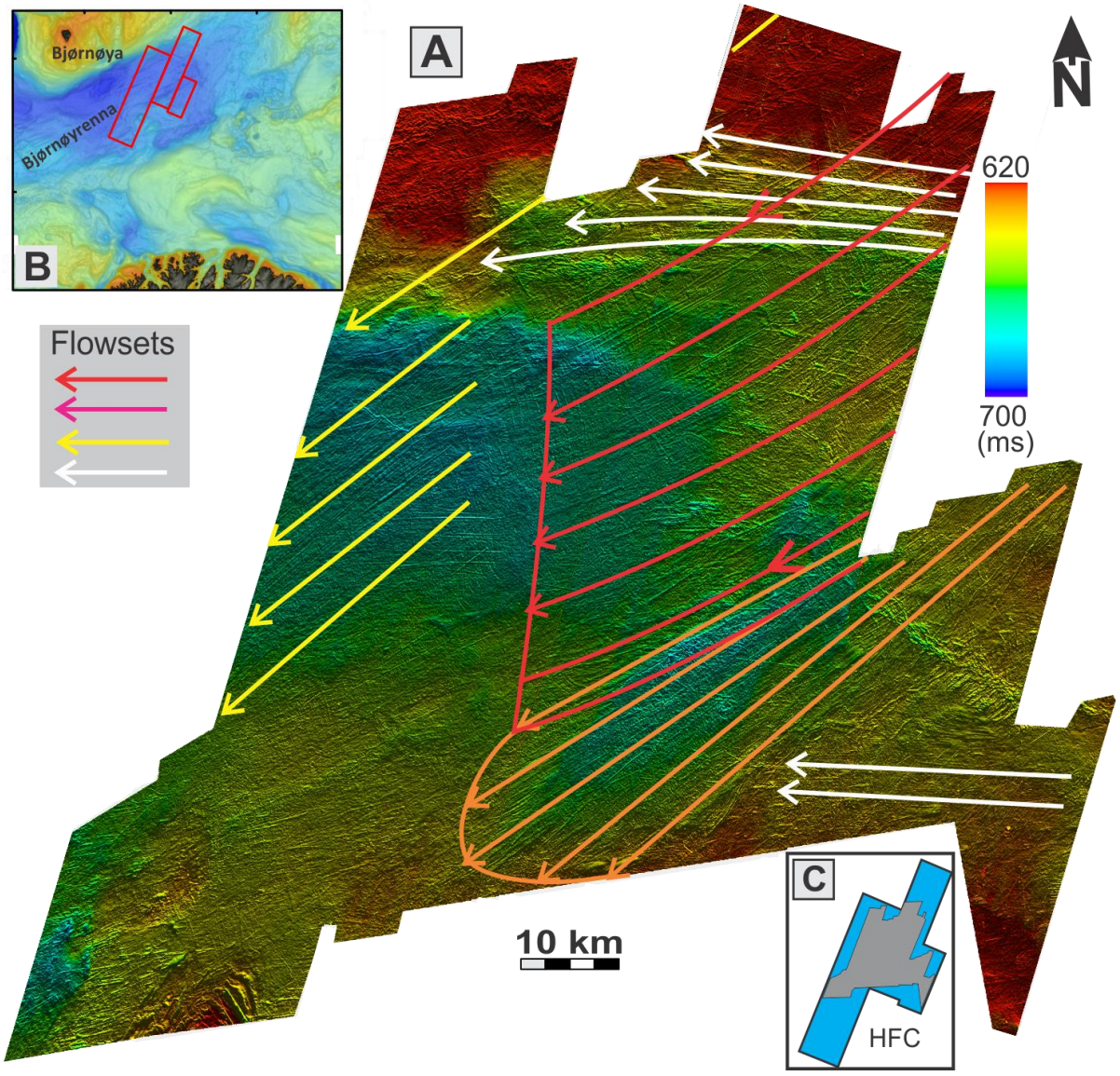

Figure 4.2: A) shaded relief time-map of URU in HFC surveys showing interpreted flowsets of various ice streams on this surface. B) Location of HFC surveys on IBCAO bathymetric map. C) Extent of interpretation in the survey.

In the southern part of URU relief time-map, MSGLs marked by orange color (Fig. 4.2) are observed with an orientation of northeast-southwest. These lineation set tend to curve more towards the southern side and diverges from the lineations set marked by red color. Also the relief is slightly deeper under these lineations. The divergence like pattern is observed in the Barents Sea (Andreassen et al. 2008; Rebesco et al. 2011) as well as in some modern ice masses like the former Larsen B ice shelf on the Antarctic Peninsula (Glasser and Scambos,

2008). The divergence in Barents Sea in Kveithola paleo-ice streams (Rebesco et al. 2011) is interpreted to be a single ice stream due to absence of cross cutting relationship however since in this study we can see the cross-cutting of the orange colored flowset by the red colored flowset (Fig. 4, it can be inferred that these flowsets generated from either (i) an ice stream that changed its orientation or (ii) these ice streams existed concurrently adjacent to each other at various times. In this case the second explanation is more likely. The ice streams with red color flow set (Fig. 4.2 A) operated from a northern source and followed the topography curving towards the eastern side whereas based on the orientation of the magenta colored flow set, it is more likely that the source for this paleo-ice stream is from the northeastern side like Sentral banken (Fig. 4.3). It should also be noted that the seismic data has a resolution of 9 m and that these lineations may not be on one single surface but from result of surfaces.

Based on the relief, the flow set marked by yellow color (Fig. 4.2 A) with northeast-southwest orientation have likely a source area from the northern side like Storbanken areas. This flow set is older than the red flow set, therefore it is likely that this paleo-ice stream might have operated in the whole area but as a new ice stream (red flow set) operated later in time, these earlier yellow lineations were eroded in that area. The red flow set does not continue further (Fig. 4.2 A) towards the west may also suggest that this may have been the grounding line for the ice stream represented by red lineations (Fig. 3.26) and eroded the earlier imprints of yellow lineations while the yellow lineations further down in the western side were preserved as these were outside the grounding line of red colored flowset. The light pink flowset in the southeastern part (Fig. 3.26) may be the same lineations as the yellow lineations which are preserved as the width of paleo-ice stream represented by the red lineations did not reach further down which can also be supported by the absence of the red lineations in this part of the URU relief map.

The white MSGLs appear dominantly in the northern and southeastern part in high relief areas of URU relief time-map (Fig. 3.26). The flow sets diverge towards the eastern side (Fig. 4.2 A). Also there is lack of other lineations where the white lineations are present. Hence it can be inferred that this was the oldest flow set recorded in the area for the ice streams which is preserved in these high relief areas.

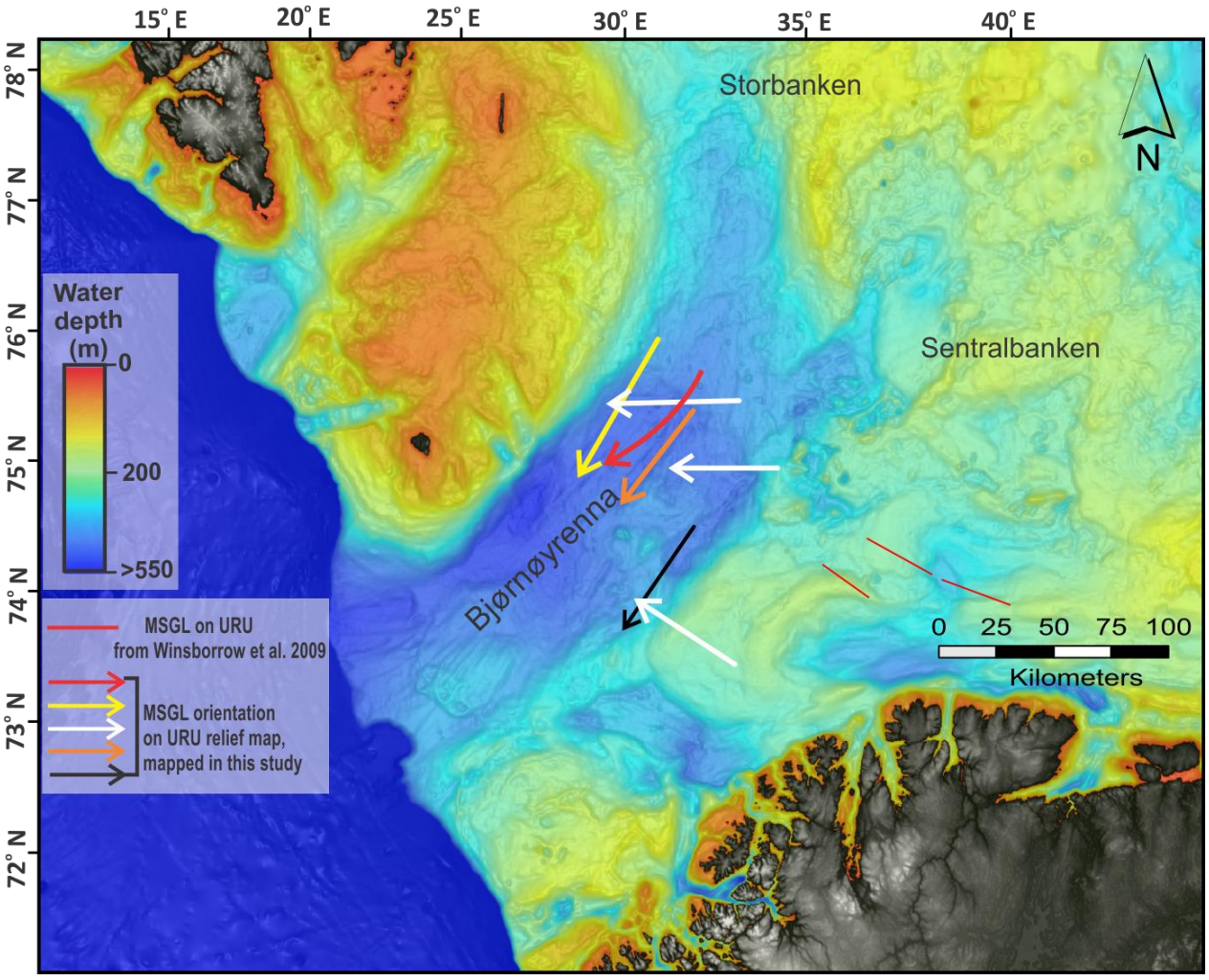

Figure 4.3: Inferred orientation of various MSGLs flow sets on IBCAO bathymetry (Jacobsen et al. 2012). Lineations on URU from Winsborrow et al. (2009) can also be observed in figure marked by red lines.

At least four ice streaming events are indicated from the mapped flowsets. The flowsets with northeast-southwest orientation (Fig. 4.2 A) are likely to have originated from a same northern source at various times however, as mass loss occurred the mass of the ice sheet changed which lead to different orientations of these flow sets. The white flow set is more likely indicate ice streaming from the east like Sentral banken (Fig. 4.3). All the megascale glacial lineations on URU are likely to have originated during the glaciation of the Barents Sea.

On the URU relief time-map of the survey SG9804, three different flow sets can be seen marked by pink, white and red color (Fig. 3.31). The various orientations of these lineations

suggests three ice streaming events while the overprinting of these lineations further suggest various timing periods for these ice streaming events.

The youngest ice streaming event on this surface is marked by red lineations with an orientation of northwest-southeast (Fig. 3.31). The lineations are likely to have caused by ice streams from Fennoscandian ice sheet near the northern coastal area towards Ingøydjupet (Fig. 4.3, marked by white arrow in the figure). The white lineations (Fig. 3.31) are although youngest of all the lineations on this surface however, the presence of just a few of them makes it difficult to assess if these could be part of a paleo ice stream.

4.1.2 Paleo-ice streams on sub-surface horizons

Only one horizon was mappable in each of the surveys (ST10020 & HFC) in Bjørnøyrenna. These horizons cannot be correlated to the horizons mapped in the surveys (SG9804 & NH0608) on Nordkappbanken however; these horizons are interpreted to be younger than 17,090 cal yrs BP (section 3.1). Based on the aforementioned information, it seems likely that these lineations were formed by ice streams that operated during the stage 3 of deglaciation model of the Barents Sea ice sheet (Winsborrow et al. 2009).

The orientation of the flow sets on hor-01 in the survey HFC suggests 3 time transgressive ice streaming events (Fig. 4.4). The red flow sets (Fig. 3.14) is the youngest event with a probable source from the north Storbanken areas (Fig. 4.4). The white flow set has almost the same orientation with a slight tilt towards eastern side and is older than the red flowset. This suggests that the white and red lineations may be part of the same ice stream that slightly changed its position. However the possibility of these lineations from separate ice streams cannot be ruled out. In both cases the source areas is suggested to be from northern areas like Storbanken (Fig. 4.4). The flow sets marked by orange color (Fig. 4.4) is the youngest. The east-west orientation suggests that this ice stream had a source area from Sentralbanken in the east.

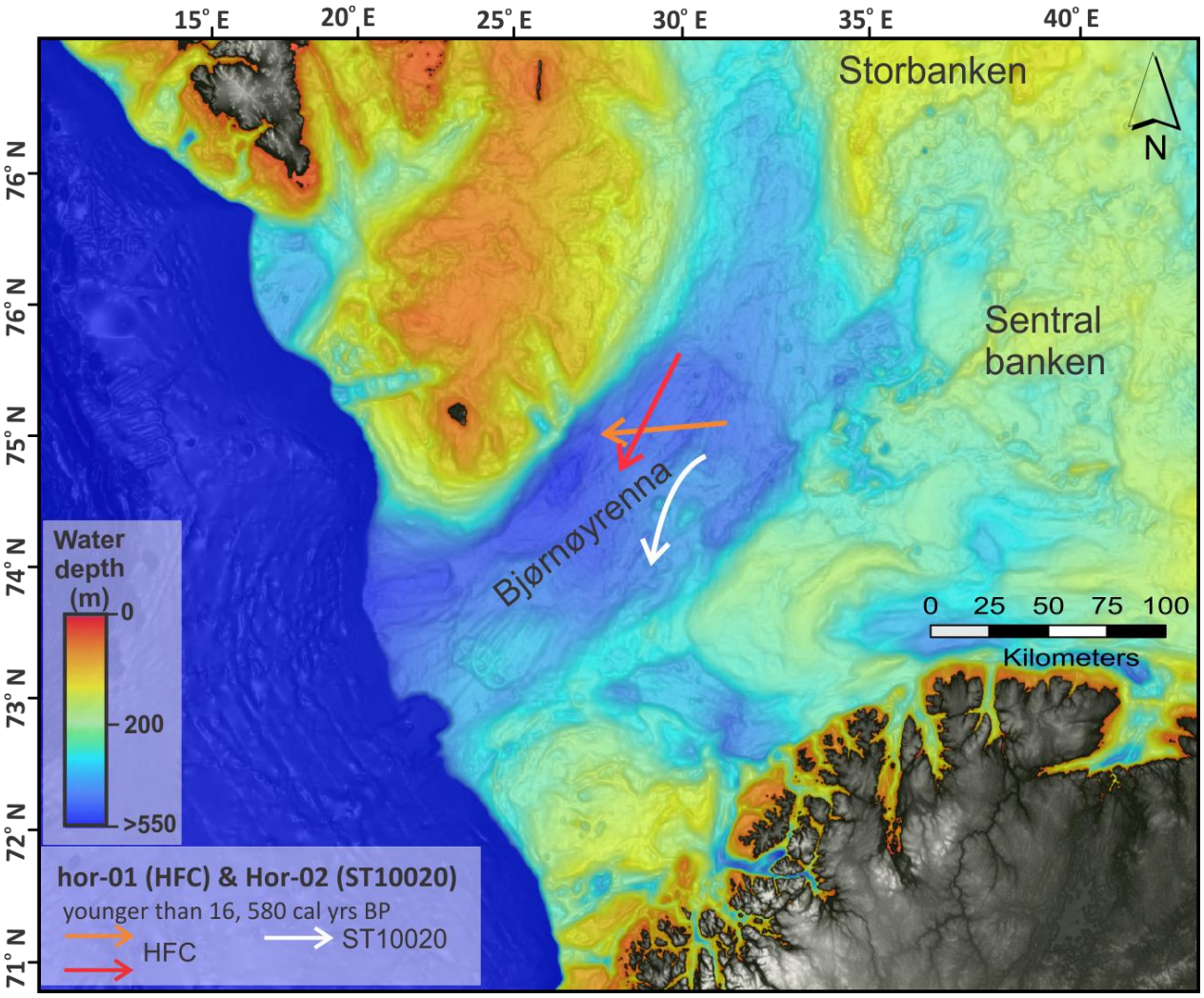

Figure 4.4: Inferred orientation of ice streams on hor-01 and hor-02 in the survey HFC and ST10020 respectively.

The orientation on hor-01 in the survey ST10020 suggests an ice stream with a northeast-southwest direction which is tending to curve towards southern part. As a result the lineations can only be found in the northeastern area on relief time-map (Fig. 3.16). It is likely that these lineations have a northern-eastern source area from Sentralbanken (Fig. 4.4). As only one flow set is present, this represent an isochronous ice streaming event.

In the Nordkappbanken area, MSGLs are observed on bE and bD in the survey NH0608, (Fig. 3.17 & Fig. 3.19) and on all sub-surfaces (bE, bD, Fig. 3.18 & Fig. 3.20) in the survey SG9804. The surface bE corresponds to the stage 2 of deglaciation model (Winsborrow et al. 2009) based on its chronology (Ruther et al. 2009; Rafaelsen et al. 2002). The flow set marked by white lines

on this horizon (Fig. 3.18 & Fig. 4.5) have northeast-southwest orientation and represents the oldest flow on this surface.

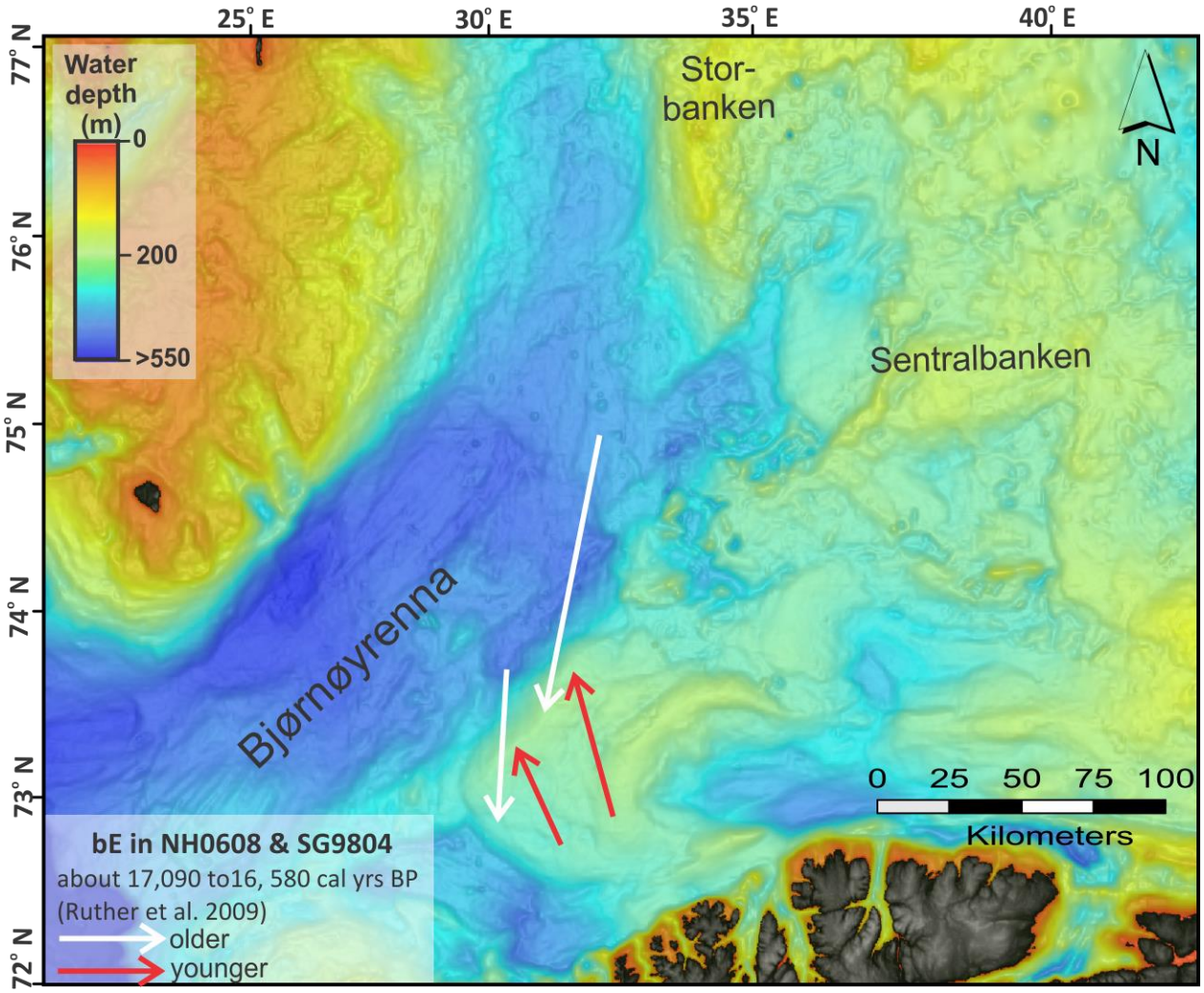

Figure 4.5: Inferred orientation of ice streams on bE in the survey NH0608 and SG9804 respectively.

Looking at the topography of the area it is likely that these are generated by an ice stream with a source from north like Sentralbanken. The same orientation of MSGLs can be observed on bE in the survey NH0608 marked by white lines (Fig. 3.17), which correlates to this surface (Fig.3.4, section 3.1) further confirms that an ice stream operated in northeast-southwest orientation with a source from the northern areas like Sentralbanken from the Barents Sea ice sheet. There is a second flow set on both the surface of bE in the survey SG9804 (marked by yellow lines in Fig. 3.18) and NH0608 (marked by red lines in Fig. 3.17) which is younger on both surfaces with roughly north-south orientation. This flow set suggests that a

second ice stream operated later in time during this time with a possible source from the Fennoscandian Ice sheet however, the possibility of the source from Barents Sea ice sheet cannot be ruled out. Based on the aforementioned discussion, the orientation for the ice streams that operated on these surfaces can be observed in Fig. 4.5.

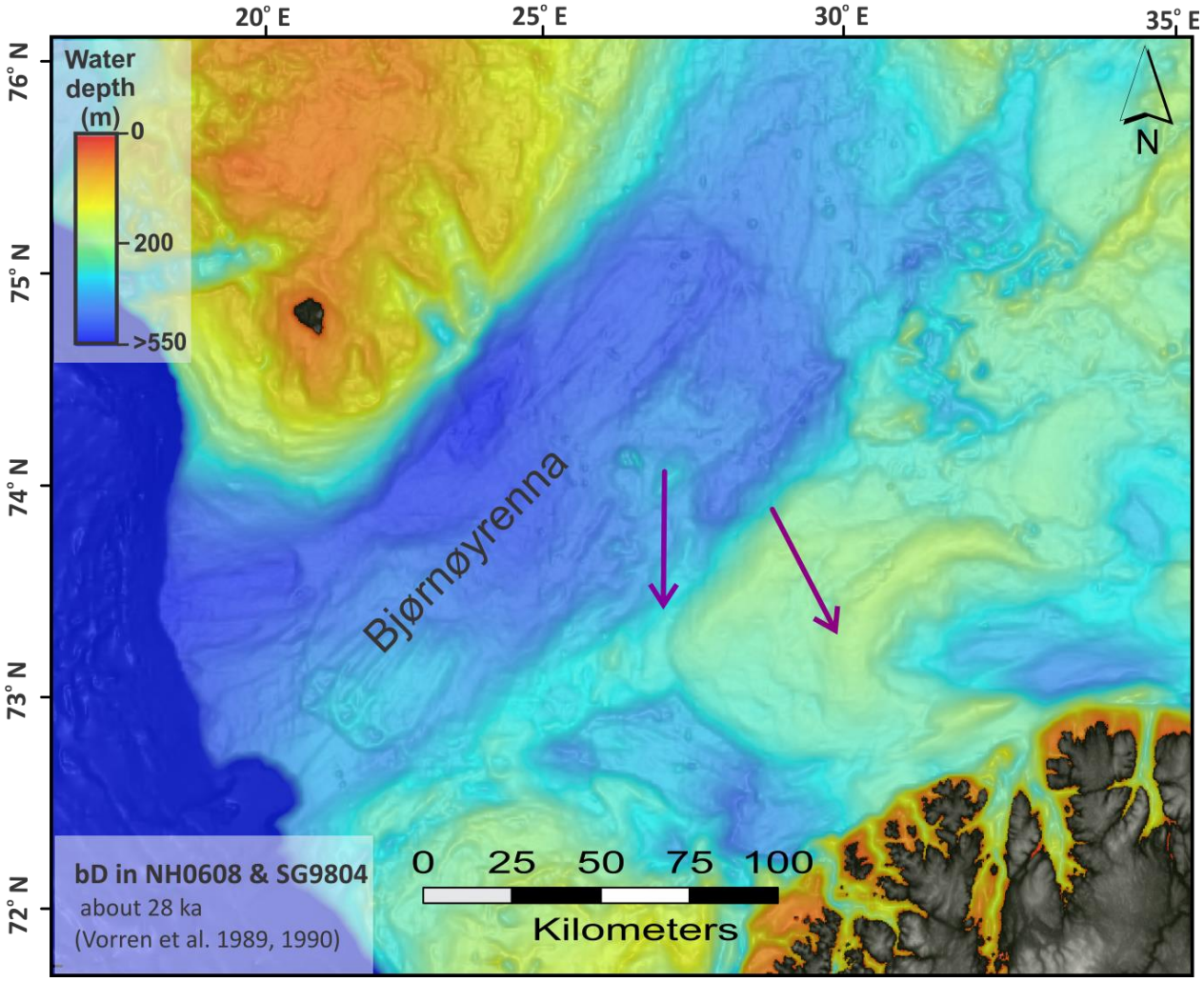

Figure 4.6: Inferred orientation of ice streams on bD in the survey NH0608 and SG9804 respectively. The yellow dashed line could be possible alternative for Fennoscandian Ice sheet source.

The horizon bD can be correlated in the survey NH0608 and SG9804 (Fig.3.4, section 3.1) in the surveys NH0608 and SG9804 respectively. Sediments in the unit D (Fig. 3.2) are radiocarbon dated to be younger than 27 320 ± 735 years BP (Rafaelsen et al. 2002; Hald et al. 1990). This may represent the early stage of deglaciation after LGM, however the formation of these lineations within the LGM cannot be ruled out. The surface bD represents an isochronous

streaming event with only one north-south oriented flow set (Fig. 3.19). The same orientation of flow set can be observed on the surface bD marked by white lines (Fig. 3.20). The source area is inferred to be from the northern areas like Bjørnøyrenna (Fig. 4.6). Another northwest-southeast flow set marked by blue colored lineations on time relief map of bD (Fig. 3.20) which is older than the white flow set but this is only present on the southeastern. The source for this ice stream could be from the Barents Sea Ice Sheet.

4.1.3 Paleo-ice streams on Seafloor

The only area where MSGLs can be observed on seafloor is in the Bjørnøyrenna HFC surveys (Fig.). The focus of this study was subsurface horizons hence it will be discussed briefly.

Three orientations of MSGL are observed on seafloor (Fig. 3.10 and Fig. 4.7).). The youngest yellow colored lineations are northeast-southwest oriented with curving following the bathymetry of Bjørnøyrenna. It seems very likely that these lineations continue further northwards and represent the stage 3 of the deglaciation model (Winsborrow et al. 2009) with a source from the northern areas like Storbanken indicated by dotted lines (Fig. 4.7). An older ice stream event represented by white lineations (Fig. 3.10) is also observed on seafloor, indicating the same orientation but curving towards the south. Although an ice stream can diverge into two lobes with different orientations (Rebesco et al. 2011), this does not seem to be the case here as cross-cutting relationships are observed. This suggests that it is a time progressive ice stream with a northern source which slightly reconfigured itself due to mass loss from the ice sheet. The lineations marked by black lines are only present on a small area in the southeast (Fig. 3.10). The relative age for it cannot be determined however this flow set also seems to have a northern source.

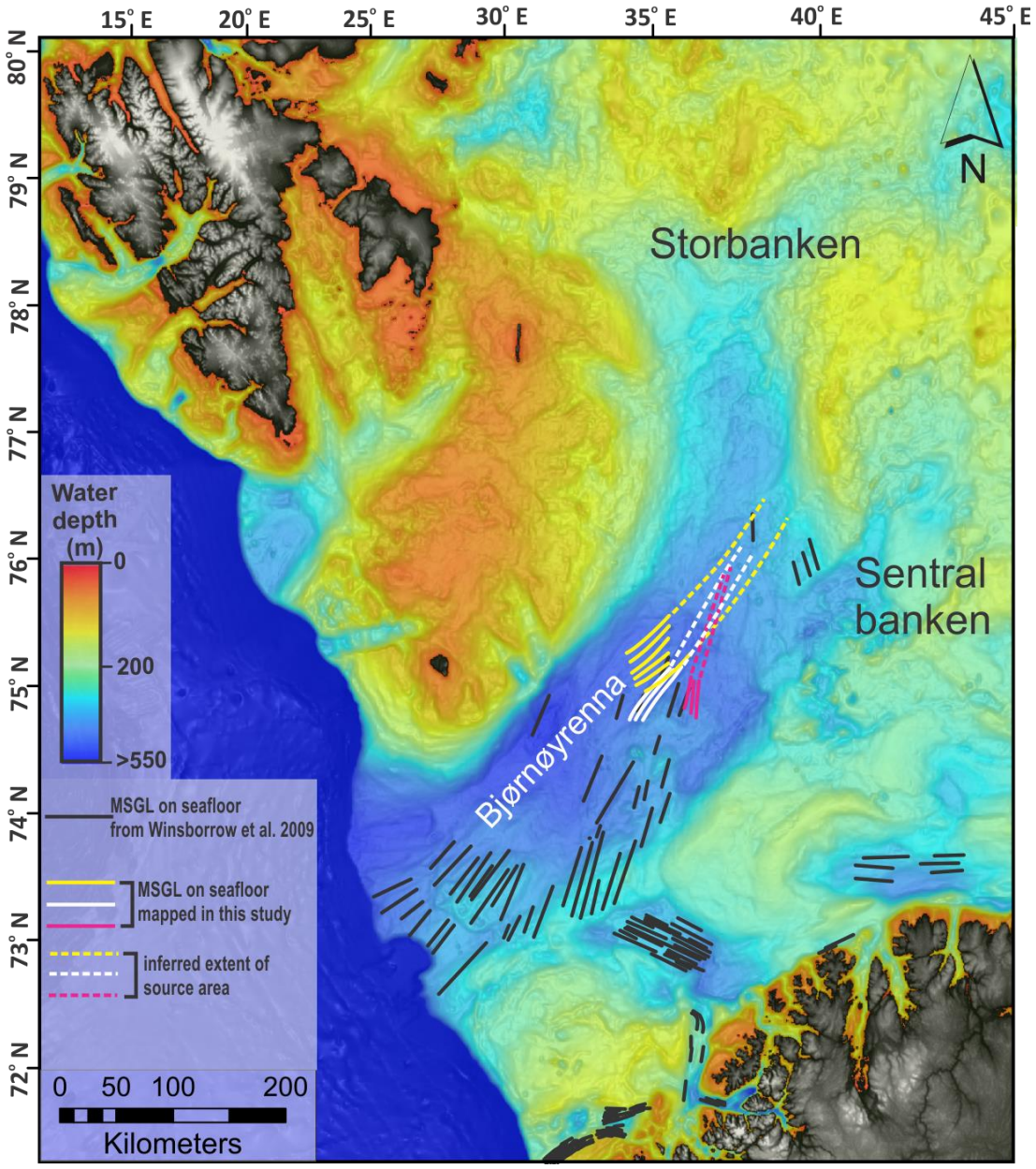

Figure 4.7: Inferred orientation of ice streams on seafloor on IBCAO bathymetry (Jacobsen et al. 2012). Inferred source areas are indicated by dotted lines in the figure.

The probable source areas are indicated by dotted lines in Fig. 4.7. Since the seafloor lineations are inferred to have been caused by last deglaciation, it can be concluded that the ice sheet was lying in the northern areas which acted as a source for these ice streams. It further suggests that Bjørnøyrenna was amongst the first areas to be deglaciated. Based on these lineations it can be inferred that there were at least three ice streaming events from approximately same source area.

4.2 Glaciotectonic depressions

On most of the subsurface horizons, large erosional depressions with distinct geomorphology are observed (e.g., Fig. 3.22, 3.23, 3.24). All depressions observed, are semi-circular except the depression observed on surface bE in the survey NH0608 which is irregular in shape (Fig. 3.23). A large depression is also observed in hor-01 in the survey ST10020 which will be discussed separately (Fig. 3.15). Type A and B like depressions have been reported from the Barents Sea (e.g., Sættem, 1990; Rafaelsen et al. 2002; Ruther et al. 2009; Deryabin, 2012; Solheim and Elverhøi, 1993). The mechanisms of the formation of these depressions are discussed to be either glacial erosion or fluid expulsion.

Based on the morphology of the depressions they are being classified into Type A, B and C depressions. Type A depressions (Fig. 3.24 A & B) are semi-circular elongated depressions with smoothed edges whereas Type B depressions (Fig. 3.25 and 4.8) are semi-circular and elongated too but the elongation is not as much as Type A. Type B depressions are also crossed by MSGLs. Type B depression also exhibit an echelon pattern (Fig. 3.24 and 4.8). Type C depressions are larger in size and have an irregular shape (Fig. 3.23 & 4.10). It seems likely that both Type A and Type B depressions are product of glacial erosion.

MSGLs are present on all the surfaces where these depressions occur with an oblique orientation to the longest axis of the depressions (Fig. 4.8 C). Type A and B depressions occur throughout the study area while Type C is present only in the survey NH0608 on Nordkappbanken area (Fig. 3.23).

All the depressions are likely to have formed by basal freezing of the glaciers and later movement of these glaciers plucked the sediments forming these depressions. Basal freeze on has been a common process on the glaciated south-western Barents Sea shelf (Sættem et al. 1992a, 1996; Ruther et al. 2009). The MSGLs present on these surfaces depicts a subglacial warm based ice stream which may have frozen during its activity due to variation in temperature and a later reactivation of these ice streams seem likely to have plucked the sediments and created these Type A and B depressions.

Type B depressions are most likely formed by an earlier subglacial freeze on as the MSGLs present seem younger than these depressions (Fig. 3.24). This further suggests that ice streams might have operated with the direction similar to the longest orientation of these depressions. However the glacial landforms created by these early ice streams were eroded by the landforms which are observed now on these surfaces.

Type A depressions (Fig. 3.24 & 4.8 A) are also likely to have formed in the same way as Type A depression but due to their smooth nature melt water under the warm ice sheets may have smoothed these depressions.

Type C depression (Fig. 3.23 & Fig. 4.10) is more likely to be formed not only by subglacial erosion but also by fluid flow expulsion. The bedrock is sub cropping just under this depression (Fig. 4.10). These inclined beds are more likely to have acted as a carrier pathway for the fluid flow. Shallow gas accumulation cannot be observed on attribute maps, which can be explained in terms of all the fluid escaping without forming any shallow gas accumulations as at few places some bright spots just underneath the depression can be observed which confirms the presence of some gas (Fig).

4.2.1 Relationship between paleo-ice stream flow and depressions

Glaciotectonic landforms and MSGLs indicate two different ice streams dynamics. Glaciotectonic landforms indicate a slowmoving or basal frozen ice stream conditions (Sættem et al. 1992) whereas MSGLs indicate a fast-flowing warmbased ice stream. The observed Type B and Type C depressions are overlain by MSGL in the survey SG9804, ST10020 and NH0608 respectively (Fig. 4.8 & 4.10).

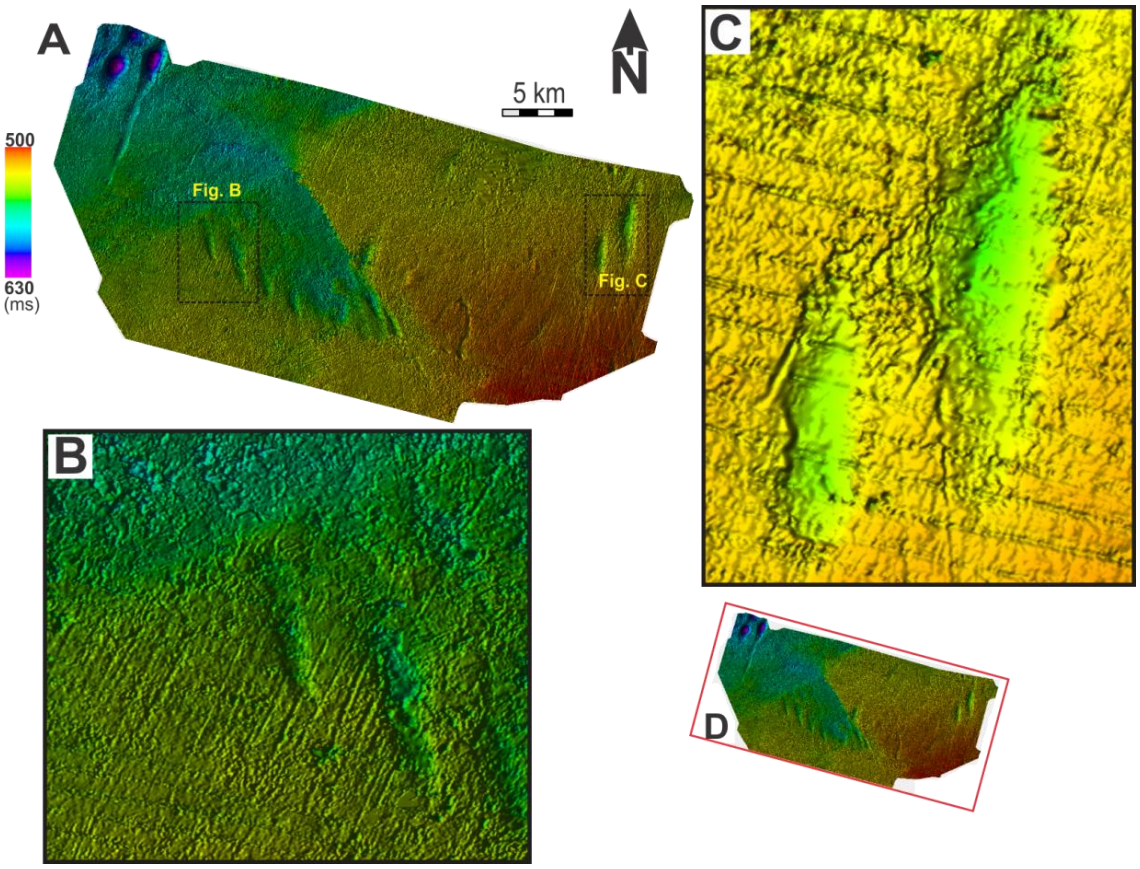

Figure 4.8: A) shaded relief time-map of bD in the survey SG9804. B) & C) Zoomed view of type B depressions showing MSGL's. D) Extent of interpretation in the survey.

This aforementioned pattern indicates that the basal freeze or slowdown of ice streams was followed by fast flowing ice stream. This trend is documented by Andreassen and Winsborrow (2009). In the study area of survey SG9804, these depressions are observed on URU and bD suggesting that cycles of fast flow and slow-down or quiescence of ice streams.

It seems likely that the Type B depressions are formed by basal freezing. The occurrence of MSGLs on the surface of this depression (Fig. 4.8 & 4.10) also is indicative of warmbased fast-flowing ice stream.

4.2.2 Relationship between fluid flow and depressions

The large depression in the survey ST10020 (Fig. 3.15) is likely to have a relationship with fluid flow. On Root Mean Square (RMS) amplitude map which is generated from a window of

20ms below URU (Fig4.9 C), high amplitudes with reverse anomalies underneath the large trough (Fig. 4.9 B & C) indicate presence of gas. Hence it can be concluded here that the main cause of this big depression could be expulsion of gas in combination with glacial erosion.

Type C depression (Fig. 4.10 A) is also likely to have formed in by fluid flow expulsion in association with glacial erosion as the underlying bedrock units (Fig. 4. 10 B) are inclined just underneath the depression. Also several faults can be seen under the depression (Fig. 4.9 b). It seems likely that along with glacial erosion fluid flow have enhanced the formation of the depression.

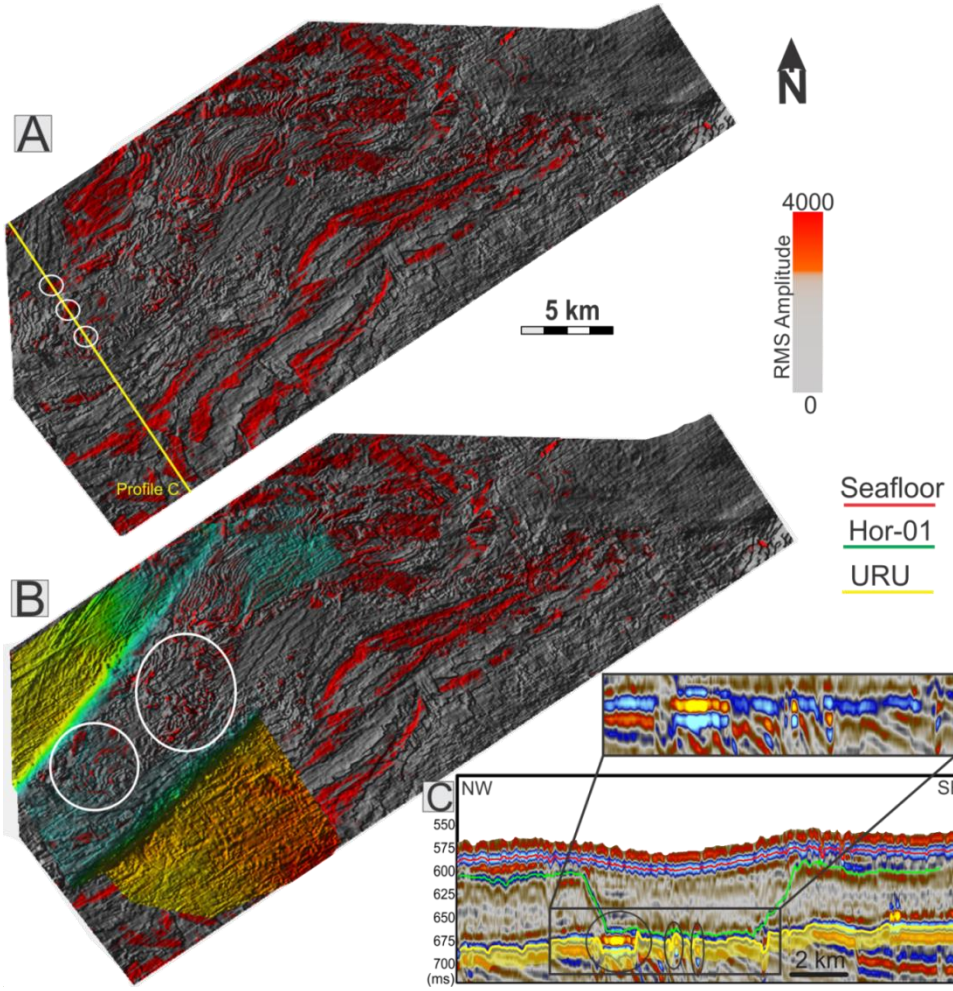

Figure 4.9: A) Root Mean Square (RMS) map 20ms below URU as marked by yellow color in Fig. C. B) RMS map overlaid by hor-01 showing high amplitudes in the center of the depression C) Seismic profile across the depression showing the volume used for generation of RMS map and high amplitude on seismic profile.

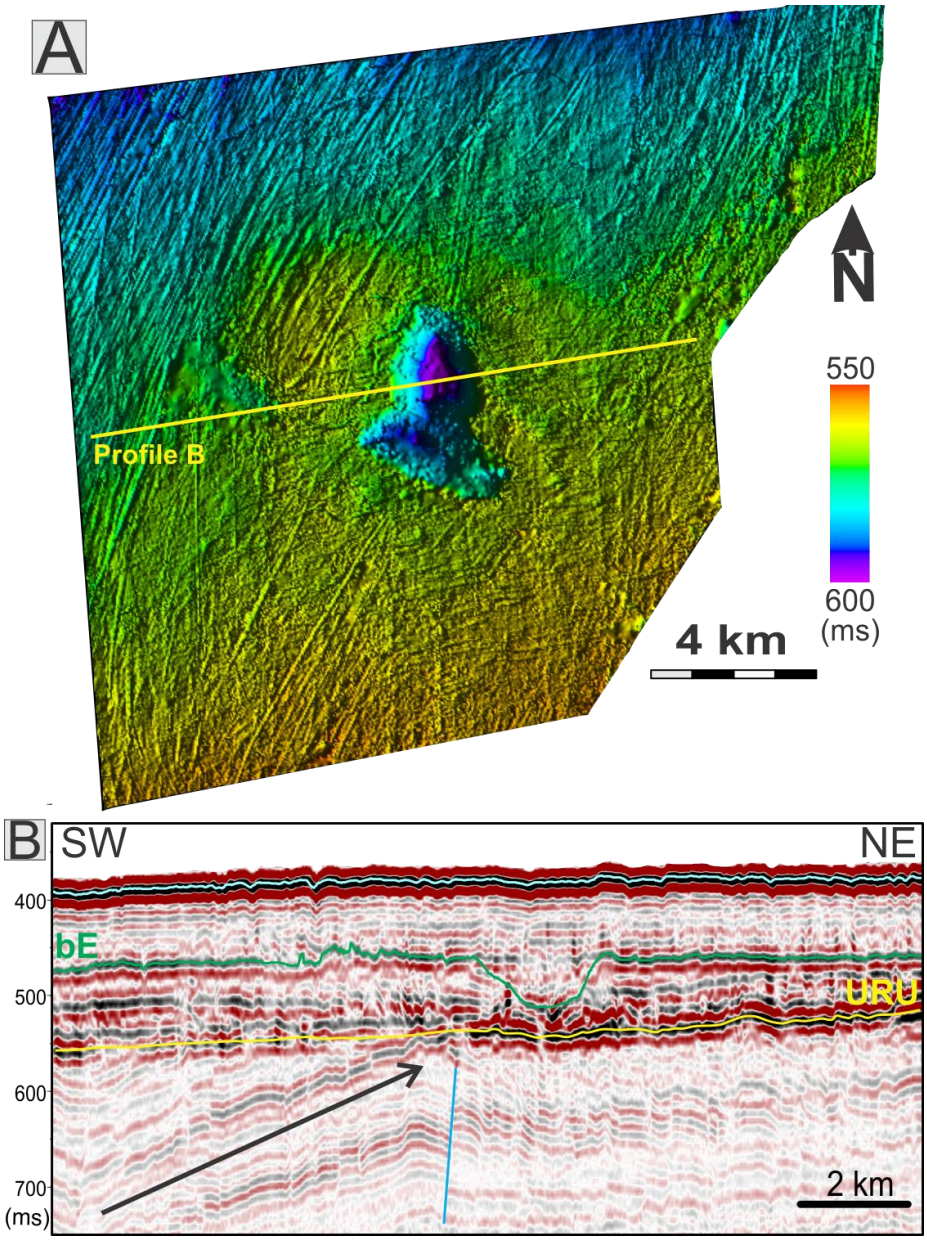

Figure 4.10: A) shaded relief time-map of bE in the survey NH0608 showing large irregular depression. B) Seismic profile across the depression showing subcropping unit and fault below the large depression.

4.3 Ice berg plough marks

Iceberg ploughmarks occur throughout the study area. These features are more common on the seafloor than at the subsurface horizons (e.g., Fig. 3.14 & Fig. 3.26). Iceberg ploughmarks indicate glaciomarine environments. Scouring of the seafloor by iceberg keels is a common process on high-latitude continental shelves (Dowdeswell and Bamber, 2007). The cross-cutting patterns of ploughmarks in the study area indicate that there was continues discharge of ice bergs.

The iceberg ploughmarks are denser on the seafloor on the Nordkappbanken area compared to in Bjørnøyrenna (Fig. 3.6) which may indicate that the source area of the ice bergs was closer to the Nordkappbanken area. The widespread occurrence of the ice bergs may also indicate that the water depth in these areas might have been shallower than the current water depth. Ice berg scours are result of deglacial and interglacial processes; hence ice bergs are produced during major deglaciation following full-glacial maxima (Dowdeswell and Bamber, 2007). This further implies that Bjørnøyrenna was ice free earlier than the areas neighboring Nordkappbanken area and the calving margin was close in the area where these ice bergs may have produced.

The absence of MSGLs on the seafloor in Nordkappbanken area can be attributed to the large ice-marginal deposits on most part of Nordkappbanken. In Bjørnøyrenna MSGLs appear widely with few ice berg plough marks (e.g., HFC surveys, Fig. 3.10 A). This suggests that the source of icebergs may have been well far from these areas. Another reason of the fewer occurrences of ice berg plough marks can also be attributed to greater water depths. The larger length (Fig. 3.10 A) of the ice berg plough marks in the HFC surveys indicates that the ice bergs were transported over a long distance with probable source coming from the east.

4.4 Channel like Features

Channel like features occur in Bjørnøyrenna on subsurface horizons; one appear on hor-02 (Fig. 3.16) in the survey ST10020 which is interpreted to be younger than 17 cal ka BP (section 3.1) and the second occur on the URU surface in the survey HFC in Bjørnøyrenna (Fig. 3.32). These channels are interpreted to be melt-water channels. Similar channels are reported from high latitude areas (e.g., Andreassen et al. 2008; Ó Cofaigh, C., 1996; Smith et al. 2009). The occurrence of melt-water beneath Rutford ice stream, west Antarctica is documented by King et al. (2004). The water is believed to occur in form of a subglacial drainage system rather than a small water pond.

Megascale glacial lineations occur obliquely across these channels which depicts a subglacial environment. The melt water under the ice sheet had been under high pressure due to overburden of the ice which may have caused the erosion of sediments forming these channels. Low sedimentation rate might have caused preservation of these channels. The presence of high values on time slice from variance cube (Fig. 3.21 B) suggests that a dense material like sands may be present in the channel. Glacio-fluvial sand is a common sedimentary infill in melt water channels (Ó Cofaigh, C., 1996).

The channel on the URU relief map in the survey HFC appears as a single channel in the southeastern part and form anastomosing like pattern towards northeastern side (Fig. 3.32). Anastomosing or net like pattern is common in channels from glacial landforms (Ó Cofaigh, C., 1996). The channel is younger than the MSGLs present on this surface. The channels here have small lobes towards southwest which is coherent to the orientation of MSGLs. This implies that movement of ice streams exerted pore pressure in the same direction as their movement forming these lobes like features.

5 Conclusions

The main conclusions from this study are:

- Three-dimensional (3D) seismic data has allowed mapping and visualizing glacial landforms in southern Barents Sea continental shelf in great detail.
- Various ice streams are inferred to have operated on the continental shelf, based on the geomorphology of the seafloor as well as the subsurface horizons in the Nordkappbanken area and Bjørnøyrenna.
- The ice streams were dynamic in nature as inferred from various orientations of the MSGLs present on different surfaces in the study area.
- The source areas for the ice streams changed during various time periods as evident from various orientations of MSGLs on different sub surface horizons. The common source for paleo-ice streams was Barents Sea Ice Sheet with some input from Fennoscandian Ice Sheet.
- Period of fast flow of ice streams is inferred from the occurrence of MSGLs while slowdown or stagnation of ice streams is inferred from the occurrence of glaciotectonic depressions.
- Ice streams dominated Bjørnøyrenna throughout the glaciation and deglaciation of the Barents Sea Ice Sheet.
- Glacial erosion was by glaciotectonic depressions was a common process on the south-western Barents Sea shelf as indicated by semi-circular depressions. Melt-water channels indicate glaciofluvial erosion. Large irregular depressions indicate fluid flow erosion along with glaciotectonic erosion.
- Glaciomarine environment is inferred to have followed subglacial conditions as indicated by presence of ice berg plough marks.
- Fluid flow expulsion along with glacial plucking have likely played a role in creating large irregular depressions.

References

Aber, J. S., and Ber, A., 2007. Glaciotectonism. Developments in Quaternary Science, 6th edn. Amsterdam: Elsevier, p. 246.

Aber, J. S., Croot, D. G., and Fenton, M. M. (1989). Glaciotectonic Landforms and Structures. p. 200.

Andreassen, K., Glad Nilssen, E., Odegaard, C.M., 2007a.Analysis of shallow gas and fluid migration within the Plio-Pleistocene sedimentary succession of the SW Barents Sea continental margin using 3D seismic data. Geo-Mar. Lett. 27, 155–171.

Andreassen, K., Ødegaard, C., and Rafaelsen, B., 2007,b, Imprints of former ice streams, imaged and I nterpreted using industry three-dimensional seismic data from the south-western Barents Sea: Geological Society, London, Special Publications, v. 277, no. 1, p. 151-169.

Andreassen, K., and Winsborrow, M.C.M., 2009, Signature of ice streaming in Bjørnøyrenna, polar North Atlantic through the Pleistocene and implications for ice stream dynamics: Annals of Glaciology, v. 50, p. 17–26,

Andreassen, K., Nilssen, L.C., Rafaelsen, L., Kuilman, L., 2004. Three-dimensional seismic data from the Barents Sea margin reveal evidence of past ice streams and their dynamics. Geology v.32 (8), p. 729–732.

Aber, J. S., and Ber, A.,2011. Glaciotectonic structures , Landforms, and processes. In Singh, Vijay P.; Singh, Pratap; Haritashya, Umesh K. : Encyclopedia of Snow, Ice and Glaciers, p. 444-458.

Badley, M. E., 1985, Practical seismic interpretation: , no. D. Reidel, Dordrecht (1985),266.

Barnes, P.W., Lien, R., 1987. Icebergs rework shelf sediments to 500 m off Antarctica. Geology v.16, p. 1130–1133.

Bulat, J., 2005, some considerations on the interpretation of seabed images based on commercial 3D seismic in the Faroe-Shetland Channel: Basin Research, v. 17, no. 1, p. 21-42.

Brown, A. R., 2004, Interpretation of three-dimensional seismic data, Soc of Exploration Geophysicists.

Brown, A. R., 1999 Interpretation of Three-Dimensional Seismic Data.: AAPG Memoir 42. SEG Investigations in Geophysics 9.

Butt, F.A., Elverhoi, A., Solheim, A., Forsberg, C.F., 2000.Deciphering Late Cenozoic development of the western Svalbard Margin from ODP Site 986 results. Mar. Geol. V. 169, p. 373–390.

Bugge, T., Elvebakk, G., Fanavoll, S., Mangerud, G., Smelror, M., Weiss, H. M., Gjelberg, J., Kristensen, S. E., and Nilsen, K., 2002, Shallow stratigraphic drilling applied in hydrocarbon exploration of the Nordkapp Basin, Barents Sea: Marine and Petroleum Geology, v. 19, no. 1, p. 13-37.

Bergendahl, E., 1989, Halokinetisk utvikling av Nordkapp bassengets sørvestre segment: Cand. Scient Oppgave, Institutt for Geologi, Universitet i Oslo, 120 p.

Bryn,P., Berg, K., Solheim, K., Kvalstad, T.J., Forsberg, C.F., 2005. Explaining the Storegga Slide. Marine and Petroleum Geology v. 22, p. 11-19.

Breivik, A.J., Faleide, J.I. and Gudlaugsson, S.T. 1998. Southwestern Barents Sea margin: Late Mesozoic sedimentary basins and crustal extension. Tectonophysics v. 293, p. 21–44.

Breivik, A.J., Gudlaugsson, S.T., Faleide, J.I., 1995. Ottar Basin, SW Barents Sea: a major Upper Palaeozoic rift basin containing large volumes of deeply buried salt. Basin Res. v.7, p. 299– 312.

Cartwright, J., Huuse, M., and Aplin, A., 2007, Seal bypass systems: AAPG bulletin, v. 91, no. 8, p. 1141.

Clark, C.D., 1993. Megascale glacial lineations and cross-cutting iceflow landforms. Earth Surface Processes and Landforms v. 18, p. 1–29.

Clark, C.D., Tulaczyk, S.M., Stokes, C.R., Canals, M., 2003. A groove-ploughing theory for the prediction of megascale glacial lineations, and implications for ice-stream mechanics. Journal of Glaciology 49 (165), p. 240–256.

Clark, C. D., and Stokes, C. R. (2003). Paleo-ice stream landsystem. In Glacial Landsystems (D. J. A. Evans, Ed.), p. 204– 227. Arnold, London.

Catania, G.A., Scambos, T.A., Conway, H., and Raymond, C.F., 2006, Sequential stagnation of Kamb ice stream, West Antarctica: Geophysical Research Letters, v. 33, no. 14, p. L14502.

Conway, H., Hall, B.L., Denton, G.H., Gades, A.M., and Waddington, E.D., 1999, Past and future grounding line retreat of the West Antarctic Ice Sheet: Science, v. 286, no. 5438, p. 280–283.

Canals, M., Urgeles, R., and Calafat, A. M., 2000, Deep sea-floor evidence of past ice streams off the Antarctic Peninsula: Geology, v. 28, no. 1, p. 31-34.

Deryabin, A., 2012, Relationship between glacial erosion and fluid flow inferred from 3D seismic data, SW Barents Sea, Master Thesis, University of Tromsø.

Dimakis, P., Braathen, B.I., Faleide, J.I., Elverhoi, A., Gudlaugsson, S.T., 1998. Cenozoic erosion and the preglacial uplift of the Svalbard-Barents Sea region. Tectonophysics v. 300 (1–4), p. 311–327

Doré A.G. 1991. The structural foundation and evolution of Mesozoic seaways between Europe and the Arctic. Palaeogeography, Palaeoclimatology, Palaeoecology v. 87, p. 441–492.

Dobhal, D.P, 2011, Glacial Geomorphology and Landforms Evolution: Glacial grooves. In Singh, Vijay P.; Singh, Pratap; Haritashya, Umesh K. : Encyclopedia of Snow, Ice and Glaciers, Springer,p.358

Dowdeswell, J.A., Villinger, H., Whittington, R.J., and Marienfeld, P., 1993, Iceberg scouring in Scoresby Sund and on the East Greenland continental shelf: Marine Geology, v. 111, p. 37-53

Dowdeswell, J.A., Hogan, K.A., Evans, J., Noormets, R., Ó Cofaigh, C., Ottesen, D., 2010. Past ice-sheet flow east of Svalbard inferred from streamlined subglacial landforms. Geology v. 38; no. 2; p. 163–166;

Evans, D. J. A., and Benn, D. I. (2001). Earth's giant bulldozers. Geography Review v. 14, p.29–33.

Evans, D.J.A. (2007). Glacitectonic structures and landforms. In Encyclopedia of Quaternary Science. Elias, S.A. Oxford: Elsevier. P. 831-83

Evans, D.J.A., Clark, C.D. & Mitchell, W.A. (2005). The last British Ice Sheet: A review of the evidence utilised in the compilation of the Glacial Map of Britain. Earth Science Reviews v. 70(3-4): p. 253-312.

Faleide et al. 1993a, Faleide, J.I., Vågnes, E. and Gudlaugsson, S.T. 1993. Late Mesozoic-Cenozoic evolution of the southwestern Barents Sea in a regional rift-shear tectonic setting. Marine and Petroleum Geology v. 10, p. 186–214.

Faleide, J.I., Gudlaugsson, S.T. and Jacquart, G. 1984. Evolution of the western Barents Sea. Marine and Petroleum Geology1, p. 123–150.

Faleide, J.I., Tsikalas, F., Breivik, A.J., Mjelde, R., Ritzmann, O., Engen, O., Wilson, J., Eldholm, O., 2008. Structure and evolution of the continental margin off Norway and Barents Sea. Episodes 31 (1), 82–91.

Faleide, Jan Inge; Bjørlykke, Knut; Gabrielsen, Roy H., 2010. Geology of the Norwegian continental shelf. I: Petroleum Geoscience: From Sedimentary Environments to rock Physics. Springer Science+Business Media B.V. 2010 ISBN 978-3-642-02331-6. p. 467-499

Forsberg, C.F., Solheim, A., Elverhoi, A., Jansen, E., Channell, J.E.T., Andersen, E.S., 1999. The depositional environment of the western Svalbard margin during the late Pliocene and the Pleistocene: Sedimentary facies changes at Site 986. In: Raymo, M., Jansen, E., Blum, P., Herbert, T.D. (Eds.), Proceeding Ocean Drilling Program. Scientific Results, v. 162, p. 233–246. Ocean Drilling Program, College Station, TX.

Faleide, J.I., Solheim, A., Fiedler, A., Hjelstuen, B.O., Andersen, E.S., Vanneste, K., 1996.Late Cenozoic evolution of the western Barents Sea–Svalbard continental margin.Global Planet. Change v. 12, p. 53–74.

Fu P, Harbor J, 2011. Glacial erosion: Glaciological variables controlling glacial erosion. In Singh, Vijay P.; Singh, Pratap; Haritashya, Umesh K. : Encyclopedia of Snow, Ice and Glaciers, Springer,p. 332-341.

Glørstad-Clark, E., Faleide, J. I., Lundschien, B. A., and Nystuen, J. P., 2010, Triassic seismic sequence stratigraphy and paleogeography of the western Barents Sea area: Marine and Petroleum Geology, v. 27, no. 7, p. 1448-1475 Sættem, J., Bugge, T., Fanavoll, S., Goll, R., Mork, A., Mork, M., Smelror, M., and Verdenius, J., 1994, Cenozoic margin development and erosion of the Barents Sea: Core evidence from southwest of Bjørnøya: Marine Geology, v. 118, no. 3-4, p. 257-281

Gudlaugsson, S.T., Faleide, J.I., Johansen, S.E., and Breivik, A.J., 1998, Late Paleozoic structural development of the south-western Barents Sea: Marine and Petroleum Geology, v. 15, p. 73–102

Gabrielsen et al. 1990 ; Gabrielsen, R.H., Færseth, R.B., Jensen, L.N., Kalheim, J.E., Riis, F., 1990. Structural elements of the Norwegian continental shelf, Part I. The Barents Sea Region. Norwegian. Petroleum Directorate Bulletin v.6,

Glasser, N.F., Scambos, T.A., 2008. A structural glaciological analysis of the 2002 Larsen B ice shelf collapse. Journal of Glaciology v. 54 (184).

Henriksen, E., Ryseth, A., Larssen, G., Heide, T., Rønning, K., Sollid, K., and Stoupakova, A., 2011, b, Tectonostratigraphy of the greater Barents Sea: implications for petroleum systems: Geological Society, London, Memoirs, v. 35, no. 1, p. 163-195

Henriksen, E., Bjørnseth, H., Hals, T., Heide, T., Kiryukhina, T., Kløvjan, O., Larssen, G., Ryseth, A., Rønning, K., and Sollid, K., 2011, a, Uplift and erosion of the greater Barents Sea: impact on prospectivity and petroleum systems: Geological Society, London, Memoirs, v. 35, no. 1, p. 271-281.

Hjelstuen, B.O., Eldholm, O., Faleide, J.I., 2007.Recurrent Pleistocene mega-failures on the SW Barents Sea margin. Earth Planet. Sci. Lett. v. 258, p. 605–618

HALD, M., SÆTTEM, J. & NESSE, E. 1990. Middle and late Weichselian stratigraphy in shallow drillings from the southwestern Barents Sea: foraminferal, amino acid and radiocarbon evidence. Norsk Geologisk Tidsskrift, v. 70, p. 241–257.

Jakobsson, M., L. A. Mayer, B. Coakley, J. A. Dowdeswell, S. Forbes, B. Fridman, H. Hodnesdal, R. Noormets, R. Pedersen, M. Rebesco, H.-W. Schenke, Y. Zarayskaya A, D. Accettella, A. Armstrong, R. M. Anderson, P. Bienhoff, A. Camerlenghi, I. Church, M. Edwards, J. V. Gardner, J. K. Hall, B. Hell, O. B. Hestvik, Y. Kristoffersen, C. Marcussen, R. Mohammad, D. Mosher, S. V. Nghiem, M. T. Pedrosa, P. G. Travaglini, and P. Weatherall, 2012, The International Bathymetric Chart of the Arctic Ocean (IBCAO) Version 3.0, Geophysical Research Letters,

Judd, A. G., and Hovland, M., 2007, Seabed fluid flow: the impact of geology, biology and the marine environment, Cambridge University Press.

Jebsen, C. and Faleide, 1998, Tertiary rifting and magmatism at the western Barents Sea margin (Vestbakken volcanic province): III international conference on Arctic margins, ICAM III; abstracts; plenary lectures, talks and posters,

King, E.C., Woodward, J., and Smith, A.M., 2004, Seismic evidence for a water filled canal in deforming till beneath Rutford Ice Stream, West Antarctica: Geophysical Research Letters, v. 31,

King, E.C., Hindmarsh, R.C.A., Stokes, C.R., 2009. Formation of megascale glacial lineations observed beneath a West Antarctic ice stream. Nature Geoscience 2, p. 585-588.

Linch, L, D., van der Meer, J. J. M., and Menzies, J., 2012, Micromorphology of iceberg scour in clays: Glacial Lake Agassiz, Manitoba, Canada: Quaternary Science Reviews, v. 55, p. 125-144

Løseth, H., Gading, M., and Wensaas, L., 2009, Hydrocarbon leakage interpreted on seismic data: Marine and Petroleum Geology, v. 26, no. 7, p. 1304-1319.

Larssen, G.B., Elvebakk, G., Henrikson, L.B., Kristensen, S.E., Nilsson, I., Samsuelsberg, T.J., Svånå, T.A., Stemmerik L., and Worsley, D., 2002, Upper Palaeozoic Lithostratigraphy of the Southern Norwegian Barents Sea, NPD Bulletin v. 9.

Laberg, J.S., Andreassen, K., Vorren, T, O., The late Cenozoic erosion of the high-latitude south-western Barents Sea shelf revisited. Geological Society of America Bulletin. v. 124, no. 1/2, p. 77-88.

Marfurt, K.J., Scheet, R.M., Sharp, J.A. & Harper, M.G., 1998. Suppression of the acquisition footprint for seismic sequence attribute mapping. Geophysics, v. 62, p. 1774-1778.

Mattingsdal, R., 2009, Glasial geomorfologi og deglasiasjon av Nordkappbanken-området, sørvestlige Barentshav, basert på 3D- og 2D-seismiske data, Master Thesis, University of Tromsø.

Nyland, B., Jensen, L.N., Skagen, J., Skarpnes, O. & Vorren, T.O. 1992: Tertiary uplift and erosion in the Barents Sea: magnitude, timing and consequences. In Larsen, R.M., Brekke, H., Larsen, B.T. & Tallerås, E. (eds.): Structural and tectonic modelling and its application to petroleum geology, 153-162. Norwegian Petroleum Society Special Publication 1, Elsevier, Amsterdam.

Nyland, B., Jensen, L.N., Skagen, J., Skarpnes, O. & Vorren, T.O. 1992: Tertiary uplift and erosion in the Barents Sea: magnitude, timing and consequences. In Larsen, R.M., Brekke, H., Larsen, B.T. & Tallerås, E. (eds.): Structural and tectonic modelling and its application to petroleum geology, p. 153-162. Norwegian Petroleum Society Special Publication 1, Elsevier, Amsterdam.

Ó Cofaigh, C., 1996. Tunnel valley genesis. Progress in Physical Geography v. 20, p. 1–19.

Ó Cofaigh, C., Dowdeswell, J.A., Allen, C.S., Hiemstra, J., Pudsey, C.J., Evans, J., Evans, D.J.A., 2005. Flowdynamics and till genesis associatedwith amarine-basedAntarcticpalaeoice stream. Quaternary Science Reviews v. 24, p. 709–740.

Ohm, S.E., D.A. Karlsen, and T.J.F. Austin, 2008, Geochemically driven exploration models in uplifted areas: Examples from the Norwegian Barents Sea: AAPG Bulletin, v. 92, p. 1191-1223.

REEMST, P., CLOETINGH, C. & FANAVOLL, S. 1994. Tectono-stratigraphic modelling of Cenozoic uplift and erosion in the SW Barents Sea. Marine and Petroleum Geology, v. 11, p. 478-490.

ROUFOSSE, M. C., 1987: The formation and evolution of sedimentary basins in the Western Barents Sea.In: J. Brooks & K. Glennie (eds.): Petroleum Geology of North West Europe. (Graham & Trotman), p. 1149-1161.

Ryseth, A., Augustson, J.H., Charnock, M., Haugerud, O., Knutsen, S.-M., Midbøe, P.S., Opsal, J.G. and Sundsbø, G., 2003. Cenozoic stratigraphy and evolution of the Sørvestsnaget Basin, southwestern Barents Sea. Norwegian Journal of Geology v. 83, p. 107–130.

Rebesco, M., Liu, Y., Camerlenghi, A., Winsborrow, M., Laberg, J.S., Caburlotto, A., Diviacco, P., Accettella, D., Sauli, C., Wardell, N., Tomini, I., 2011. Deglaciation of the western margin of the Barents Sea Ice Sheet - A swath bathymetric and sub-bottom seismic study from the Kveithola Trough. Marine Geology v.279, p. 141-147.

Solheim, A., Berg, K., Forsberg, C.F. & Bryn, P. 2005: The Storegga Slide Complex: repetitive large scale sliding with similar cause and development. Marine and Petroleum Geology v. 22, p. 97-107.

Stemmerik, L., & Worsley,D. 1989. Late Paleozoic sequence correlation, North Greenland and the Barents Shelf. In J.D. Collinson (Ed), Correlation in hydrocarbon exploration. London: Graham and Trotman, p. 99-111

Solheim, A., Kristoffersen, Y., 1984. Sediments above the upper regional unconformity: thickness, seismic stratigraphy and outline of the glacial history. Nor. Polarinst. Skr. 179B, 26 pp.

Sejrup, H., Larsen, E., Haflidason, H., Berstad, I., Hjelstuen, B.O., Jonsdotter, H.E., et al., 2003. Configuration, history and impact of the Norwegian Channel Ice stream. Boreas v. 32, p. 18–36.

Solheim, A., and Elverhøi, A., 1993, Gas-related sea floor craters in the Barents Sea: Geo-Marine Letters, v. 13, no. 4, p. 235-243.

Solheim, A., Andersen, E.S., Elverhoi, A., Fiedler, A., 1996. Late Cenozoic depositional history of the western Svalbard continental shelf, controlled by subsidence and climate. Global Planet. Chance v. 12, p. 135–148.

Sejrup, H.P., Hjelstuen, B.O., Dahlgren, K.I.T., Haflidason, H., Kuijpers, A., Nygard, A., Praeg, D., Stoker, M.S., Vorren, T.O., 2005. Pleistocene glacial history of the NW European continental margin. Mar. Petrol. Geol. V. 22, p. 1111–1129.

Stoker, M. S., and Long, D., 1984, A relict ice-scoured erosion surface in the central North Sea: Marine Geology, v. 61, no. 1, p. 85-93.

Stokes, C.R., Clark, C.D., Storrar, R., 2009. Major changes in ice stream dynamics during deglaciation of the north-western margin of the Laurentide Ice Sheet. Quaternary Science Reviews v. 28 (7–8), p. 721–738.

Sheriff, R. E., 2002, Encyclopedic dictionary of applied geophysics, Society of exploration geophysicists.

Solheim, A., Faleide, J.I., Andersen, E.S., Elverhoi, A., Forsberg, C.F., Vanneste, K., Uenzelmann-Neben, G., Channell, J.E.T., 1998.Late Cenozoic seismic stratigraphy and glacial geological development of the East Greenland and Svalbard-Barents Sea continental margins. Quat. Sci. Rev. 17, 155–184.

Sættem, J., Poole, D.A.R., Ellingsen, L., Sejrup, H.P., 1992a. Glacial geology of outer Bjørnøyrenna, southwestern Barents Sea. Marine Geology v.103, p. 15–51.

Sættem, J., Rise, L. & Westgaard, D. A. 1992, b. Composition and properties of glacigenic sediments in the southwestern Barents Sea. Marine Geotechnology, v.10, p.229–255.

Sættem, J., 1990, Glaciotectonic forms and structures on the Norwegian continental shelf: observations, processes and implications: Norsk geologisk tidsskrift, v. 70, no. 2, p. 81-94.

Selley, R. C., 1998, Elements of petroleum geology. San Diego, Academic Press Ltd.

Svendsen, J.I., Alexanderson, H., Astakhov, V.I., Demidov, I., Dowdeswell, J.A., Funder, S., Gataullin, V., Henriksen, M., Hjort, C., Houmark-Nielsen, M., Hubberten, H.W., Ingolfsson, O., Jakobsson, M., Kjar, K.H., Larsen, E., Lokrantz, H., Lunkka, J.P., Lysa, A., Mangerud, J., Matiouchkov, A., Murray, A., Moller, P., Niessen, F., Nikolskaya, O., Polyak, L., Saarnisto, M., Siegert, C., Siegert, M.J., Spielhagen, R.F., Stein, R., 2004. Late Quaternary ice sheet history of northern Eurasia. Quat. Sci. Rev. v. 23, p. 122–127

Smith, A.M., Murray, T., 2009. Bedform topography and basal conditions beneath a fast flowing West Antarctic ice stream. Quaternary Science Reviews v.28, p. 584–596.

Tulaczyk, S. M., Scherer, R. P., and Clark, C. D., 2001, A ploughing model for the origin of weak tills beneath ice streams: a qualitative treatment: Quaternary International, v. 86, no. 1, p. 59-70.

Vorren, T.O., Kristoffersen, Y., Andreassen, K., 1986.Geology of the inner shelf west of North Cape, Norway. Norsk Geologisk Tidsskrift 66, 99–105.

VORREN, T.O., LEBESBYE, E. & LARSEN, K. B. 1990. Geometry and genesis of the glacigenic sediments in the southern Barents Sea. In: DOWDESWELL, J.A. & SCOURSE, J. D. (eds) Glacimarine Environments: Processes and Sediments. Geological Society, London, Special Publications, v. 53, p. 269–288.

Vorren, T.O., Laberg, J.S., 1997. Trough mouth fans—paleoclimate and ice-sheet monitors. Quatern. Sci. Rev. v. 16, p. 865–881

Vorren, T.O., Laberg, J.S., Blaume, F., Dowdeswell, J.A., Kenyon, N.H., Mienert, J., 1998. The Norwegian Greenland Sea continental margins: morphology and late Quaternary sedimentary processes and environment. Quatern. Sci. Rev. v. 17, p. 273–302

Wellner, J.S., Heroy, B.C., Anderson, J.B., 2006. The death mask of the Antarctic ice sheet: comparison of glacial geomorphic features across the continental shelf. Geomorphology v. 75, p. 157–171.

Worsley D., Agdestein T., Gjelberg J., Kirkemo K., Mørk A., Nilsson I., Olaussen S., Steel R.J. & Stemmerik L. 2001. The geological evolution of Bjørnøya, Arctic Norway: implications for the Barents shelf. Norwegian Journal of Geology v. 81, p. 195–234.

Worsely D., 2006, The post-Caledonian geological development of Svalbard and the Barents Sea, NGF Abstracts and Proceedings, no. 3, p. 5-21

Woodworth-Lynas, C.M.T., Dowdeswell, J.A., 1994. Soft-sediment striated surfaces and massive diamicton facies produced by floating ice. In: Deynoux, M., Miler, J.M.G., Domack, E.W., Eyles, N., Fairchild, I.J., Young, G.M. (Eds.), Earth's Glacial Record. Cambridge University Press, Cambridge, p. 241-259

Winsborrow, M.C.M., Clark, C.D., and Stokes, C.R., 2010,b, what controls the location of ice streams: Earth-Science Reviews, v. 103, p. 45–59,

Winsborrow, M.C.M., Andreassen, K., Corner, G.D., and Laberg, J.S., 2009, Deglaciation of a marine-based ice sheet: Late Weichselian paleo–ice dynamics and retreat in the southern Barents Sea reconstructed from onshore and offshore glacial geomorphology: Quaternary Science Reviews, v. 29, p. 424–442.

Yilmaz, Ö., 1987. Seismic Data Analysis, Vol II, Second Edition. Society of Exploration Geophysicists, Tulsa, Oklahoma, 2027